SAND2018-9357 PE
SAND2021-11113 PE
SAND2022-12146 PE
SAND2022-12412 PE

Sandia National Laboratories

Securing the future of Nuclear Energy

MELCOR

MELCOR Applications & Best Practices

KC Wagner

EMUG 2023

Sandia National Laboratories is a multimission laboratory managed and operated by National Technology and Engineering Solutions of Sandia, LLC., a wholly owned subsidiary of Honeywell International, Inc., for the U.S. Department of Energy's National Nuclear Security Administration under contract DE-NA0003525.

LWR MELCOR CODE DEVELOPMENTS

MELCOR

MODELS

- Convecting Molten Pool
- Curved Lower Head
- Stefan Model
- Point Kinetics
- Smart Restart
- RN Activity (Bonus)
- H2 Production
- Turbulent Deposition
- Mechanistic Fan Cooler
- Multi-rod
- CORQUENCH
- LHC
- LHC
- Vector CFs
- Homologous Pump
- Resuspension
- Radiation Enclosure
- Heat Pipe Reactor
- Fluid Fuel Point Kinetics
- Molten Salt Fission Product Chemistry
- Molten Salt Equation of state enhancement
- TRISO Fission Product Release Enhancements
- FHR TRISO Fission Product Release Modeling

2000 2001 2002 2003 2004 2005 2006 2007 2008 2009 2010 2011 2012 2013 2014 2015 2016 2017 2018 2019 2020 2021 2022 2023

EMPHASIS

- Conversion from F77 to F95
- MELCOR 2.X Robustness and User Flexibility
- SFP Models
- Molten Pool/ Lower Head
- HTGR Models
- Code Performance Improvements
- Na Fire Models
- Non-LWR Models
- SMR Models
- HPR Public Demonstration Meeting
- HTGR Public Demonstration Meeting
- FHR Public Demonstration Meeting

OFFICIAL RELEASE

- MELCOR 1.8.5
- MELCOR 1.8.6
- MELCOR 2.0 (BETA)
- M2.1.1576
- M2.1.3649
- M2.1.4803
- M2.1.6342
- MELCOR 2.2
- MELCOR 2.2.21402
- MELCOR 2.2.2023

SOARCA

Outline

- SOARCA UA Insights
  - Focus on recently released Surry UA (NUREG/CR-7262)
  - Also include interesting insights from the Peach Bottom and Sequoyah UAs

- Some examples of recent Non-LWR work
  - Fluoride high-temperature reactor (FHR)
  - Molten salt reactor (MSR)
  - Sodium fast reactor (SFR)

- Point kinetics feedback example
  - Forming feedbacks using vector control functions

SOARCA Uncertainty Analysis Case Studies

Background on SOARCA

SOARCA was initiated to develop a body of knowledge on the realistic outcomes of severe reactor accidents; three pilot plant analyses complete

Peach Bottom

- Boiling water reactor with Mark I containment
- Located in Pennsylvania
- UA on LTSBO

Surry

- 3-loop Westinghouse pressurized reactor with large, dry containment
- Located in Virginia
- UA on STSBO/ induced SGTF

Sequoyah

- 4-loop Westinghouse pressurized reactor with ice condenser containment
- Located in Tennessee
- UA on STSBO (no SGTF)

Background on Original SOARCA (2)

- State-of-the-Art Reactor Consequence Analyses
- Multi-year effort by the NRC and SNL completed January 2012
- Considered select accident scenarios postulated for Peach Bottom Atomic Power Station and Surry Power Station
  - NUREG/CR-7110 “State-of-the-Art Reactor Consequence Analyses Project, Volume 1: Peach Bottom Integrated Analysis”
  - NUREG/CR-7110, “State-of-the-Art Reactor Consequence Analyses Project, Volume 2: Surry Integrated Analysis”
  - NUREG-1335, “State-of-the-Art Reactor Consequence Analyses (SOARCA) Report”
- Integrated modeling of nuclear reactor accident progression and offsite consequences using modern computational tools and best modeling practices
- Included sensitivity analyses but not an uncertainty assessment (UA)

Objectives of the SOARCA UAs

- Considering one accident scenario specific to each of the Peach Bottom, Surry and Sequoyah plants:
  - Identify the uncertain input parameters potentially influential to accident progression and source term
  - Define informed distributions for the possible values of the uncertain parameters
  - Randomly exercise for the specific scenario, thru Monte Carlo sampling, a MELCOR model of the plant across the possible values of the uncertain parameters generating a distribution of source term outcomes
  - Determine from the distribution of outcomes the importance of the uncertain parameters relative to the metrics of Cs and I release to the environment
  - Identify the variations in accident phenomena driving differences in the Cs and I release metrics
  - Identify the linkages between the uncertain parameters and the driving phenomena
  - Develop insight into overall sensitivity of results and conclusions from the original SOARCA studies to uncertainty in model inputs

Uncertain MELCOR parameters chosen for the SOARCA UAs

Peach Bottom – BWR with Mark I Containment	Sequoyah – PWR with Ice Condenser Containment	Surry – PWR with Large, Dry Sub-atmospheric Containment
Sequence Related Parameters		
• Safety relief valve stochastic failure to reclose • Battery duration	• Primary safety valve stochastic number of cycles until a failure to close • Primary safety valve open area fraction after failure • Secondary safety valve stochastic number of cycles until failure-to-close • Secondary safety valve open area fraction after failure	• Primary safety valve stochastic number of cycles until failure-to-close • Primary safety valve open area fraction after failure • Secondary safety valve stochastic number of cycles until failure-to-close • Secondary safety valve open area fraction after failure • Reactor coolant pump seal leakage • Normalized temperature of hottest steam generator tube • Steam generator non-dimensional flaw depth • Main steam isolation valve leakage
Time within the Fuel Cycle		
Not varied	Time in the cycle sampled at three points in the refueling cycle – near Beginning- (BOC), Middle- (MOC), and End-of-Cycle (EOC)	Time in the cycle was discretely sampled at 14 times from 0.5 days to 550 days
In-Vessel Accident Progression		
• Zircaloy melt breakout temperature • Molten clad drainage rate • SRV thermal seizure criterion • SRV open area fraction upon thermal seizure • Main steam line creep rupture area fraction • Fuel failure criterion • Radial debris relocation time constants	• Melting temperature of the eutectic formed from fuel and zirconium oxides • Oxidation kinetics model	• Zircaloy melt breakout temperature • Molten clad drainage rate • Melting temperature of the eutectic formed from fuel and zirconium oxides • Oxidation kinetics model

SOARCA UA NUREG/CRs and NUREG

- NUREG/CR 7155, “State-of-the-Art Reactor Consequence Analyses Project, Uncertainty Analysis of the Unmitigated Long Term Station Blackout of the Peach Bottom Atomic Power Station,” U.S. Nuclear Regulatory Commission, Washington, DC, May 2016.
- NUREG/CR 7245, “State-of-the-Art Reactor Consequence Analyses Project: Sequoyah Integrated Deterministic and Uncertainty Analysis,” U.S. Nuclear Regulatory Commission, Washington, DC, October 2019.
- NUREG/CR-7262, “State-of-the-Art Reactor Consequence Analyses Project: Uncertainty Analysis of the Unmitigated Short Term Station Blackout of the Surry Power Station,” U.S. Nuclear Regulatory Commission, Washington, DC, December 2022.
- NUREG-2254, “Summary of the Uncertainty Analyses for the State-of-the-Art Reactor Consequence Analyses Project,” U.S. Nuclear Regulatory Commission, Washington, DC, October 2022.

Key Insights from the SOARCA UAs

- Importance varied based on plant design and study emphasis
  - Peach Bottom and Surry UAs → source to the environment
  - Sequoyah UA → containment response
- Post-SOARCA analysis identified the following important responses affecting the accident progression
  - Time in the fuel cycle
  - Valve failures
  - Consequential steam generator tube failure
  - Hydrogen behavior
  - Containment failure
  - Primary system pump leakage
  - Other insights

Time in the fuel cycle - inventory and decay heat

- Only included in the PWR UAs
  - Non-uniform impact on the radionuclide inventory

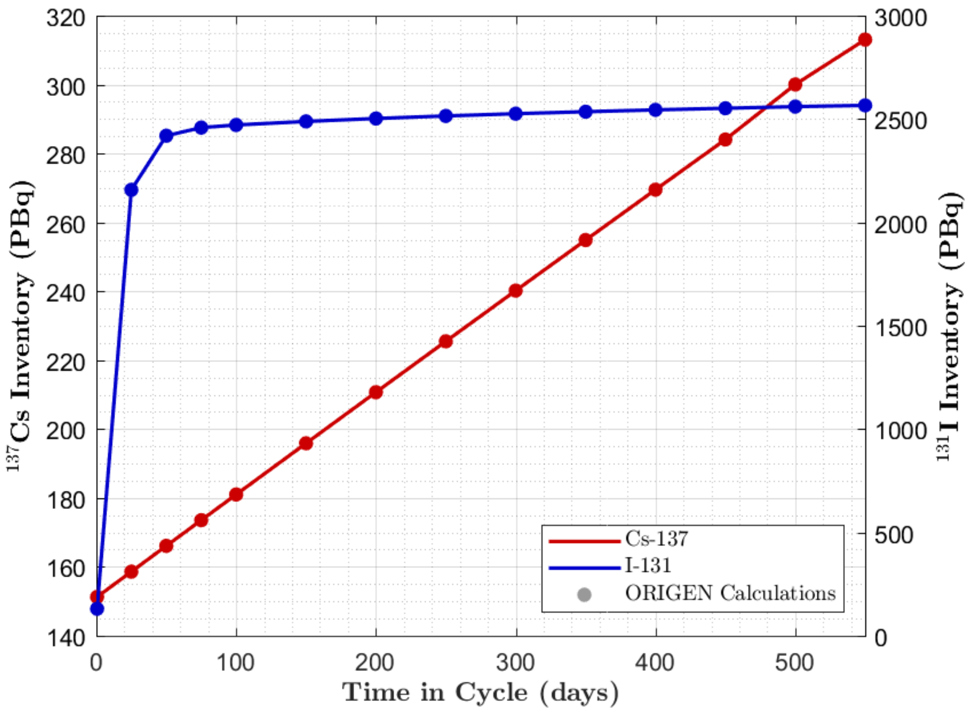

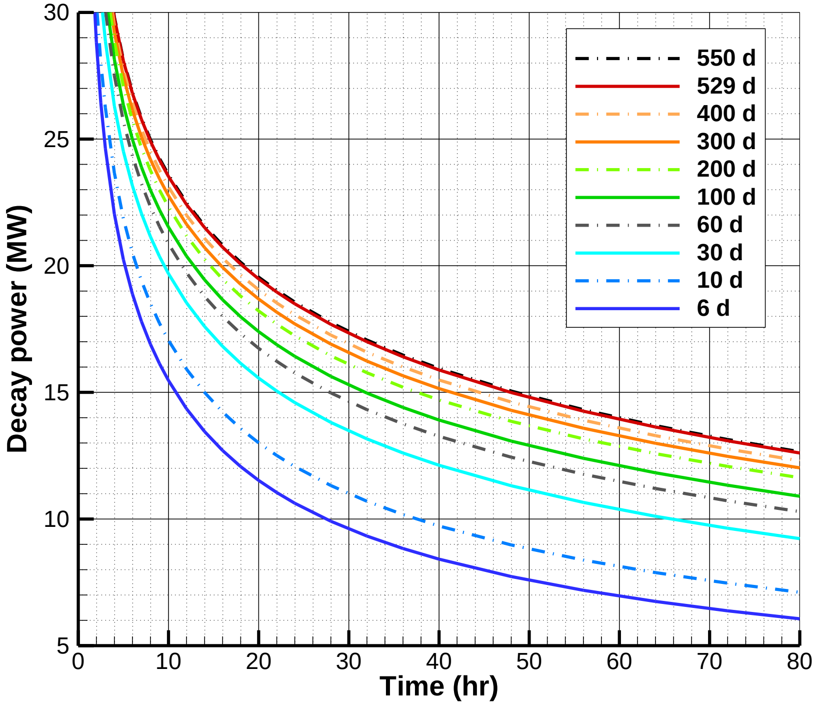

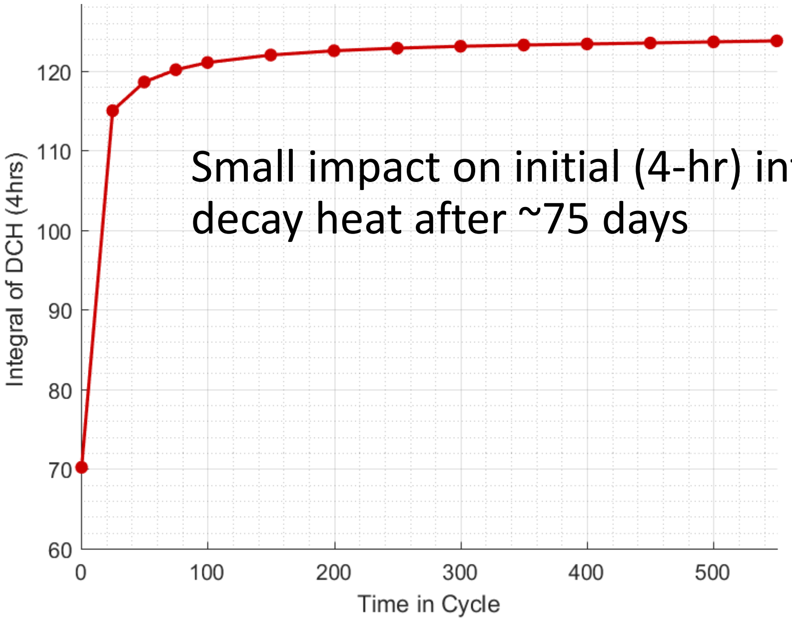

Small impact on initial (4-hr) integrated decay heat after ~75 days

Time in the fuel cycle – hot leg failure and in-vessel H_2 insights

- Earliest time in the fuel cycle had substantially delayed hot leg failure

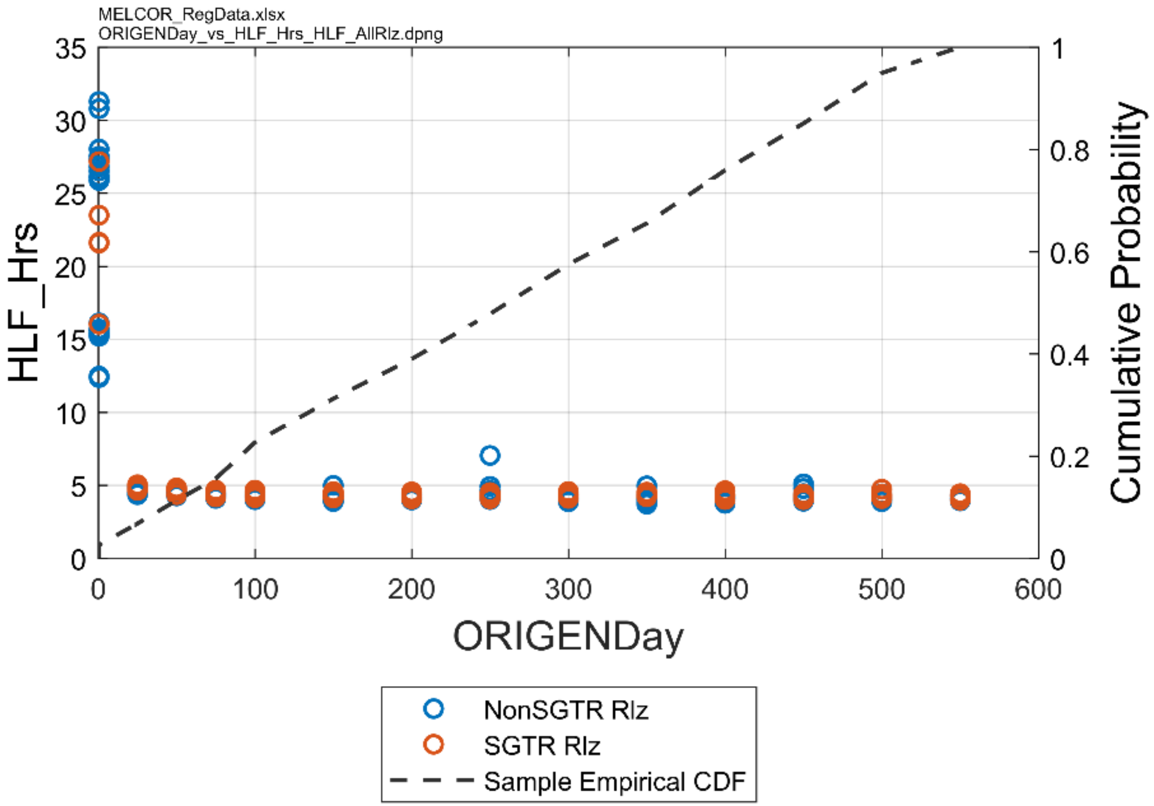

- Earliest time in the fuel cycle had substantially later & higher in-vessel hydrogen production

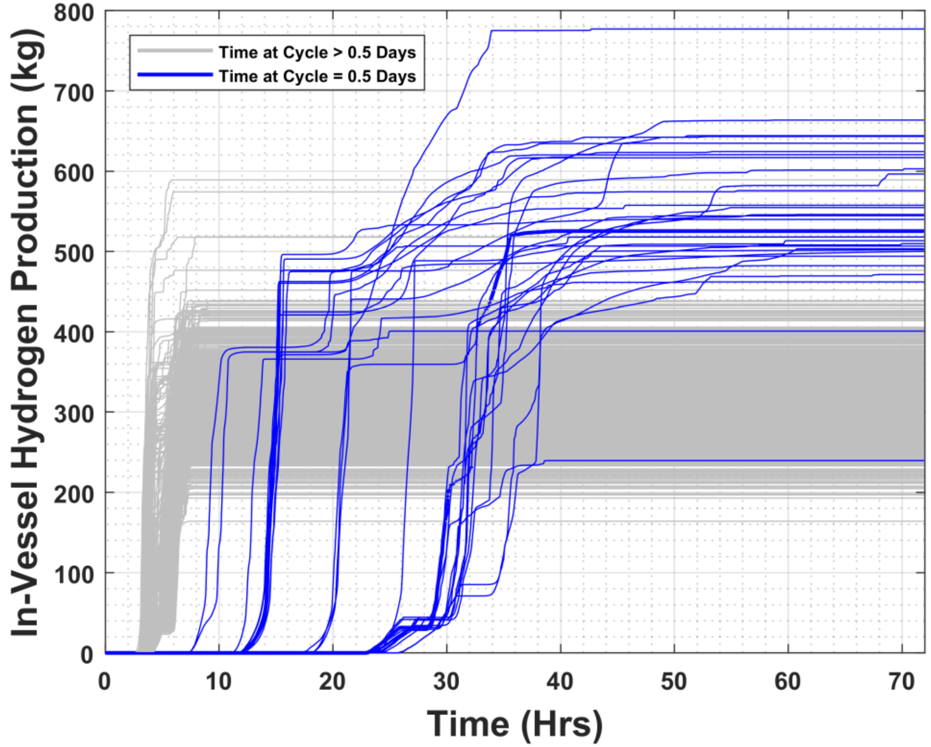

Time in the fuel cycle – containment failure insights

- Earliest time in the fuel cycle did not progress to containment failure in <72 hr (no LHF) in Surry UA

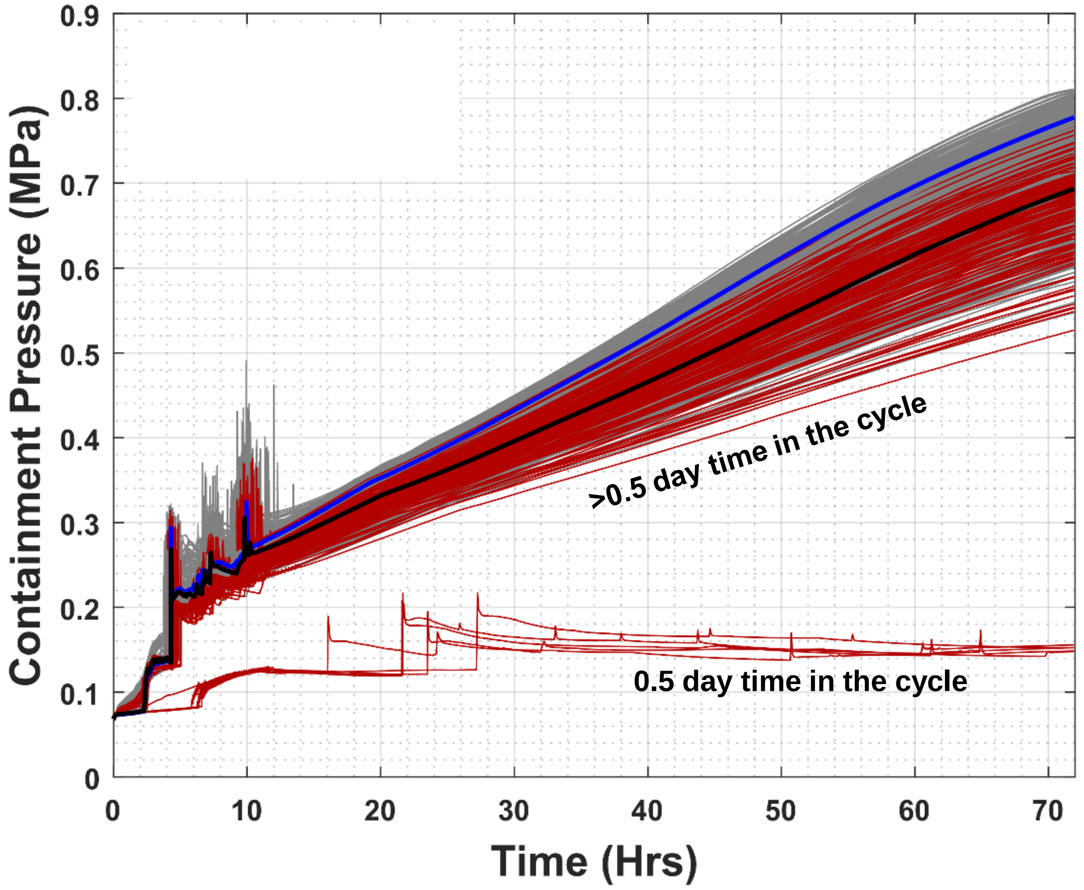

- Similar impact in the Sequoyah ice condenser UA

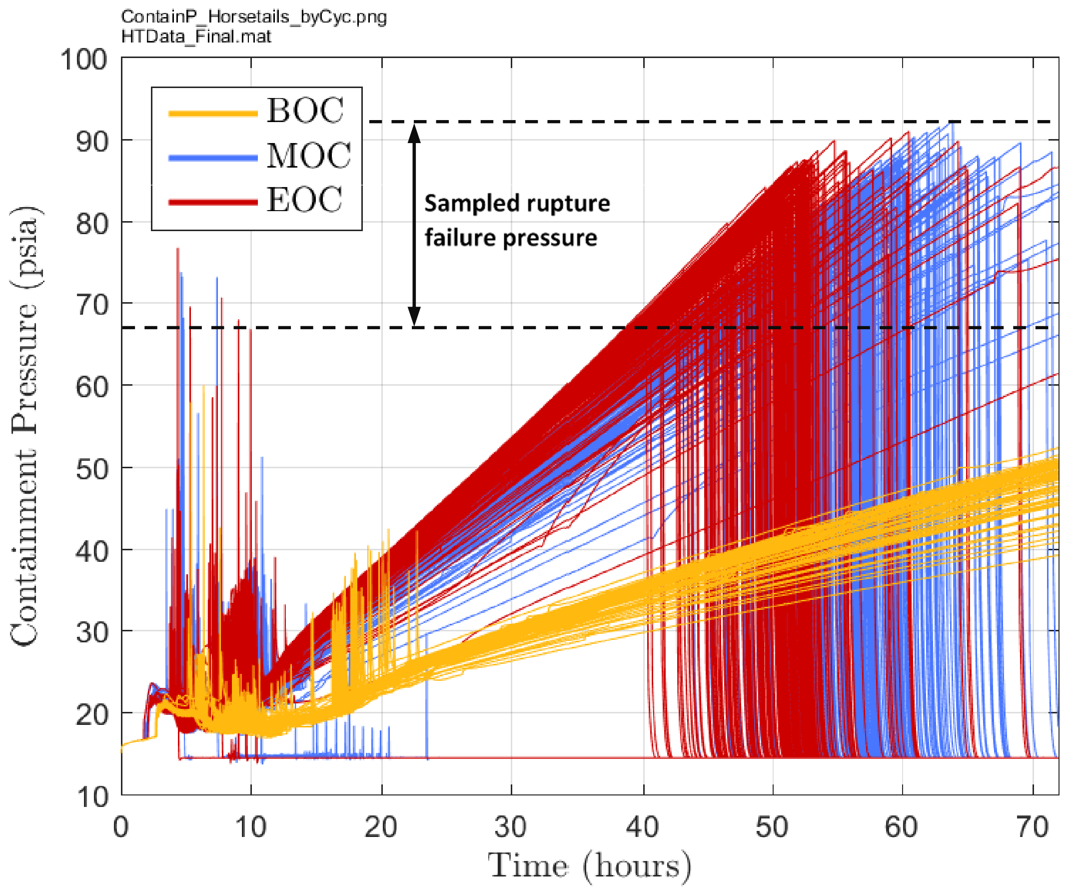

Time in the fuel cycle – environmental source term insights

- Generally upward trend in iodine release to the environment (i.e., includes some gaseous component)
- Generally upward trend in cesium release to the environment (i.e., also impacted by 72 hr simulation and CF timing)

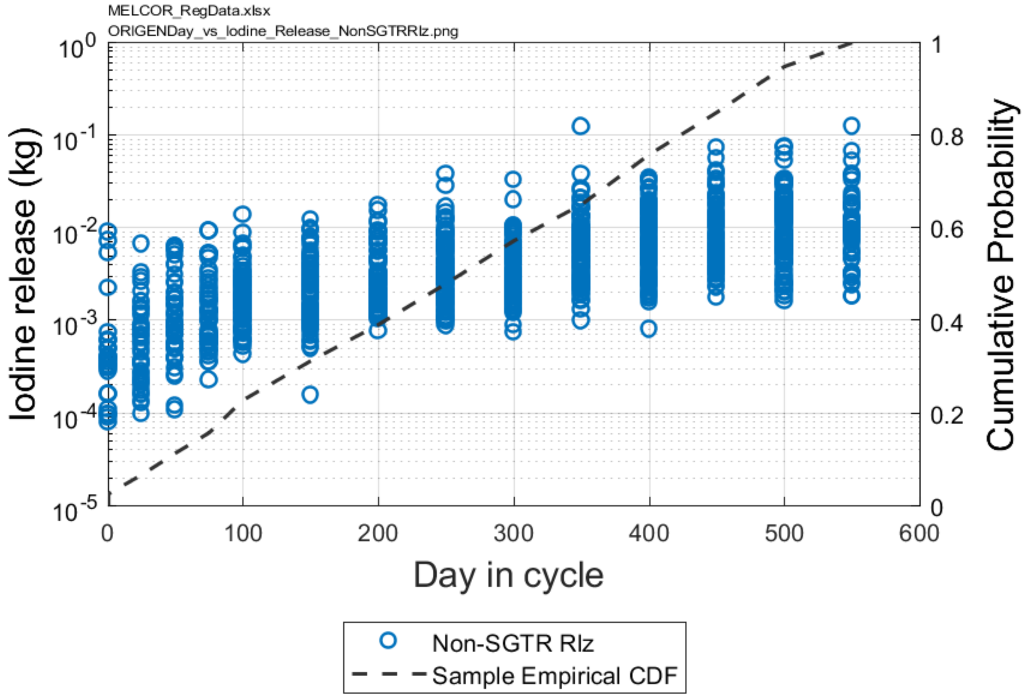

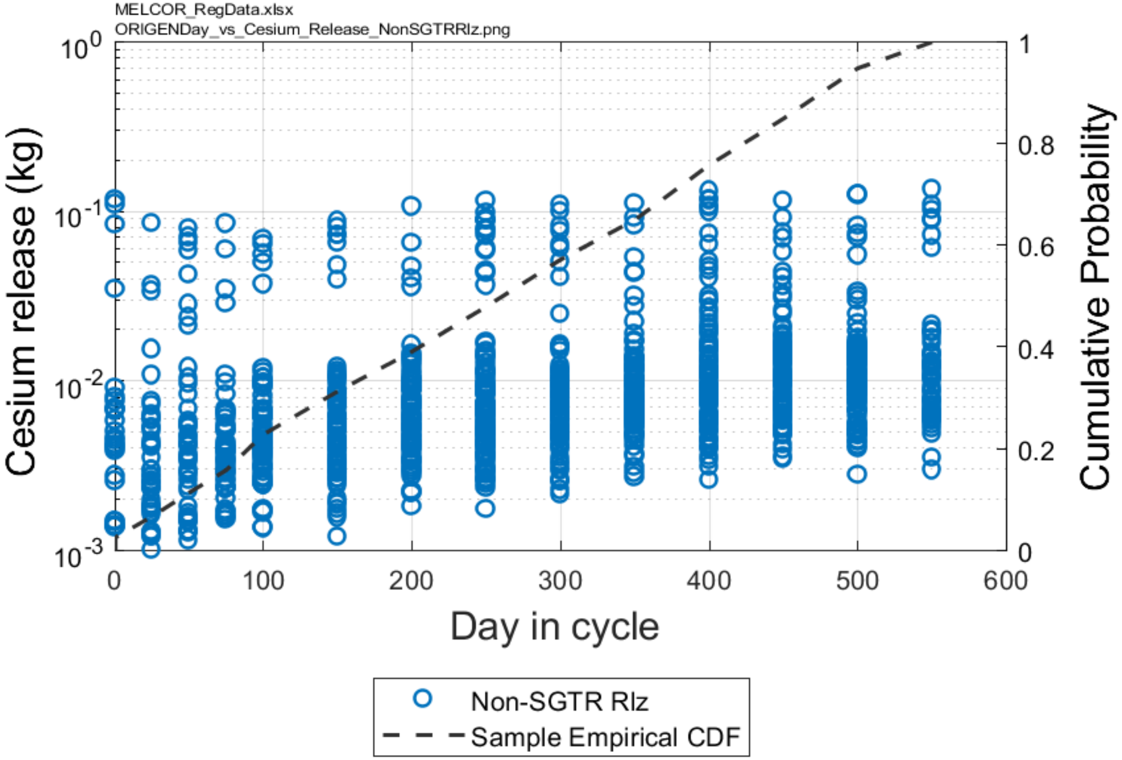

Valve failure methodology – PWRs

- Important and highly uncertain – few data for SV failure
- Research reviewed each US occurrence (licensing event report), contacting nuclear valve testing personnel, and a review of NUREG/CR-7037
  - SV FTC is most likely on the initial demand
  - If an SV functioned per design on the initial demand, then it would most likely function on all subsequent demands
  - SVs that fail to close are most likely to fail in either a weeping (i.e., mostly closed) or a mostly open position.
  - The probability per demand of a valve to fail to open (FTO) is sufficiently small compared to the FTC such that FTO may be neglected.
  - A valve is more likely to fail if cold water flows through the valve than if saturated water flows through the valve.
  - Applying MSL SV operational data to pressurizer SVs was judged acceptable due to the lack of pressurizer SV operational data.

Valve failure uncertainty distributions – PWRs

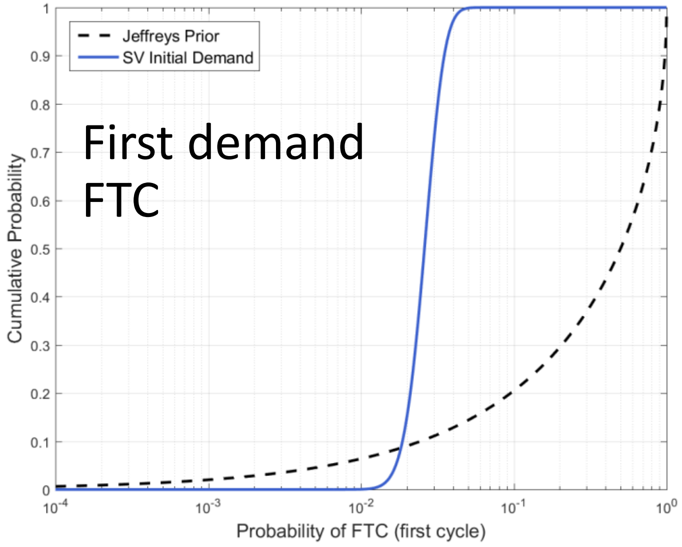

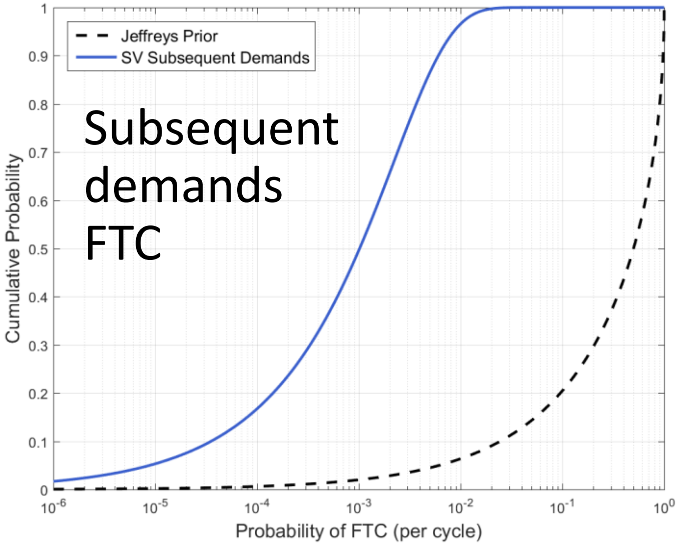

- Each pressurizer SV and SG MSS SV is sampled separately

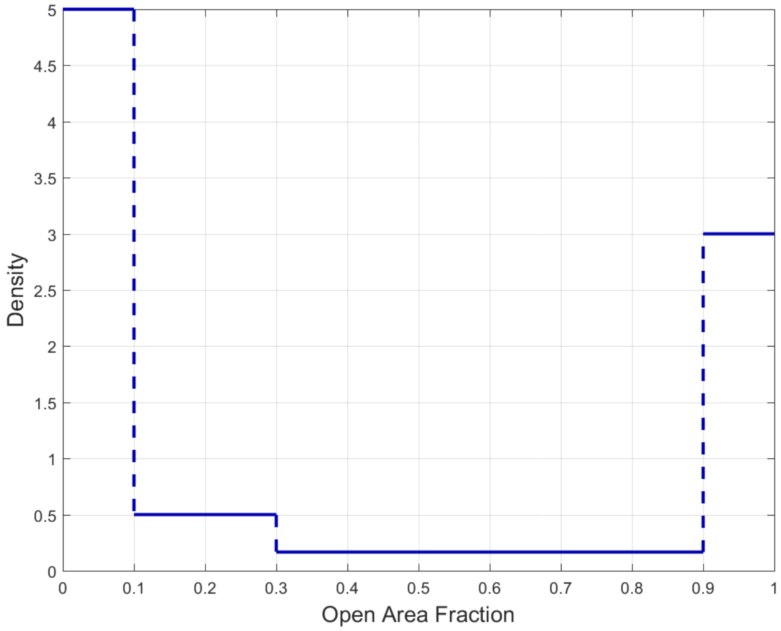

Failure fraction

Valve failure methodology - additional considerations

- MSIV leakage can impact SG MSS SV cycling
- PWR MSIVs do not have tech specs like BWRs
  - PWR MSIV LERs reviewed for insights
  - Uniform distribution from 0.01 in^2 to 1 in^2
  - BWR tech spec is 11.5 scfm (< 0.01 in^2)
  - MSIV leakage impacts SG MSS SV demands

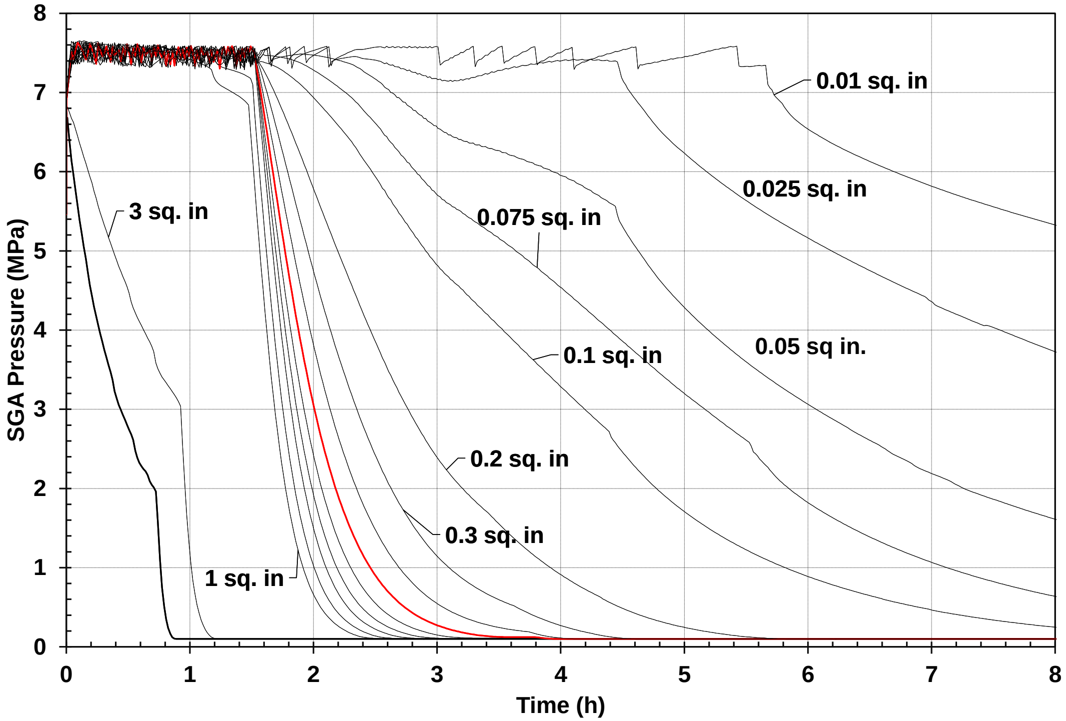

- Impact on the accident progression
  - SG MSS SV failure or MSIV leakage
    - Increased mechanical stress for C-SGTF
  - Pressurizer SV failure
    - Reduced stress for hot leg failure
    - Increased inventory discharged to the pressurizer relief tank
- Surry UA results - MSS SV failures occurred in 10% of the UA realizations on each SG

Pressurizer valve failure – Insights

- Pressurizer SV cycled ~70 times before hot leg failure (small variation with time-in cycle)
  - C-SGTF only occurred with no failures or small failure areas (<0.1)
  - Most tube ruptures occurred with >50 cycles
- Large SV failure area delayed or prevented hot leg failure
- Small SV failure area accelerated hot leg failure
- Fail to open of all pressurizer SVs examined as a sensitivity study →
  - Pump seal failure (480 gpm) x 3 loops

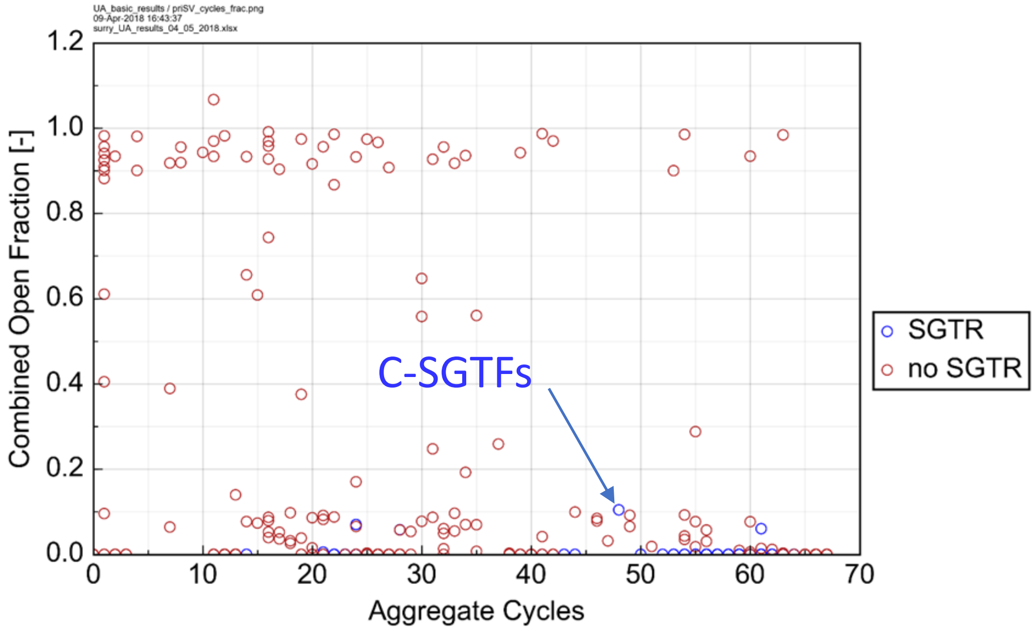

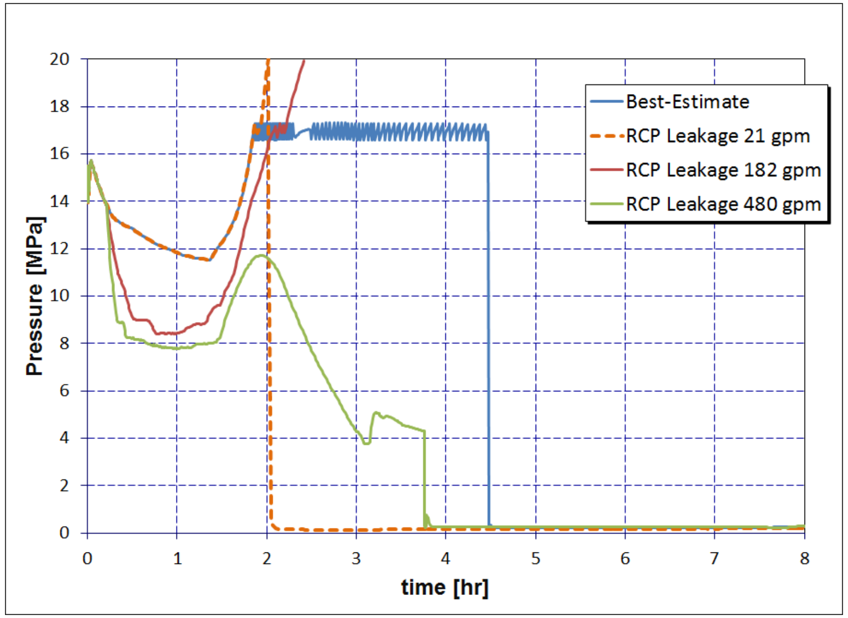

Pressurizer valve failure – Insights

- 54 of 56 SV failure cases with area fraction >0.36 led to boiloff and dryout of the pressurizer relief tank (PRT) –
  - Dryout and revaporization source term
  - Revaporization dependent on chemical form
  - Occurred before containment failure (time for settling)

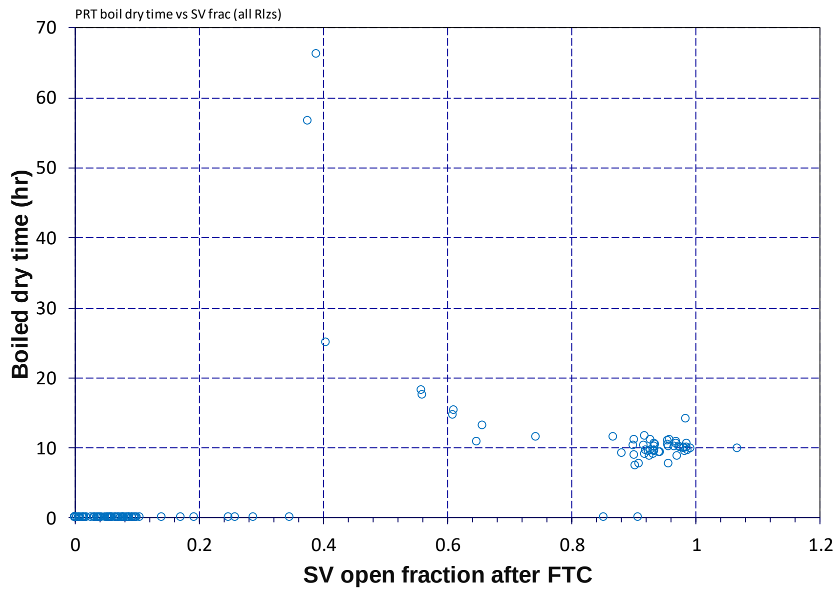

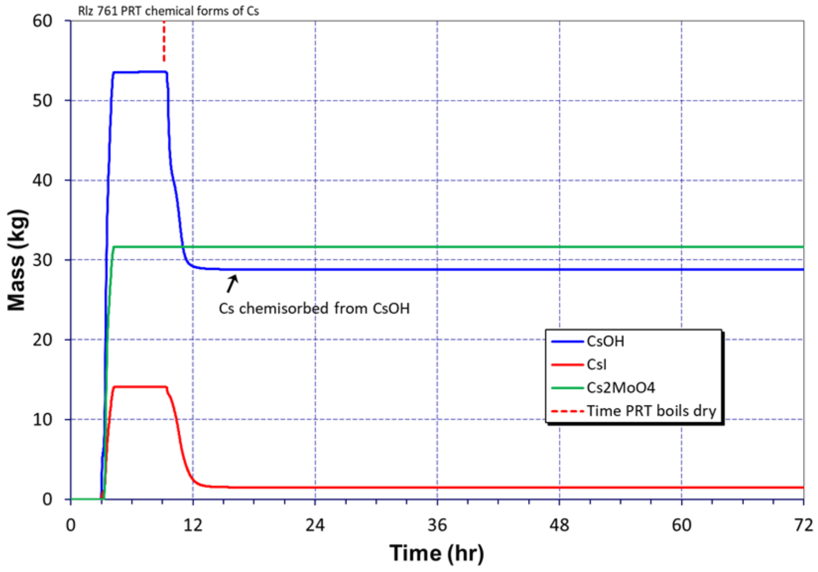

Pressurizer relief tank (PRT) modeling

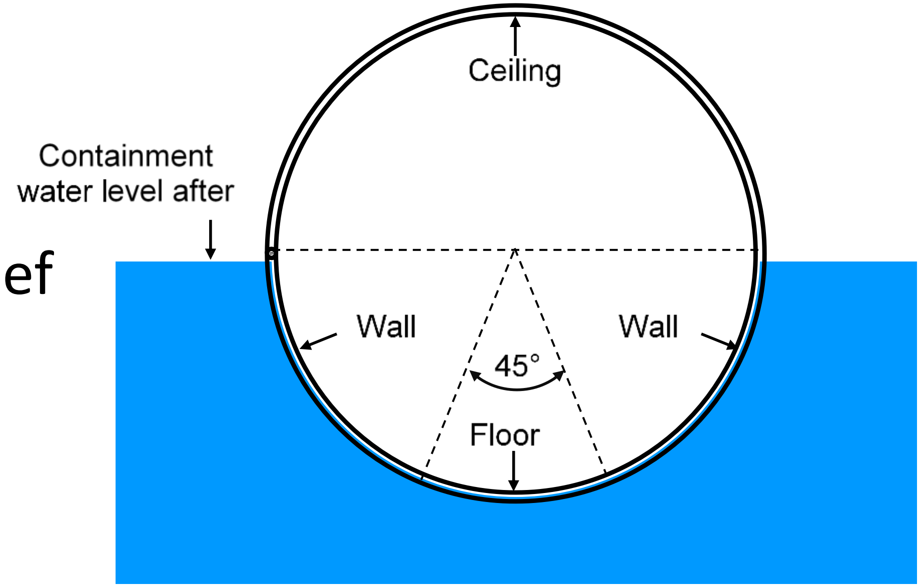

Valve failure methodology – BWR results

- BWR SRVs results showed 3 distinct accident progressions
  - ~50% had a stochastic failure prior to core damage
  - ~33% had a thermal failure without a MSL failure
  - ~17% had a thermal failure with a MSL failure
- MSL failure leads to fastest accident progression
  - Earlier vessel dryout and vessel failure
  - Earlier drywell liner melt-through
  - Largest environmental source term
    - Bypasses torus scrubbing

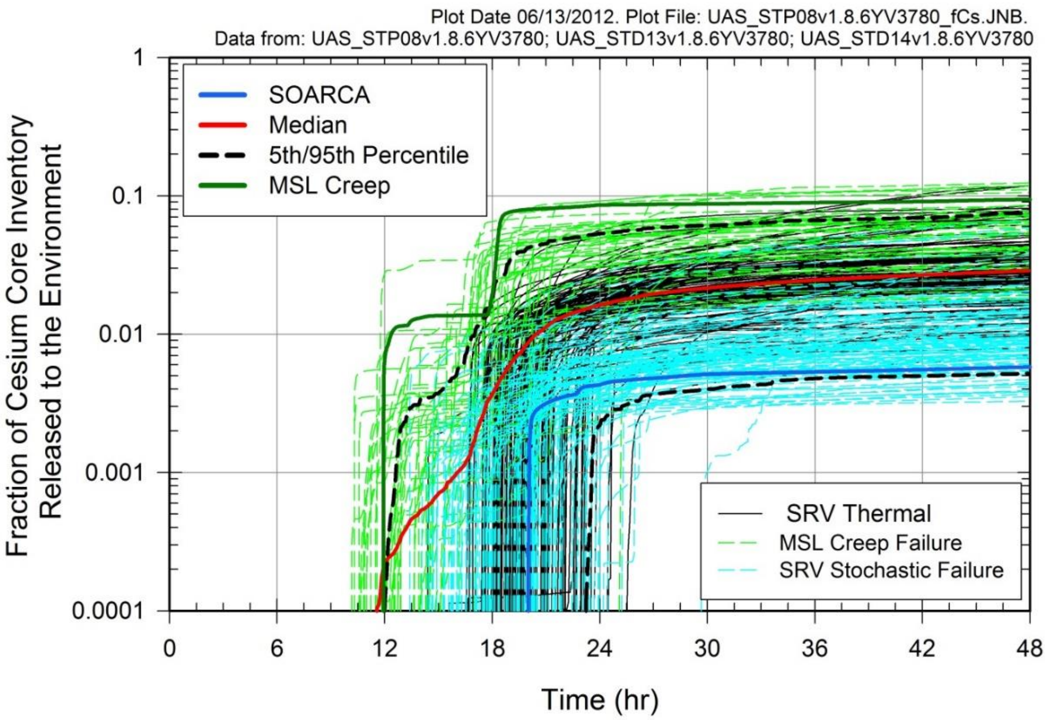

Valve failure methodology – Peach Bottom (BWR) UA

- Large impact on accident progression, MSL failure, and magnitude of the source term
  - SRV stochastic failure to reclose (SRVLAM) - Beta distribution fit to mean value in Peach Bottom IPE (the SOARCA value) using the methodology in NUREG/CR-7037
  - SRV thermal seizure criterion (temperature) (SRVFAILT)
  - SRV open fraction given thermal seizure (SRVOAFRAC)

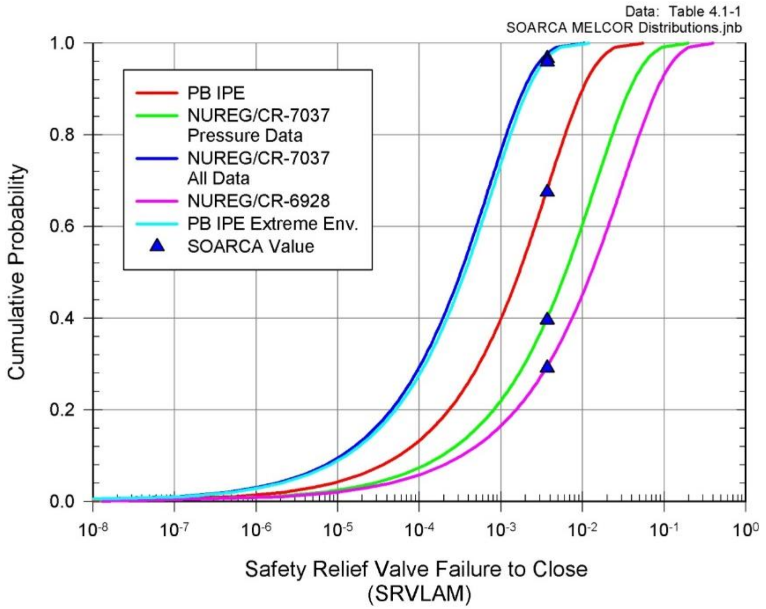

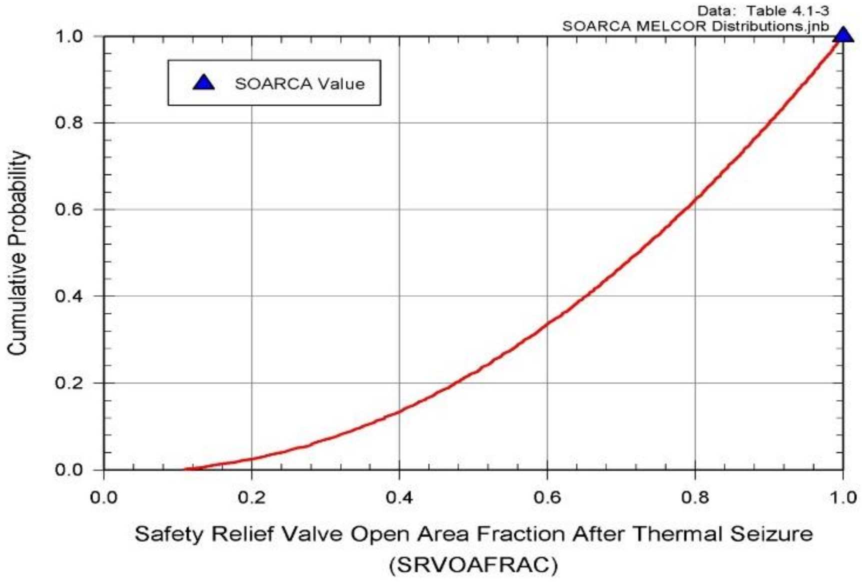

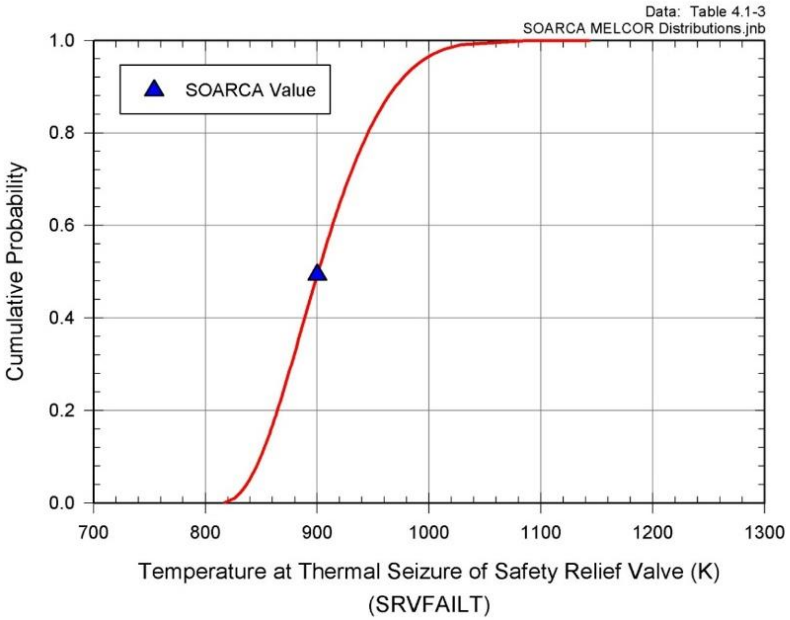

Consequential steam generator tube failure methodology

- C-SGTF monitored in 12 locations
  - Hottest tube model with a sampled flaw
  - Hot tube in SG with a sampled flaw
  - Average tube in SG with a sampled flaw
  - Average tube in SG without a flaw
- Hottest plume temperature uncertainty distribution determined from CFD calculations [NUREG-1922]
  - CFD results quantified plume variability

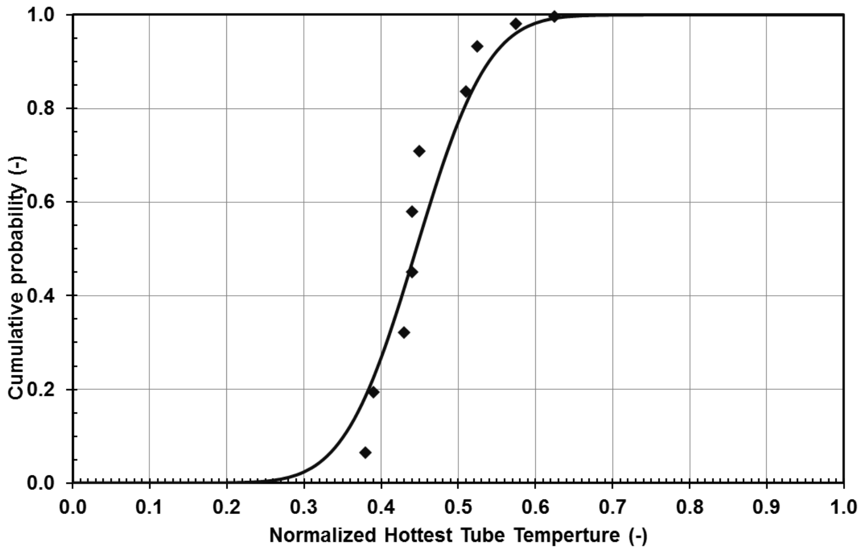

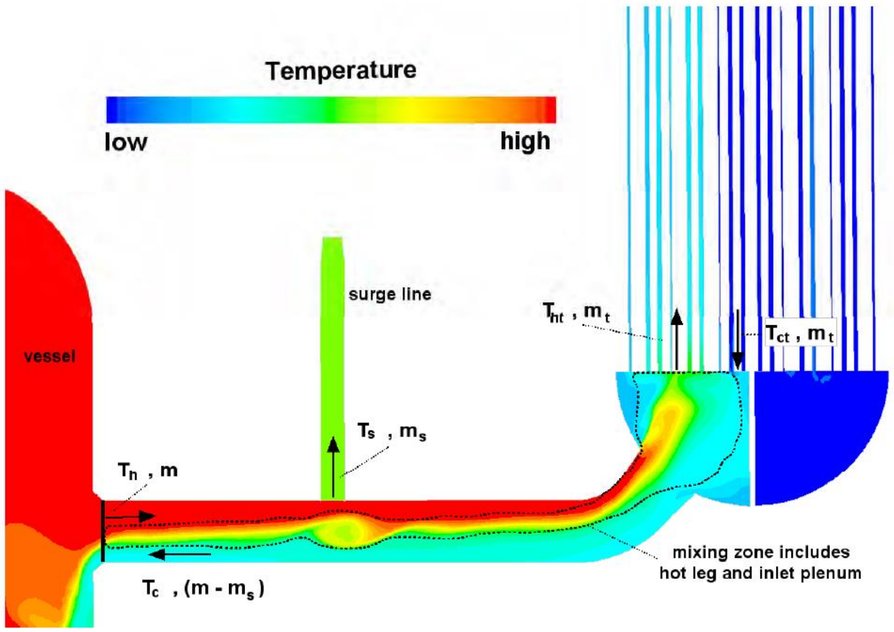

$$T_n = \frac{T_{ht} - T_{ct}}{T_h - T_{ct}}$$

T_n	Normalized hot tube temperature
T_{ht}	Hottest tube temperature
T_h	Hot leg hot stream temperature
T_{ct}	Cold tube temperature

Consequential steam generator tube failure methodology

- SG flaw distribution primarily determined from two sources
  - NUREG-2195
  - Surry Units 1 & 2 in-service inspection reports from 1980 to 2013
  - 76 flawed tubes required replacement (loose parts, anti-vibration bar wear, lancing equipment damage from historical sludge issue)
  - 70% on the SG inlet side & 61% below the first grid
  - Currently, 100% inspection per 2 outages
  - Only flaws >0.3 (NUREG/CR-6995) have the potential for a C-SGTF (stress multiplier >1.4)
- Flaw distribution is hybrid of all Inconel tube SGs for flaw depths <0.5 and Surry ISI data for flaw depths >0.5
  - Generic + plant-specific match for estimated number for flaws >0.5
  - Much more generic data for flaws <0.5
  - Overall 4.26 tubes >0.3 but only 0.15 tubes >0.5 between inspections
  - Distribution considers hottest (3%), hot (22%), and cold (75%) zones

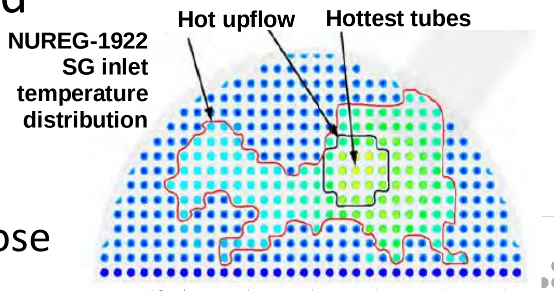

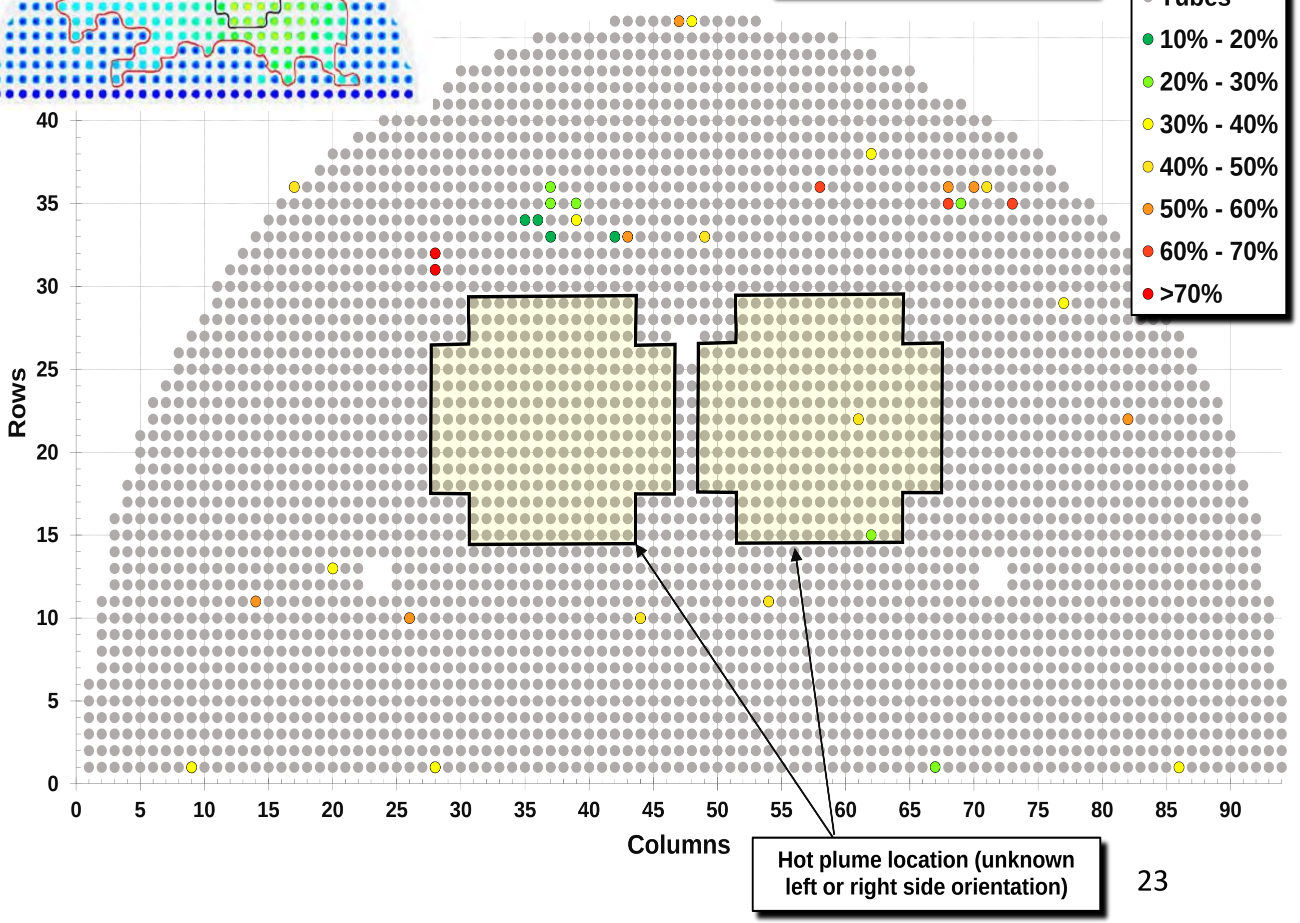

Consequential steam generator tube failure methodology

- For each realization, five flaw samples are randomly selected
  - The maximum of three of the samples are used for the cold region flaw depth as only the most severely flawed tube in this region will be modeled
  - One sample will be used for the upflow region
  - The fifth flaw sample will be used for the hot zone flaw
    - The cumulative flaw distribution for the hot region is specified so that the sampled flaw is used 14% of the time because there is no flaw 86% of the time in this small region

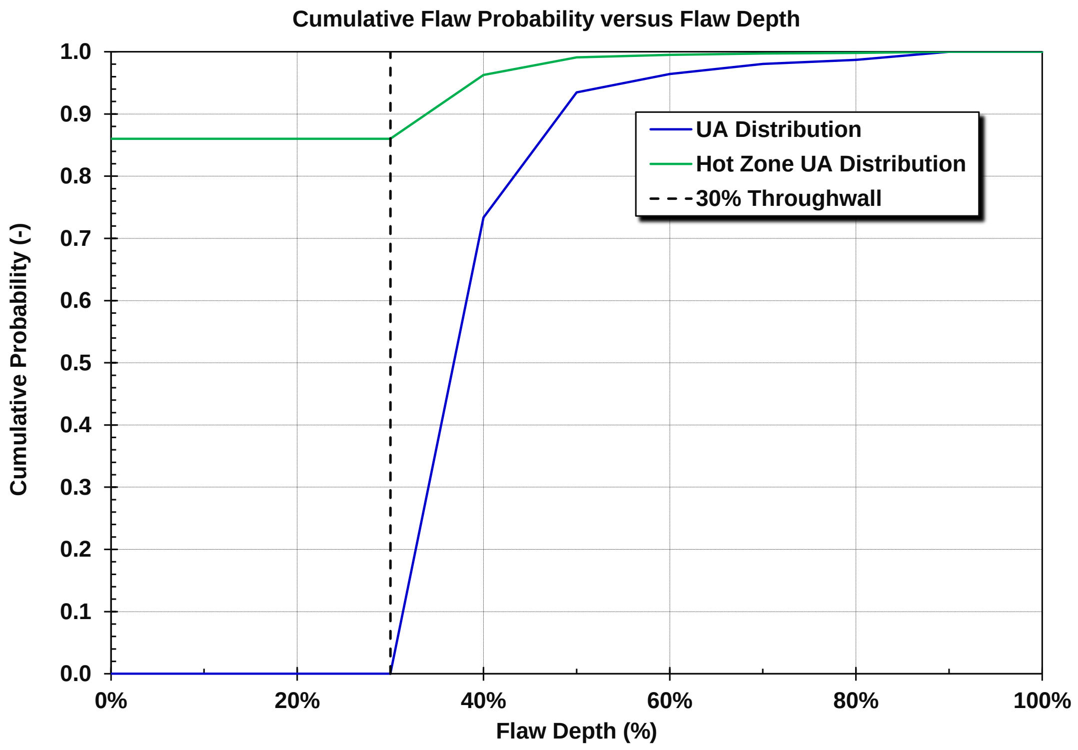

Consequential steam generator tube failure results

- C-SGTF occurred in 12.5% of the realizations (144 realizations)
- Always included a hot leg rupture
- C-SGTF more likely if
  - Flaw >0.8 m in the cold flow region
  - Flaw >0.68 in hot upflow region

Surry UA Creep Damage to the Hottest Steam Generator Tubes

	Rank Regression		Quadratic		Recursive Partitioning		MARS		Main Contribution	Conjoint Contribution
Final R^2	0.63		0.90		0.78		0.97			
Input	R^2 contr.	SRRC	S_i	T_i	S_i	T_i	S_i	T_i		
tubeHotA_NFD	0.18	0.75	0.50	0.72	0.81	0.98	0.11	0.99	0.341	0.395
ThotA_norm	0.19	0.42	0.02	0.22	0.03	0.21	0.00	0.05	0.057	0.126
msiv_leak_a	0.14	0.39	0.01	0.04	0.00	0.02	0.00	0.20	0.037	0.078
priSVcyc	0.06	0.41	0.00	0.10	0.01	0.00	0.00	0.52	0.018	0.195
RCP_Leak	0.03	-0.23	0.01	0.17	---	---	0.00	0.00	0.010	0.050
secSVfrac1	0.02	0.28	---	---	---	---	0.00	0.02	0.005	0.005
priSVfrac	0.01	-0.19	0.00	0.06	---	---	0.01	0.00	0.004	0.018
Zr_brkout_T	---	---	0.00	0.00	---	---	0.01	0.06	0.004	0.015
secSVcyc1	---	---	0.01	0.04	0.01	0.03	0.00	0.00	0.004	0.016

** highlighted if main contribution larger than 0.02 or conjoint contribution larger than 0.1*

- C-SGTF more likely in the hottest region if
  - Flaw >0.42
  - Flaw >0.31 and peak hot plume temperature (T_n) was > 0.48

$$T_n = \frac{T_{ht} - T_{ct}}{T_h - T_{ct}}$$

Back-up with regression explanations

Surry UA Creep Damage to the Hottest Steam Generator Tubes

	Rank Regression		Quadratic		Recursive Partitioning		MARS		Main Contribution	Conjoint Contribution
Final R^2	0.63		0.90		0.78		0.97			
Input	R^2 contr.	SRRC	S_i	T_i	S_i	T_i	S_i	T_i		
tubeHotA_NFD	0.18	0.75	0.50	0.72	0.81	0.98	0.11	0.99	0.341	0.395
ThotA_norm	0.19	0.42	0.02	0.22	0.03	0.21	0.00	0.05	0.057	0.126
msiv_leak_a	0.14	0.39	0.01	0.04	0.00	0.02	0.00	0.20	0.037	0.078
priSVcyc	0.06	0.41	0.00	0.10	0.01	0.00	0.00	0.52	0.018	0.195
RCP_Leak	0.03	-0.23	0.01	0.17	---	---	0.00	0.00	0.010	0.050
secSVfrac1	0.02	0.28	---	---	---	---	0.00	0.02	0.005	0.005
priSVfrac	0.01	-0.19	0.00	0.06	---	---	0.01	0.00	0.004	0.018
Zr_brkout_T	---	---	0.00	0.00	---	---	0.01	0.06	0.004	0.015
secSVcyc1	---	---	0.01	0.04	0.01	0.03	0.00	0.00	0.004	0.016

** highlighted if main contribution larger than 0.02 or conjoint contribution larger than 0.1*

- R^2 = total explained variance
- R^2contr = incremental variance attributable to a variable by itself (sum to R^2)
- SRRC = relative strength and direction of a variable's influence
- S_i = analogous to R^2contr but only relative (don't sum to R^2)
- T_i = S_i + contribution conjoint with other variables
- Main contribution = relative influence of a variable by itself all methods considered
- Conjoint contribution = relative influence of a variable conjoint with other variables all methods considered
- Meaningful influences highlighted yellow

Consequential steam generator tube failure – source term

- Detailed insights from the C-SGTF reference case
  - No over cycling FTC SV occurred on any of the SGs
  - No over cycling FTC occurred on the pressurizer SV
  - No reactor coolant pump seal failures, which is the most likely outcome from the uncertainty distribution.
  - The hot leg nozzle rupture occurred on Loop C where the pressurizer surge line connects. Loop C heated faster due to the cycling pressurizer SV, which led to the preferential failure on this loop.
  - Hydrogen deflagrations occurred in containment after the hot leg failure, but they did not pose a significant over pressure challenge to the containment boundary.
  - The containment design pressure and the pressure associated with liner yield were both exceeded. However, the containment pressure was below the rebar failure pressure at 72 hr, which is the most likely outcome at 72 hr.
  - Although the containment pressure associated with rebar yield was not reached by 72 hr, the pressure was expected to exceed this value shortly thereafter.
  - The largest contributor to containment pressurization was the continuous heating of RCS coolant recast as steam in the containment (rather than addition of non condensable gases to the atmosphere from core-concrete interaction [CCI]).
  - The C SGTF significantly increased the release to the environment. The reference realization without a C SGTF released 0.028% and 0.003% of the iodine and cesium inventory, respectively. However, the C SGTF reference realization released 1.42% and 0.92% of the iodine and cesium inventory, respectively.
  - The concrete ablation from CCI had not slowed by the end of the MELCOR calculation at 72 hr. The concrete erosion rate and non condensable gas generation was relatively constant after the start of the CCI

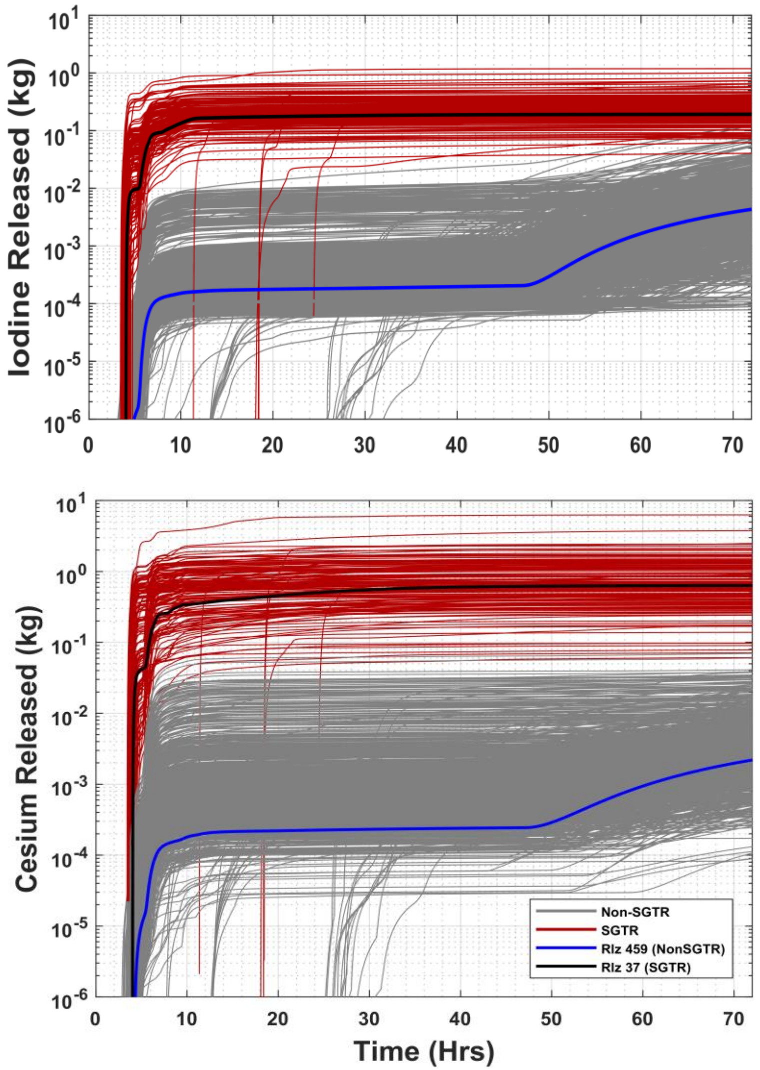

Consequential steam generator tube failure – source term

- Detailed insights from the C-SGTF reference case
  - Hot leg failure stops tube creep accumulation
  - C-SGTF leakage rate drops after hot leg failure
  - C-SGTF leakage is greater than containment leakage through 72 hr
  - Only 2.7% and 5% of the total Cs and I are released to environment <5 hr
  - 99.9% and 98.8% of the Cs and I to the environment go via the C-SGTF

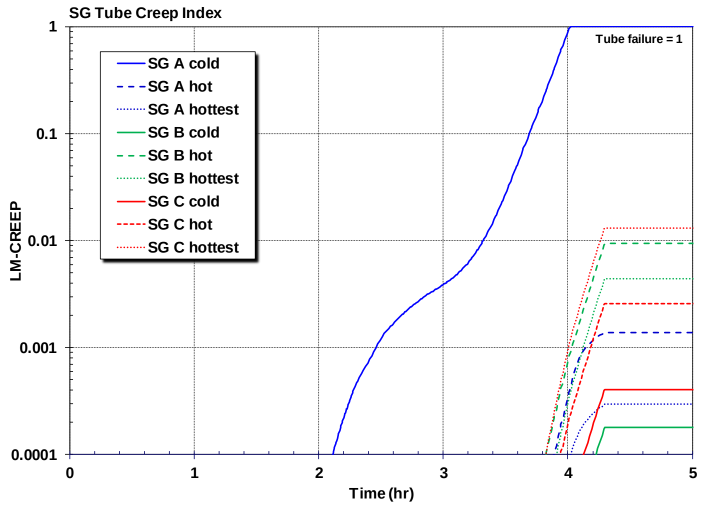

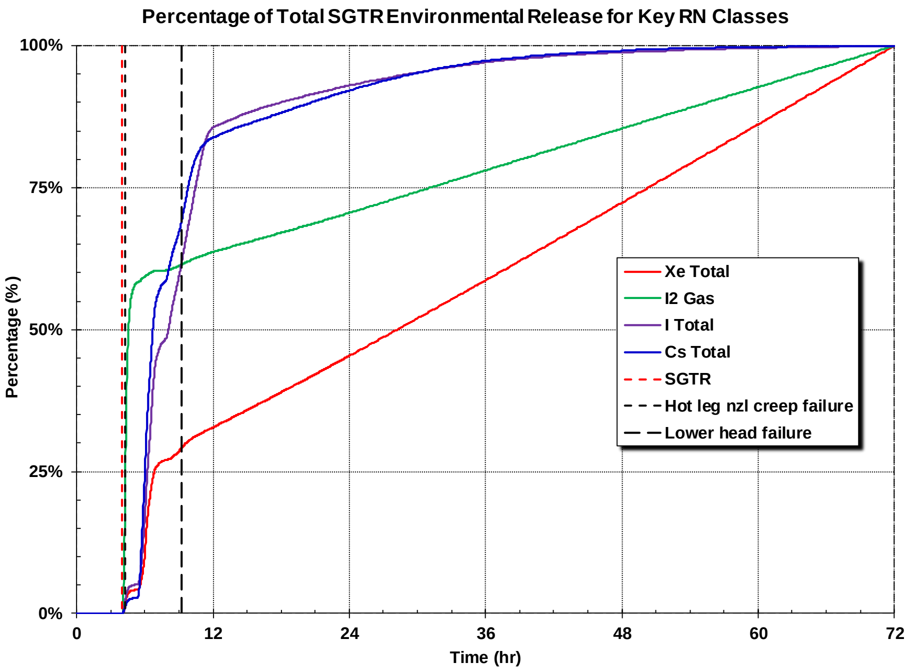

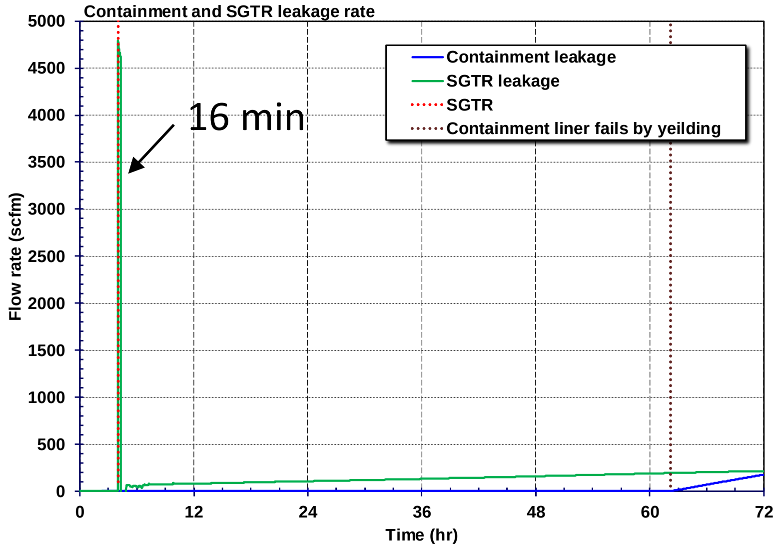

Consequential steam generator tube failure – source term

- Focused uncertainty study with multiple tube failures
  - Sampled a deep flaw in the hot plume region with other boundary conditions that ensured a C-SGTF (tube leakage area varied from 1 to 5 tubes)
  - The SG pressurized with >3 C-SGTFs and was controlled by MSIV leakage
  - 1 & 2 C-SGTFs have initial puff and gradual buildup during core degradation
  - >3 C-SGTF delayed hot leg failure and overwhelms natural circulation flows to unaffected SGs (preferentially sending radionuclides to the affected SG)

- Applicability to other PWRs
  - SG design
    - T_n ~ 0.43 for Westighouse Model 51 SG (Surry)
    - T_n ~ 0.95 for CE SG (shallow inlet plenum)

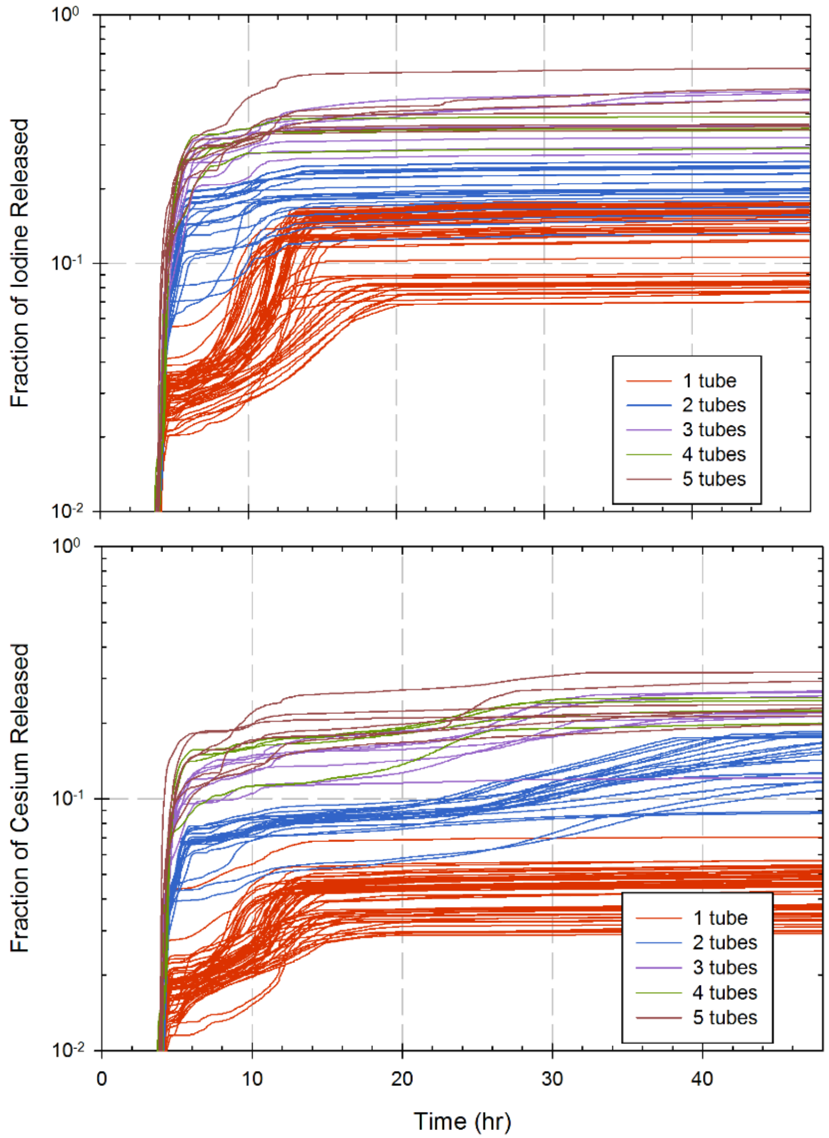

Hydrogen behavior – methodology

- Uncertain parameters used to explore hydrogen behavior and containment failure
- Sequoyah UA – focus on early containment failure
  - Low-design pressure, free-standing steel containment
  - Uncertain parameters
    - Oxidation kinetics correlation
    - Lower flammability limit for combustion
    - Containment rupture pressure
    - Barrier seal failure pressure and area
    - Ice chest open fraction
- Surry UA
  - Steel-reinforced concrete containment
  - Uncertain parameters
    - Oxidation kinetics correlation
    - Hydrogen ignition criteria
    - Containment fragility curve
    - Containment wall heat transfer rate

- Peach Bottom UA
  - Inerted BWR Mark I containment
  - Uncertain parameter
    - Reactor building hydrogen ignition criteria

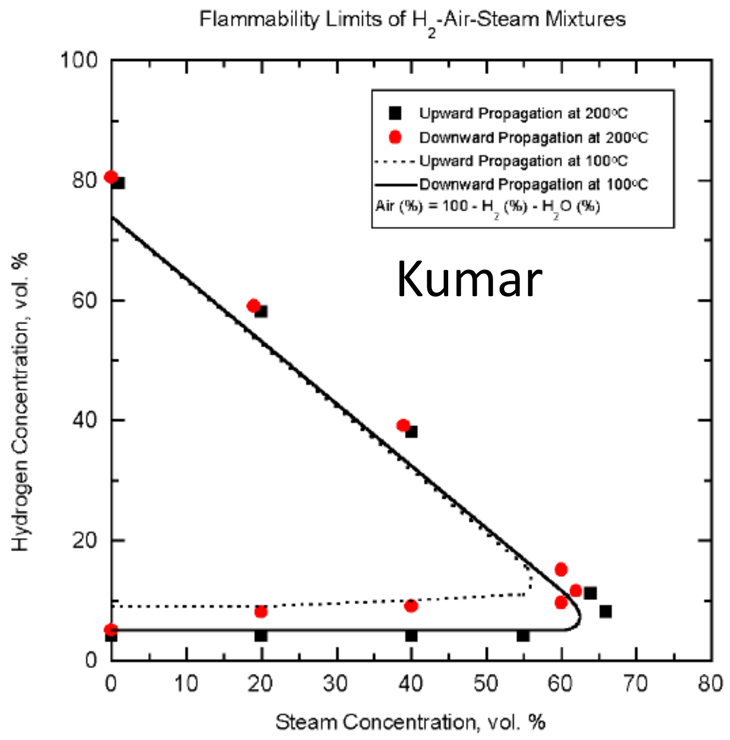

Hydrogen behavior – Surry UA results

- No hydrogen induced containment failure
  - Early burn with hot leg failure
    - Hot leg failure occurs early in the core degradation with limit hydrogen production
  - Steam generation from accumulator discharge into degrading core after HL failure led to steam inerting in the containment

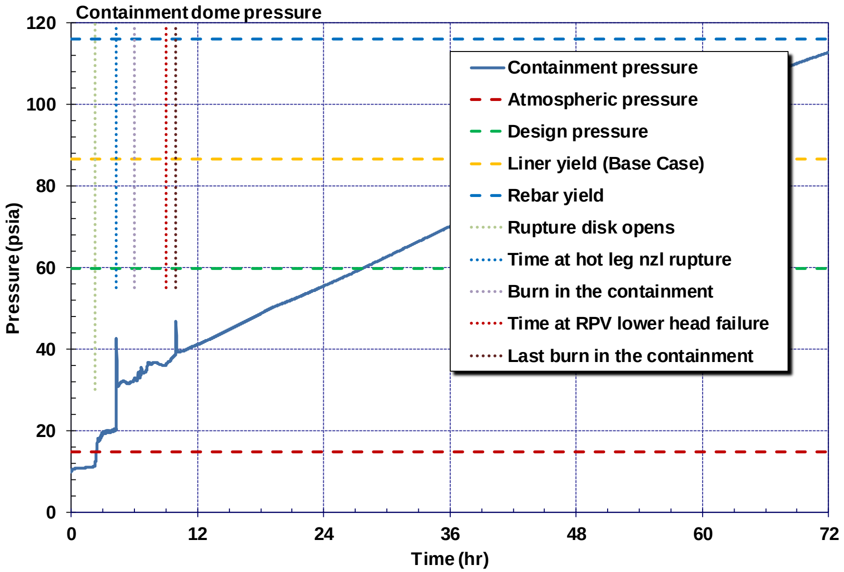

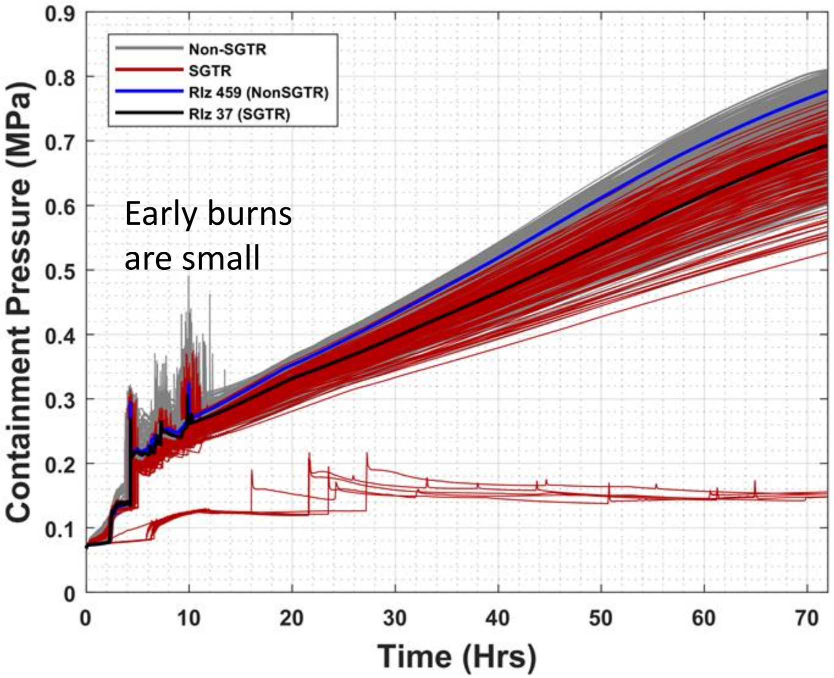

C-SGTF slows the containment pressurization

C-SGTF with new core shows no significant containment pressurization

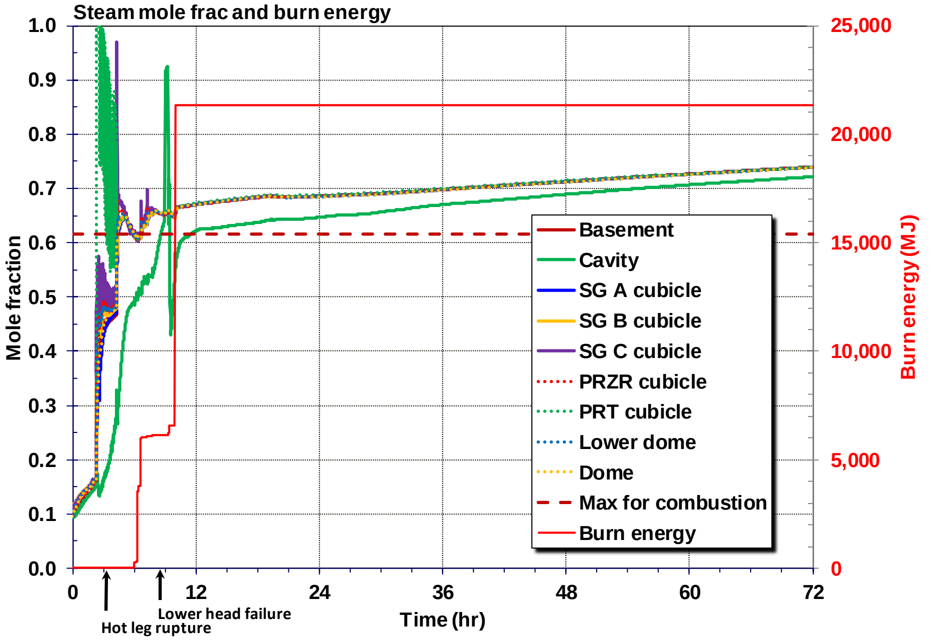

Hydrogen behavior – Sequoyah UA results

- More vulnerable to an early hydrogen induced containment failure (ice condenses the steam)
    - In-vessel hydrogen generation is ~300 kg
    - Ex-vessel hydrogen generation is ~1000 kg by 72 hr
- Only 4 realizations had an early containment failure
    - Requires specific & limited range of uncertain parameter values
    - Pressurizer SV FTC with <45 cycles and SV failure area > 0.3
    - Lower sampled containment failure pressure
    - Kinetics correlations with higher low temperature oxidation (Urbanic-Heidrich and Catchart-Pawel/Urbanic-Heidrich)
    - Small burns from CCI reduced oxygen concentration
    - Containment became oxygen-limited with steam and CCI pressurization
- Early pressurizer FTC (<45 cycles) had the highest with iodine releases and contributor to early containment failure
    - Pressurizer SV FTC with <45 cycles and SV failure area > 0.3
    - Focused UA study used to better understand uncertain parameter influence failure dynamics & confirmed importance of time in the cycle & in-vessel oxidation kinetics model

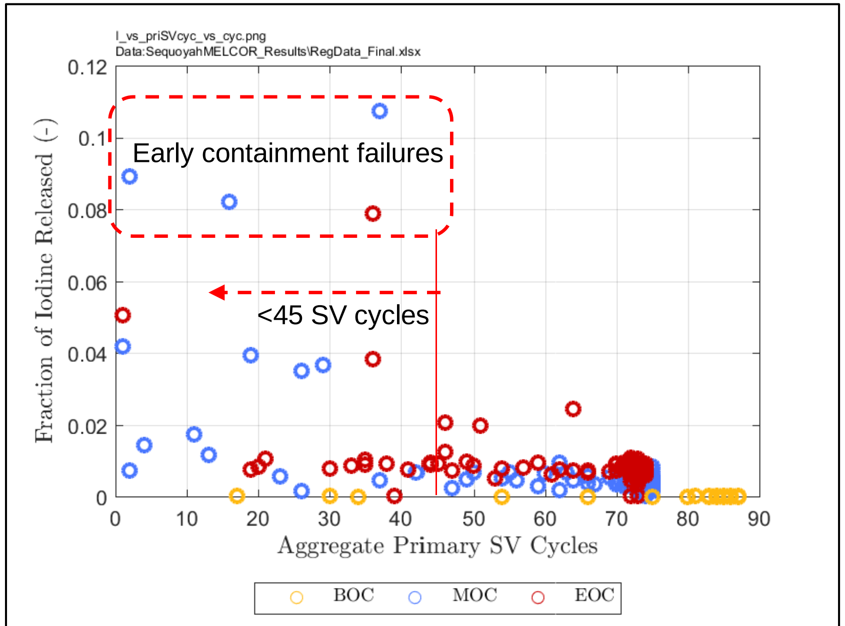

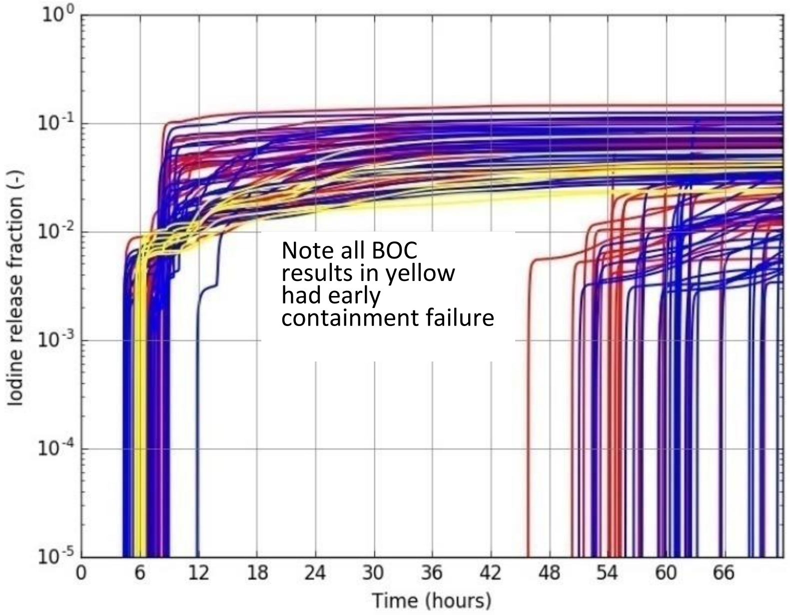

Hydrogen behavior – Surry UA results

- Some focused calculations of the Surry long-term station blackout (LTSBO) were performed
  - LTSBO initially has DC power and successful turbine-driven auxiliary feedwater until the batteries are exhausted
  - Much slower accident progression
- Delaying ignition until the first burn increases the peak pressure and containment failure likelihood
  - All calculations include a pressurizer FTC
  - **Green line** credits ignitors (Ignite hydrogen at a 7% concentration)
  - **Red line** assumes no ignitors but high temperature gases exiting the pressurizer relief tank is the first ignition source
  - **Blue line** assumes no ignitors but high temperature gases exiting the vessel following hot leg failure is the first ignition source
  - Confirms UA results of accumulation of hydrogen gas in the dome prior to the first burn

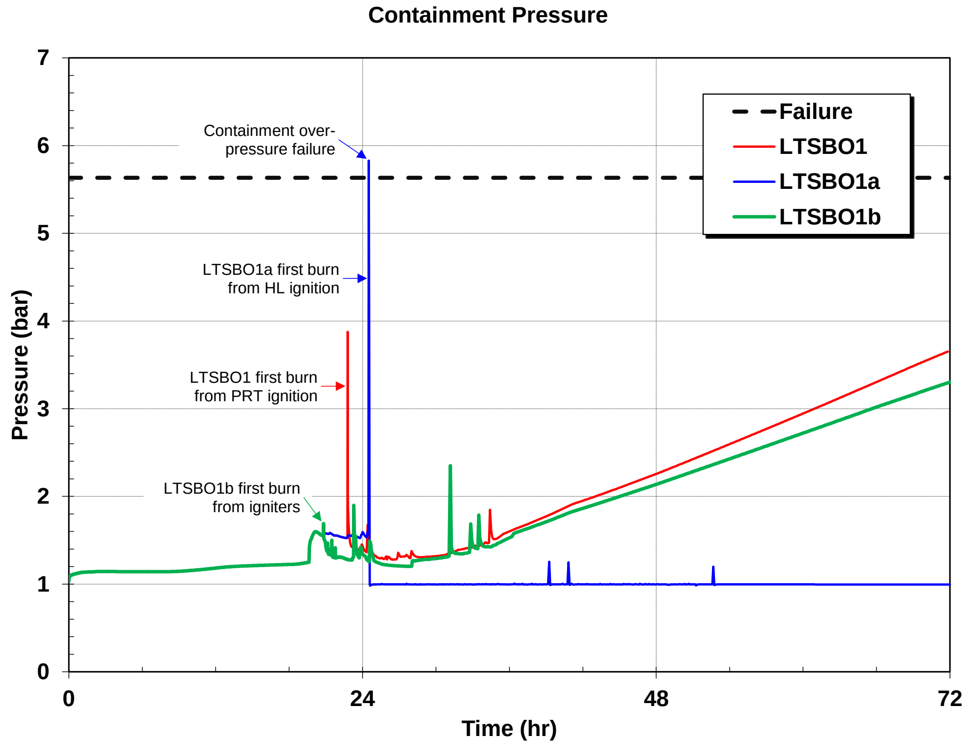

Hydrogen behavior – Fukushima Unit 1 results

Hydrogen behavior – Fukushima Unit 3 results

Hydrogen behavior – Fukushima results

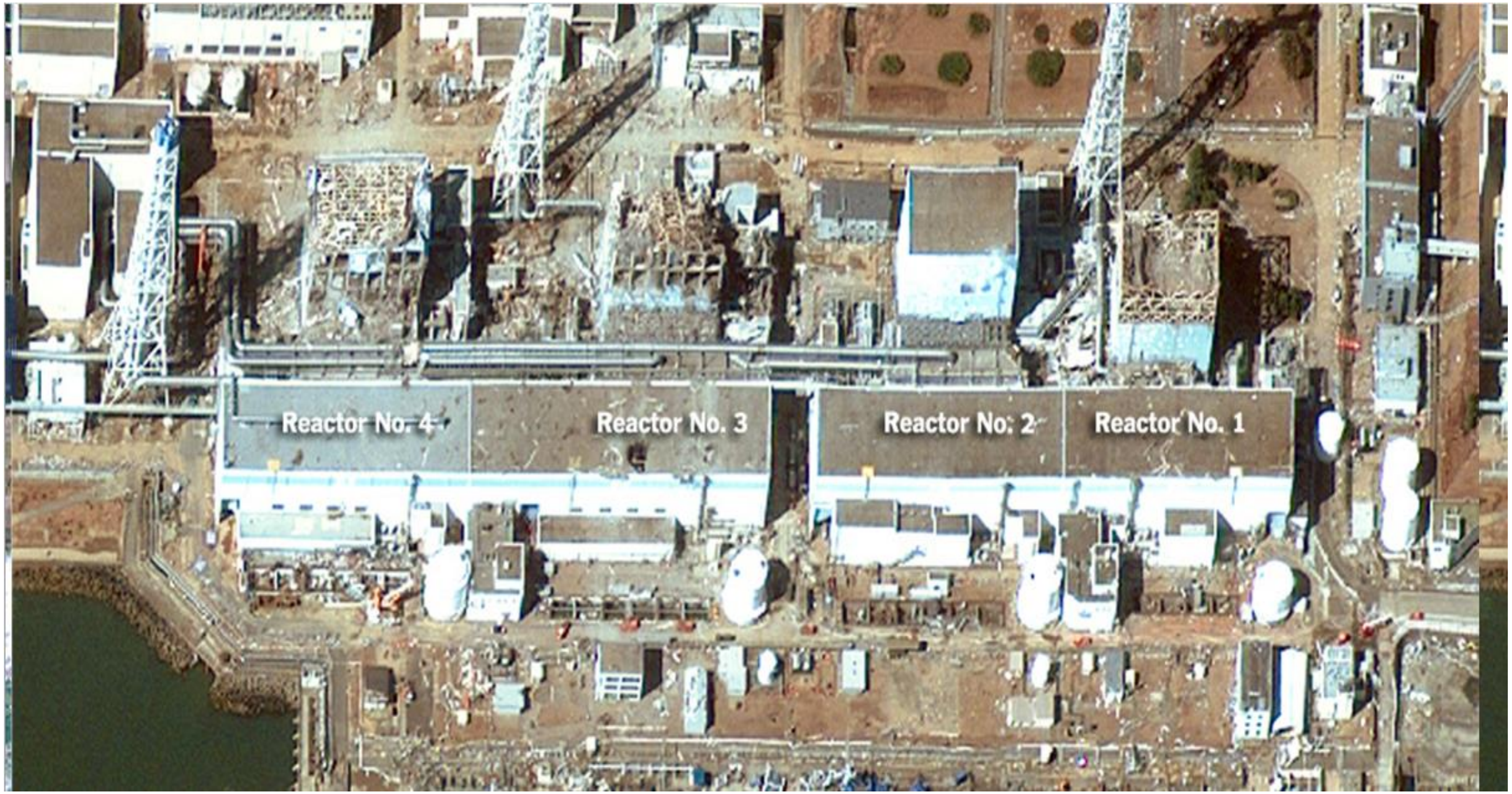

Containment over-pressurization led to release of H_2 into the reactor buildings

Hydrogen behavior – TMI-2 results

Telephone in containment scorched in one area by H_2 combustion event.

55 gal. drum collapsed by overpressure from the H_2 combustion event.

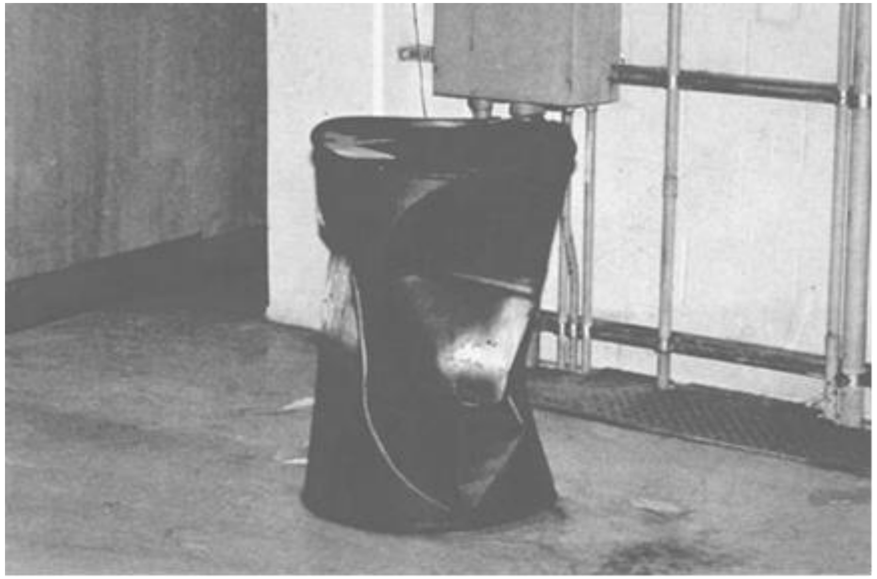

Hydrogen behavior – TMI-2 results

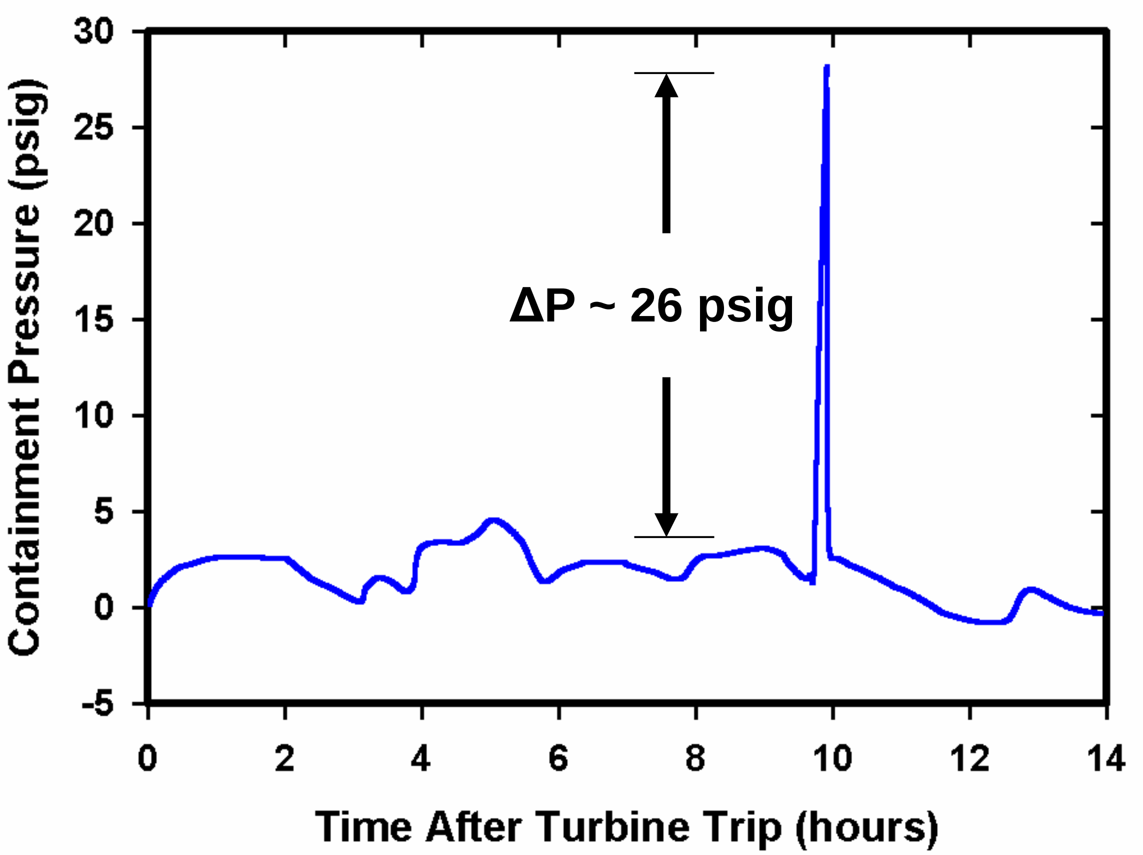

Hydrogen behavior – Peach Bottom BWR UA results

- An intact reactor building retains some of the released radionuclides
- Peach bottom model included the following reactor building failure modes
  - Blowout panels
  - Roof
  - Railroad doors at grade level
- When the railroad doors blow open, a buoyant draft is established in the reactor building
  - Yellow → closed doors
  - This contributed to a higher source term

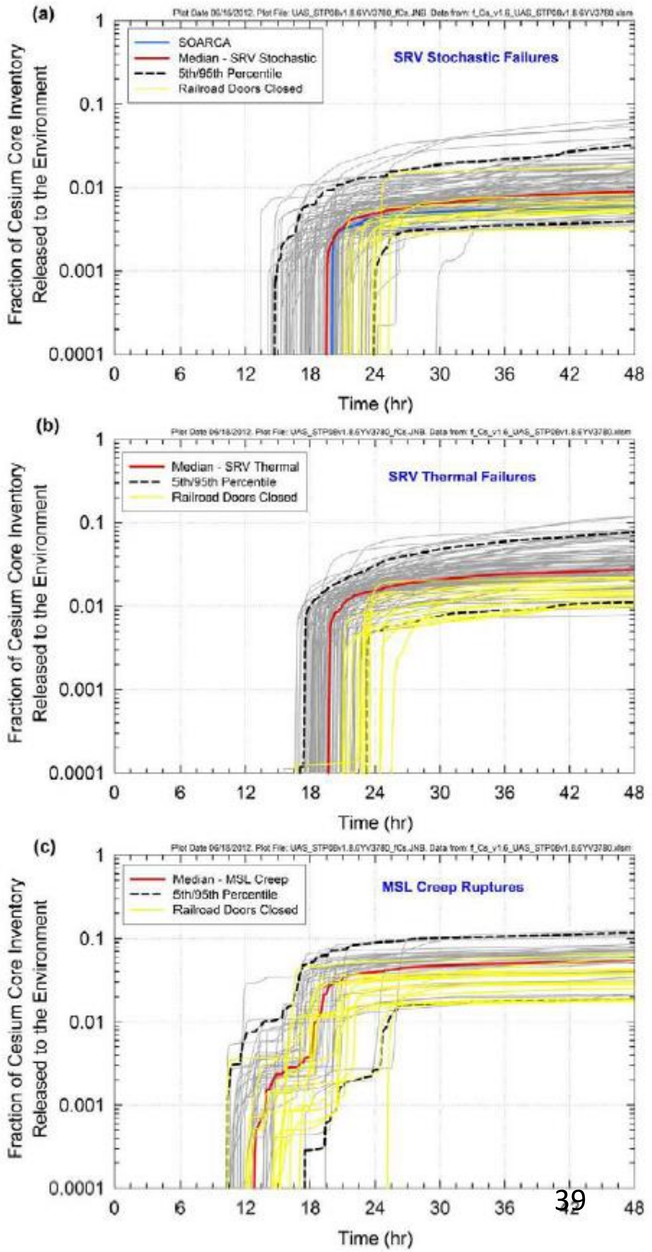

Containment failure methodology – Peach Bottom

- BWR containment failure focused on drywell head leakage, melt-spreading, and drywell liner failure (i.e., a thermal contact failure versus over-pressurization)
  - Reexamination of MELCOR 1.8.6 UA results using MELCOR 2.2
  - Pump seal leakage impact on melt spreading
  - Delayed liner melt-through promotes more drywell leakage (i.e., a higher containment leakage pathway)

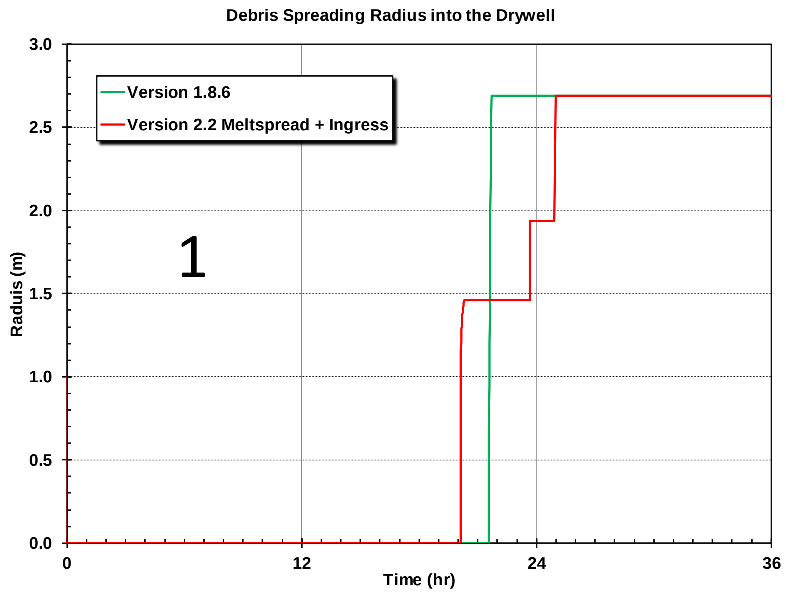

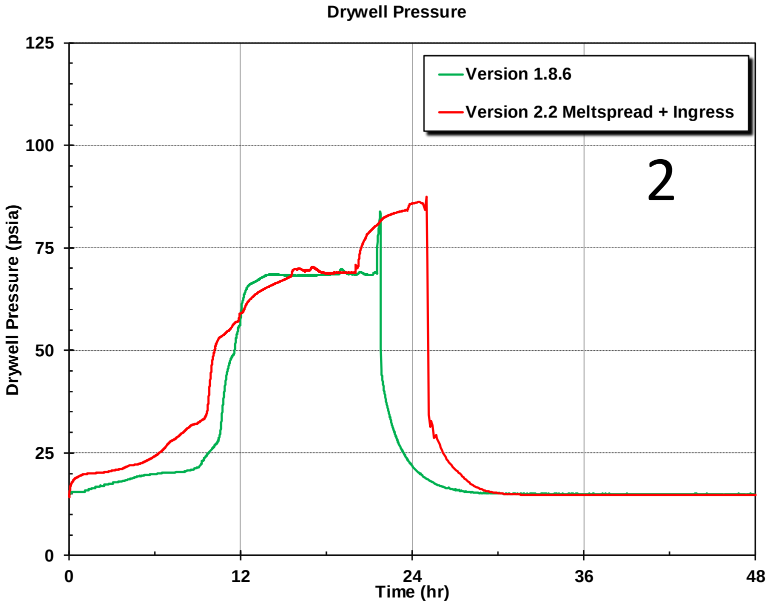

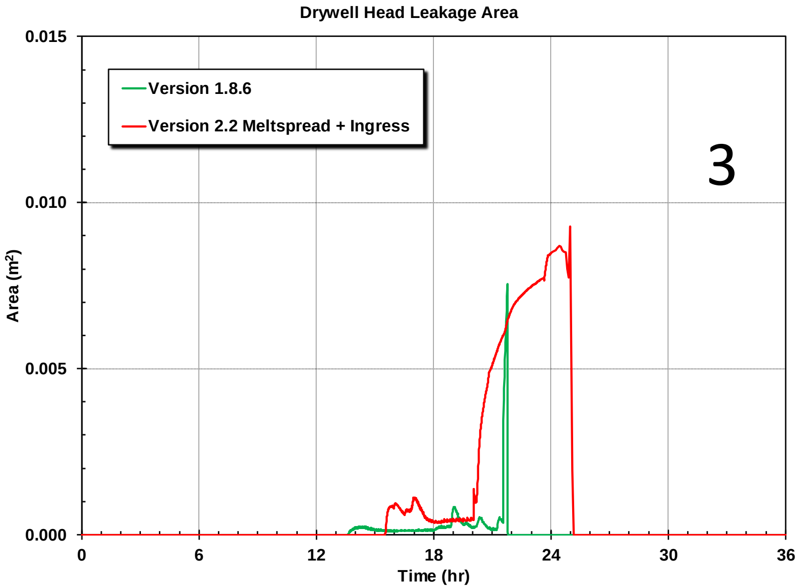

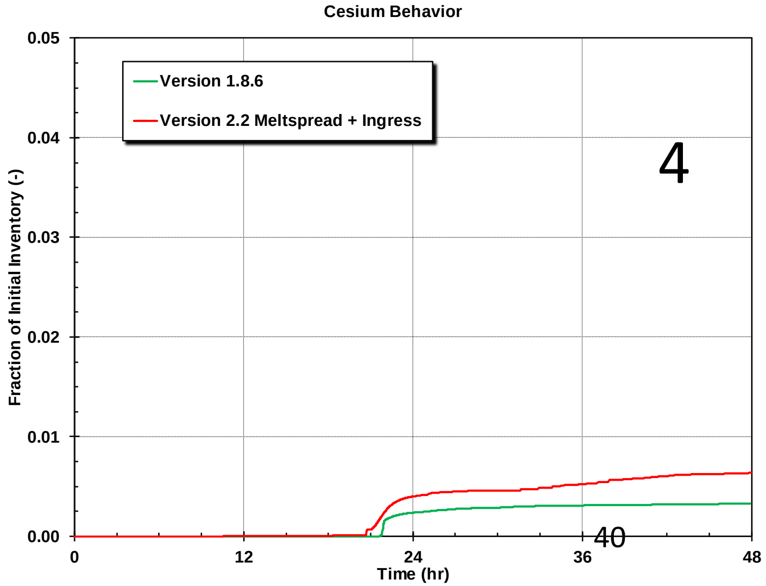

Containment failure – Surry results

- Late over-pressurization from steam and non-condensable gases generated from CCI (95.1%),
  - Liner failure only (81.2%)
  - Liner failure and C-SGTF (12.6%)
  - Liner and rebar failure (1.4%)
- No containment failure prior to the end of the 72 hr simulation time (4.9%) – earliest time at cycle only

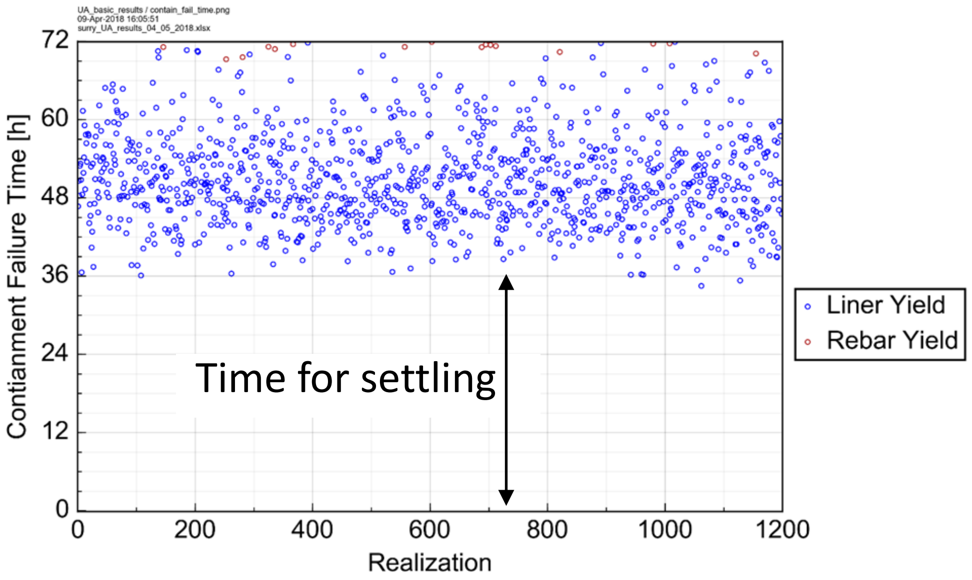

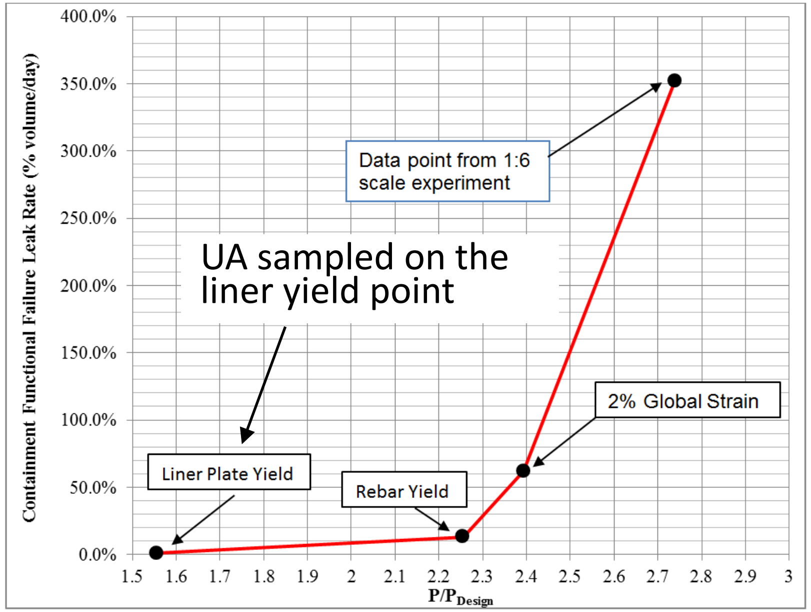

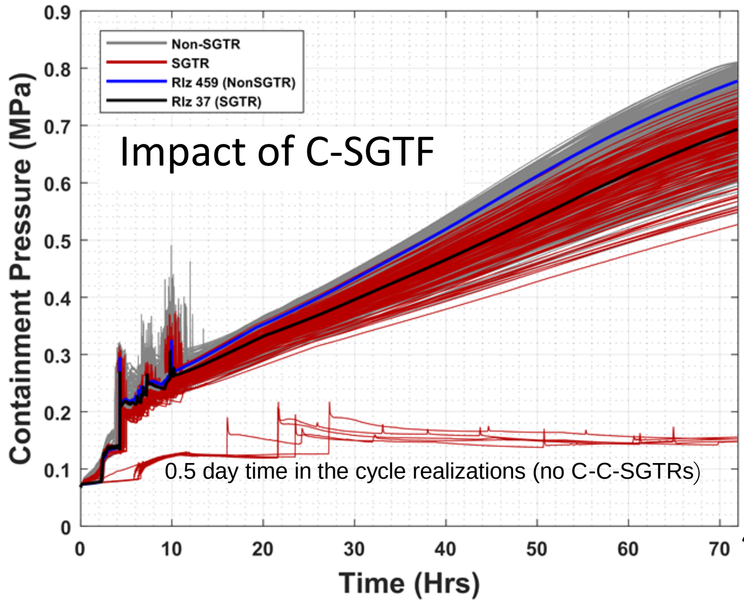

Containment failure methodology – Surry results

- Concrete type impact impacts gases generated from CCI, erosion dynamics, and containment pressurization rate
  - Basaltic generates less non-condensable gases but has a faster axial erosion rate
  - Limestone generates lots of CO and H_2 but slower axial erosion
  - Pressurization is dominated by the steam partial pressure
- Design leakage had a large impact on the cesium release to the environment
  - Only release mechanism until liner plate failure, which occurs after significant settling (non-C-SGTF)

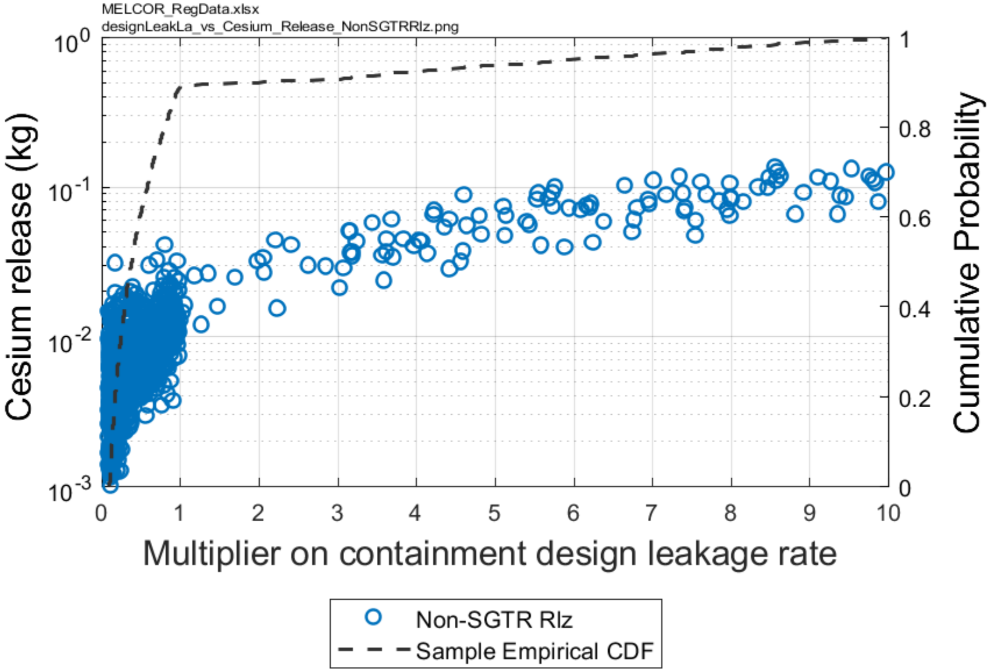

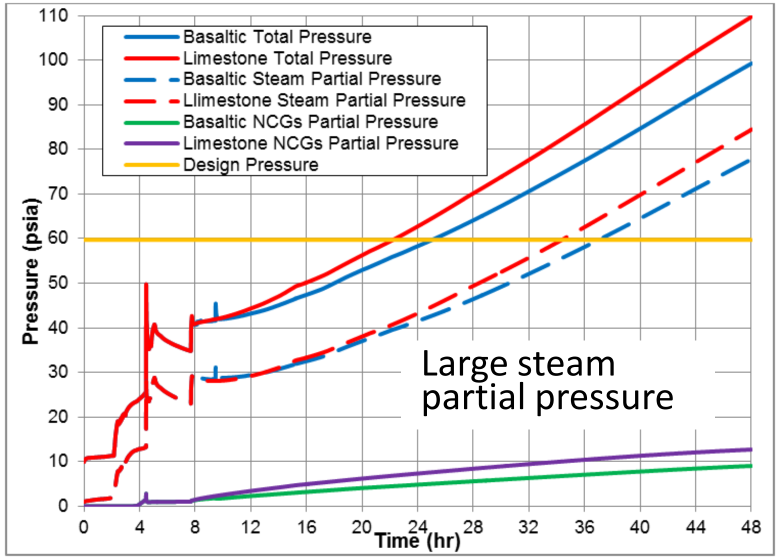

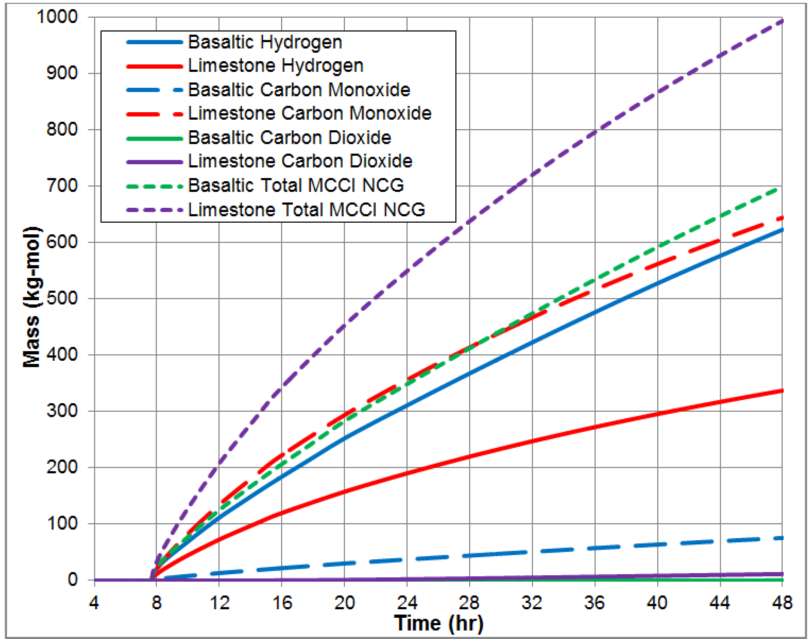

Other Surry source term results

- Surry UA sampled on iodine gas fraction based on French CEA fuel-cladding gap measurements
  - Gaseous iodine has an important impact on the environment source term due to aerosol settling with late containment failure

- Surry UA showed tighter correlation between cesium and iodine with larger releases
  - Cesium releases are strongly impacted by the design leakage and time for settling. There is less variation with high design leakage when more aerosol release occurs before settling

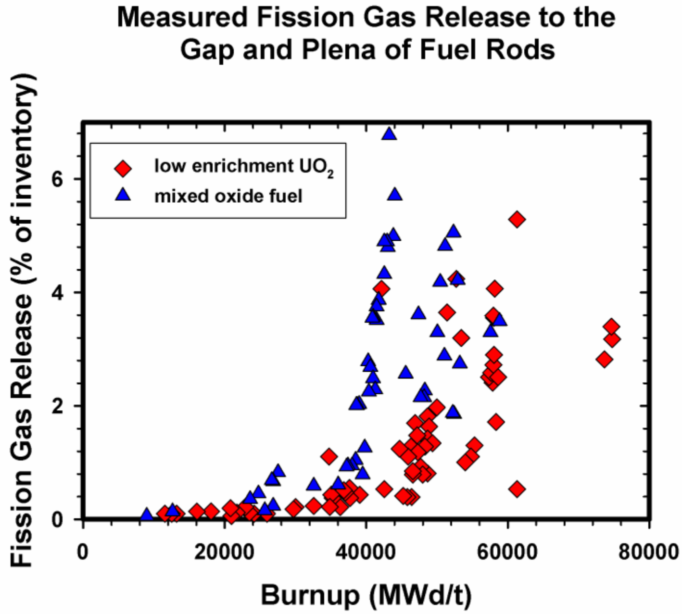

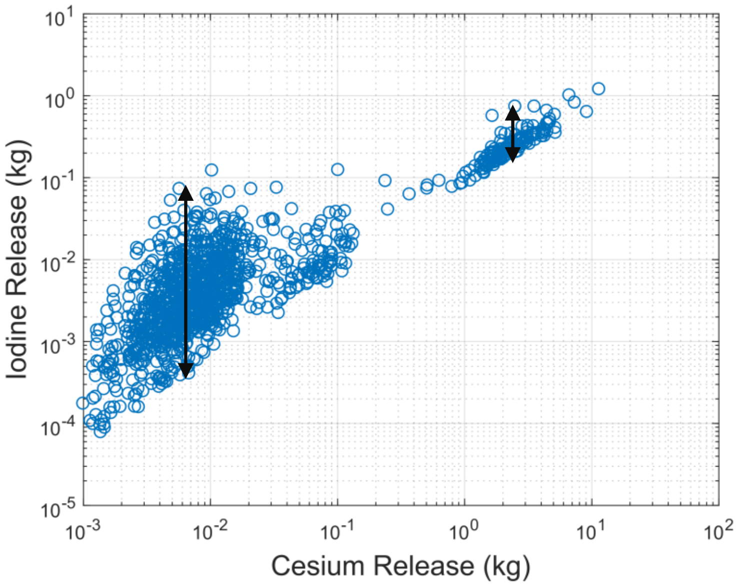

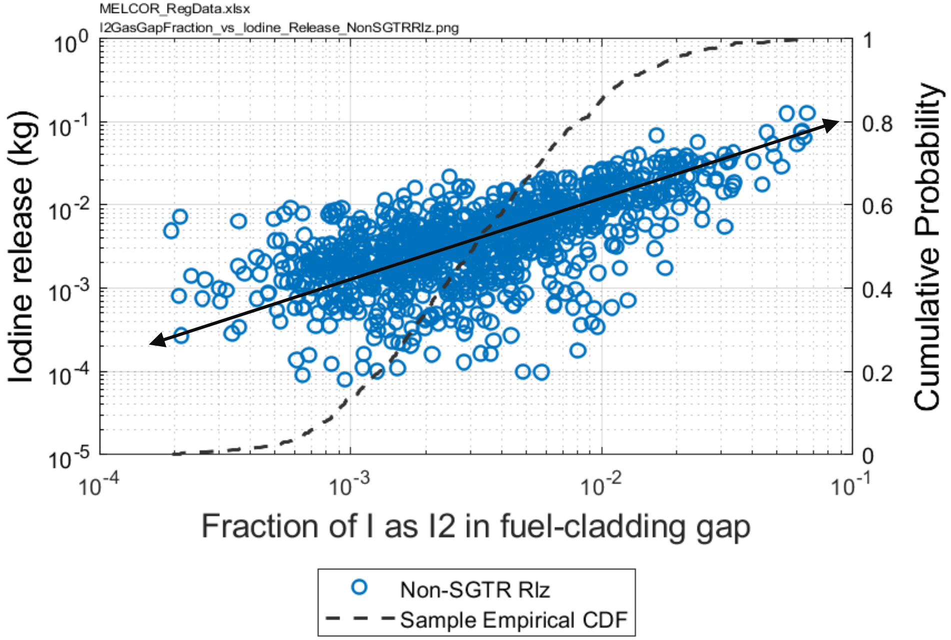

LWR MELCOR CODE DEVELOPMENTS

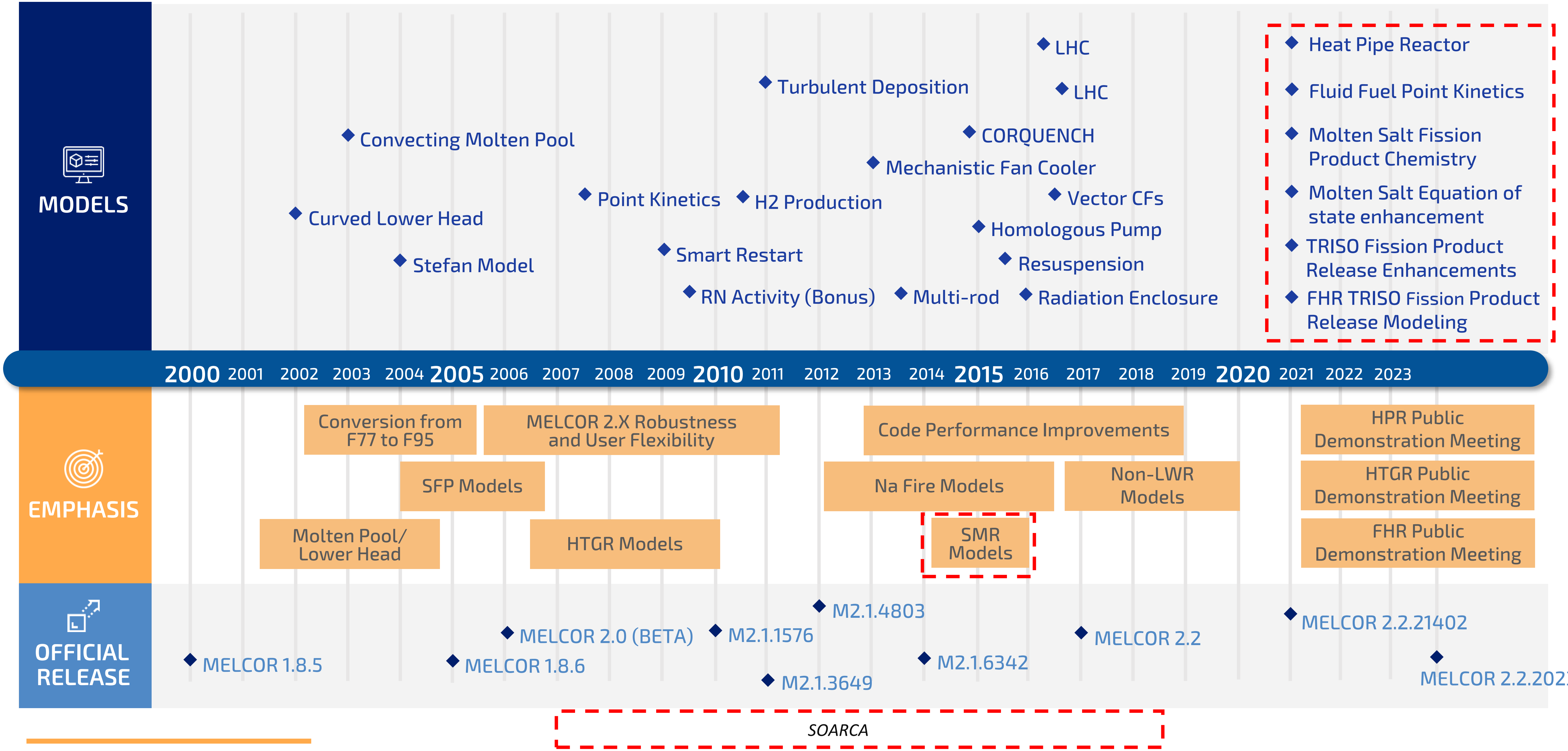

SCALE/MELCOR Non-LWR Source Term Demonstration Project – Fluoride-Salt-Cooled High-Temperature Reactor (FHR)

September 14, 2021

U.S.NRC

Oak Ridge National Laboratory

Sandia National Laboratories

U.S. DEPARTMENT OF ENERGY

NNSA

Project scope

Full-plant models and sample calculations for representative non-LWRs

2021

- Heat pipe reactor – INL Design A – public workshop 6/29/2022
- Pebble-bed gas-cooled reactor – PBMR-400 – public workshop 7/20/2022
- Pebble-bed molten-salt-cooled – UCB Mark 1 – public workshop 9/14/2022

2022

- Molten-salt-fueled reactor – MSRE – public workshop 9/13/2022
- Sodium-cooled fast reactor – ABTR – public workshop 9/20/2022

2023

- Additional code enhancements, sample calculations, and sensitivity studies

Advanced Reactor Designs

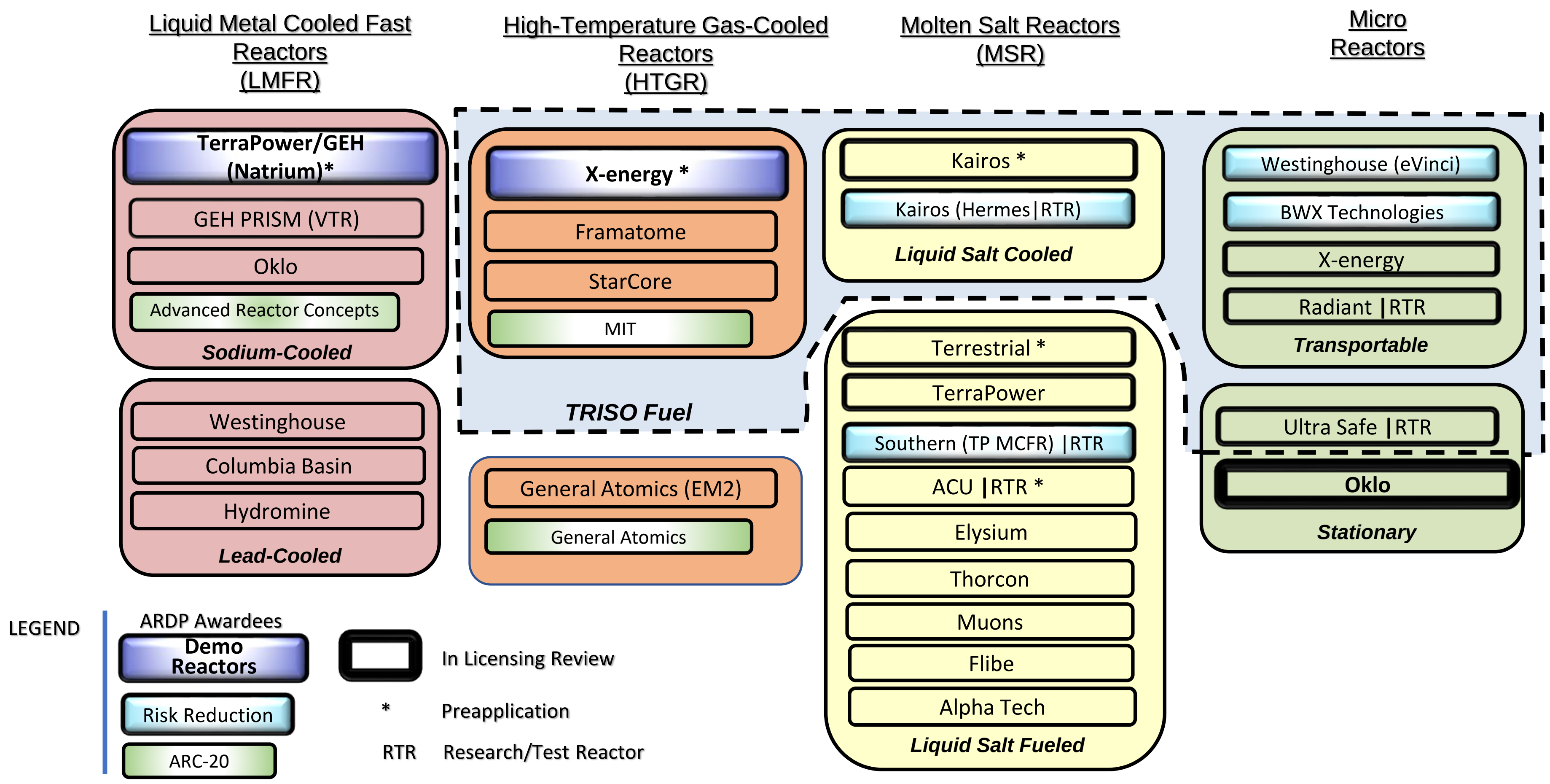

UCB Mark 1 FHR

Reactor

- 236 MW_{th} / 100 MW_e
- Atmospheric pressure
- 600°C core inlet
- 700°C core outlet
- 976 kg/s core flowrate
- FLiBe molten salt coolant

Core

- 470,000 fueled pebbles + 218,000 unfueled pebbles in core and defueling chute
- 180 MWd/kgHM discharge burnup
- 19.9% enrichment
- Online refueling

Secondary system: gas-turbine at 18.6 bar with natural gas co-firing capability

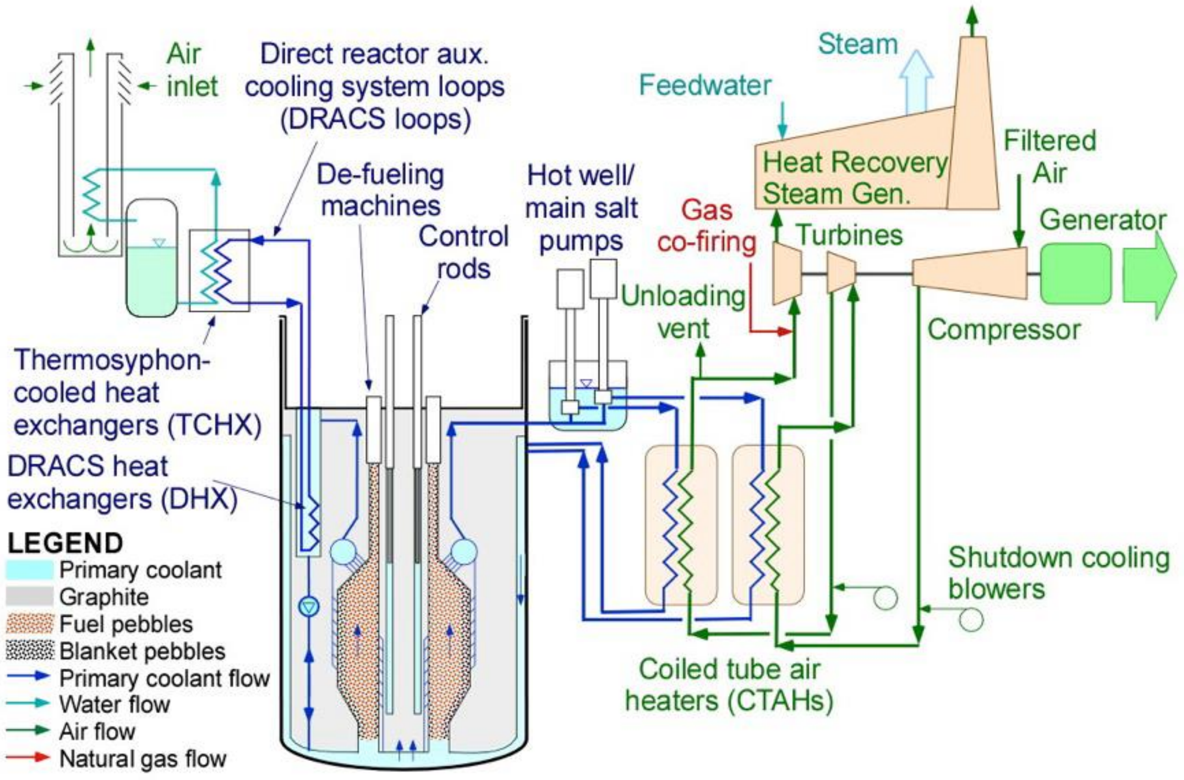

UCB Mark 1 schematic
[UCBTH-14-002]

Fluoride-salt-cooled High-Temperature Reactor Fission Product Inventory/Decay Heat Methods and Results

FHR analysis with SCALE

- Objective
  - Provide input for MELCOR accident simulation
    - Radionuclide inventory
    - Decay heat profile
    - Reactivity feedback coefficients
    - Reactivity from xenon transient
- Approach
  - Apply SCALE to generate fuel composition for an equilibrium core
  - Equilibrium core – operated for several years so the average burnups are no longer changing
  - Evaluate neutronic characteristics

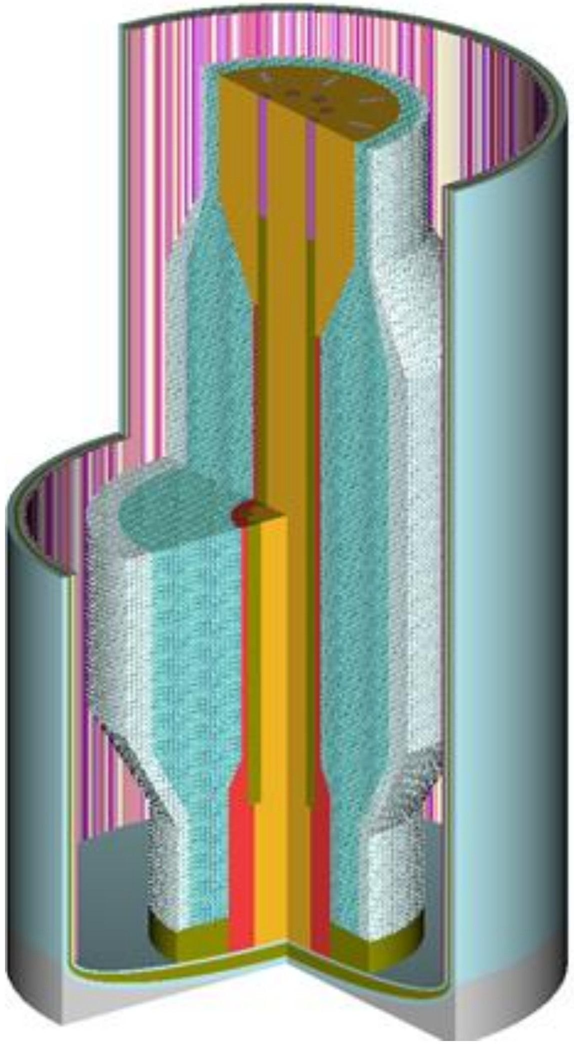

SCALE model of the UCB Mark 1 core

Isothermal reactivity temperature coefficients from SCALE

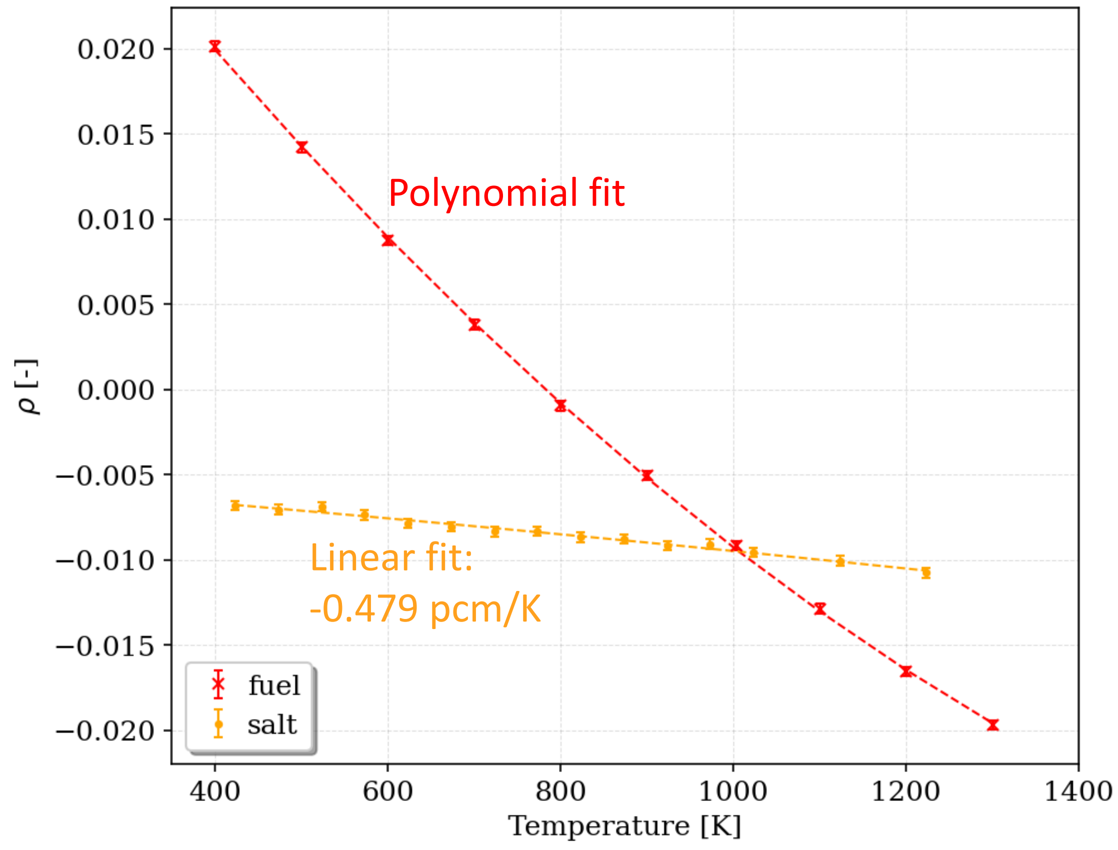

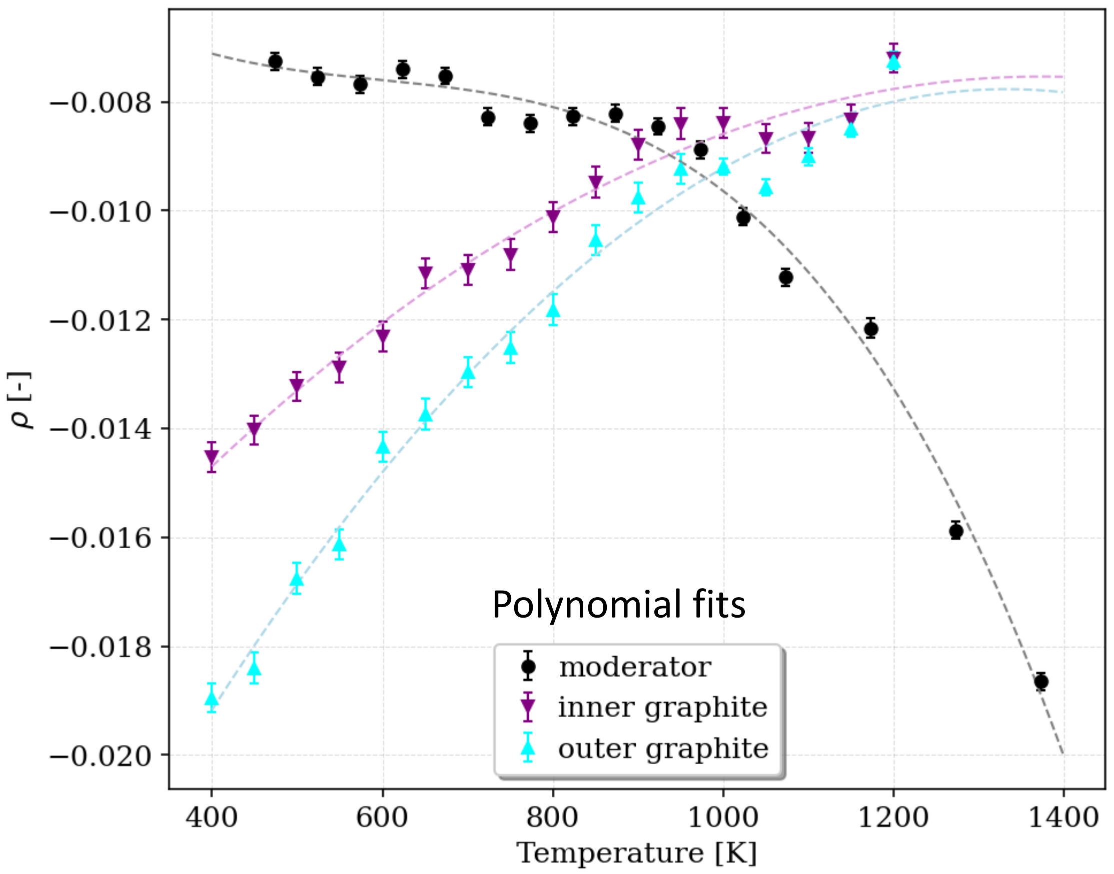

1. Linear fit for salt temperature coefficient
2. Polynomial fit or tabulated values for fuel, moderator, and graphite temperature coefficients

$$\rho = a + bT + cT^2 + dT^3$$

	a	b	c	d
Fuel	4.57E-02	-7.08E-05	1.59E-08	
Moderator	-2.02E-03	-2.48E-05	3.88E-08	-2.16E-11
Inner graphite	-2.18E-02	2.07E-05	-7.55E-09	
Outer graphite	-3.10E-02	3.49E-05	-1.31E-08	

2σ statistical error bars are displayed

MELCOR FHR Models

Radionuclide Diffusion Release Model

Intact TRISO Particles

- One-dimensional finite volume diffusion equation solver for multiple zones (materials)
- Temperature-dependent diffusion coefficients (Arrhenius form)

$$\frac{\partial C}{\partial t} = \frac{1}{r^n}\frac{\partial}{\partial r}\left(r^n \boldsymbol{D}\frac{\partial C}{\partial r}\right) - \lambda C + \beta \qquad D(T) = D_0 e^{-\frac{Q}{RT}}$$

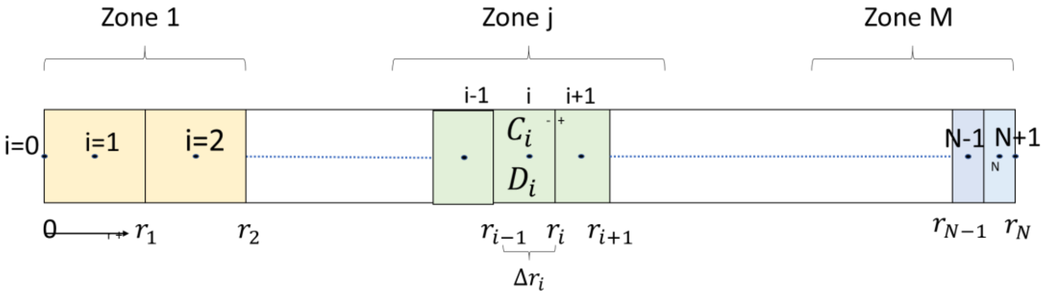

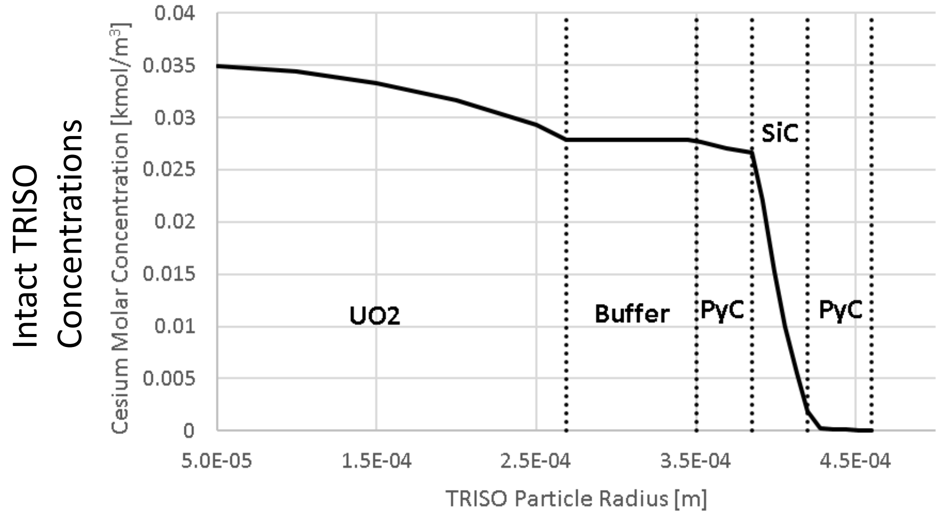

Diffusivity Data Availability

Radionuclide	UO_2	UCO	PyC	Porous Carbon	SiC	Matrix Graphite	TRISO Overall
Ag	Some	Not investigated	Some	Not found	Extensive	Some	Extensive
Cs	Some		Some		Extensive	Some	Some
I	Some		Some		Some	Not found	Not found
Kr	Some		Some		Not found	Some	Some
Sr	Some		Some		Extensive	Some	Some
Xe	Some		Some		Some	Some	Not found

Data used in the demo calculation

[IAEA TECDOC-0978]

	FP Species							
	Kr		Cs		Sr		Ag	
Layer	D (m^2/s)	Q (J/mole)	D (m^2/s)	Q (J/mole)	D (m^2/s)	Q (J/mole)	D (m2/s)	Q (J/mole)
Kernel (normal)	1.3E-12	126000.0	5.6-8	209000.0	2.2E-3	488000.0	6.75E-9	165000.0
Buffer	1.0E-8	0.0	1.0E-8	0.0	1.0E-8	0.0	1.0E-8	0.0
PyC	2.9E-8	291000.0	6.3E-8	222000.0	2.3E-6	197000.0	5.3E-9	154000.0
SiC	3.7E+1	657000.0	7.2E-14	125000.0	1.25E-9	205000.0	3.6E-9	215000.0
Matrix Carbon	6.0E-6	0.0	3.6E-4	189000.0	1.0E-2	303000.0	1.6E00	258000.0
Str. Carbon	6.0E-6	0.0	1.7E-6	149000.0	1.7E-2	268000.0	1.6E00	258000.0

Iodine assumed to behave like Kr

Radionuclide Release Models

- Recent failures – particles failing within latest time-step (burst release, diffusion release in time-step)
- Previous failures – particles failing on a previous time-step (time history of diffusion release)
- Contamination and recoil

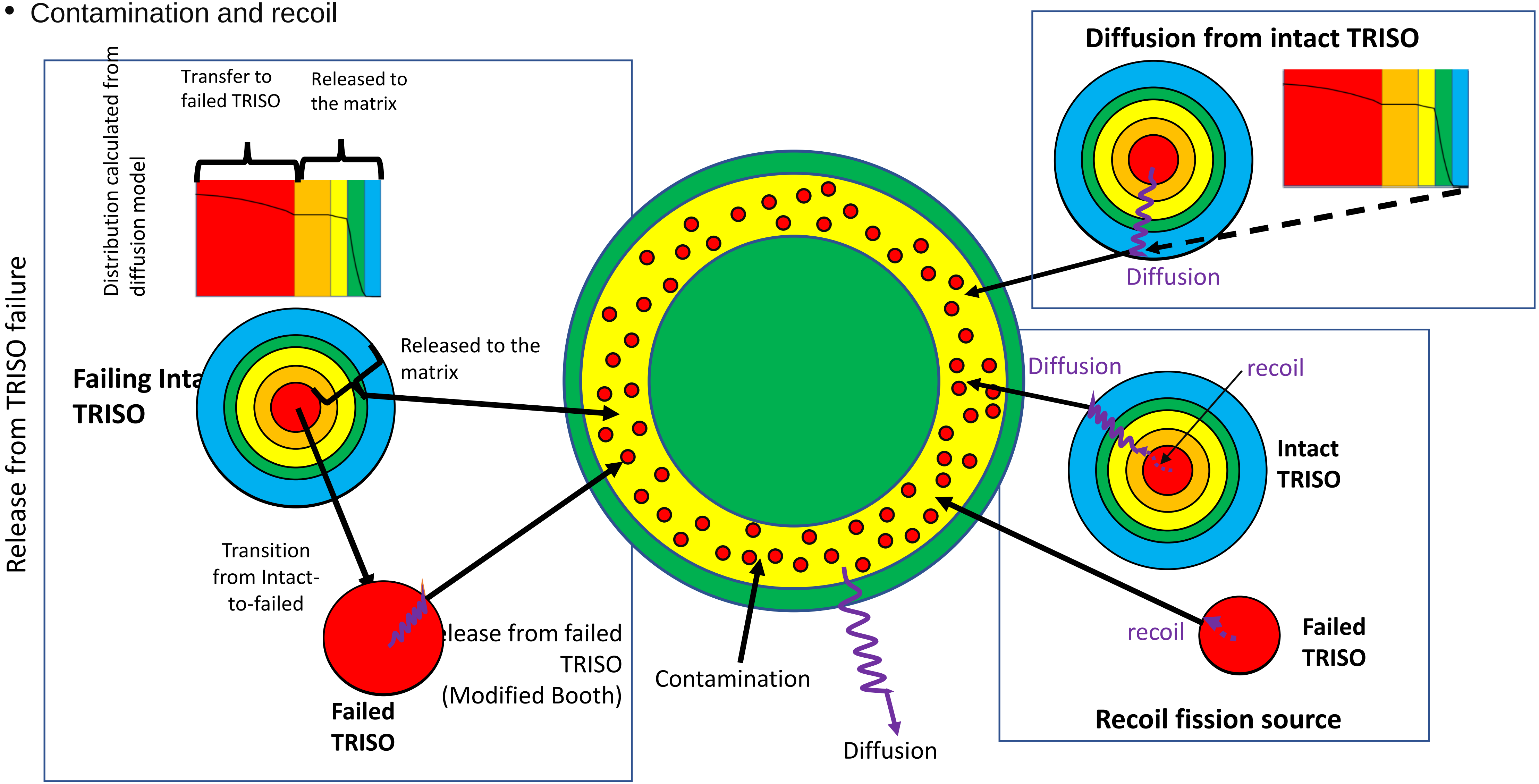

Point Kinetics Modeling

Standard treatment

$$\frac{dP}{dt} = \left(\frac{\rho - \beta}{\Lambda}\right)P + \sum_{i=1}^{6} \lambda_i Y_i + S_0$$

$$\frac{dY_i}{dt} = \left(\frac{\beta_i}{\Lambda}\right)P - \lambda_i C_i, \qquad for\ i = 1 \ldots 6$$

Feedback models

- User-specified external input
- FHR example includes multiple feedbacks
  - Fuel
  - Molten salt around the fuel
  - Inner reflector
  - Outer reflector and unfueled pebbles
  - Moderator (matrix around fueled pebbles)

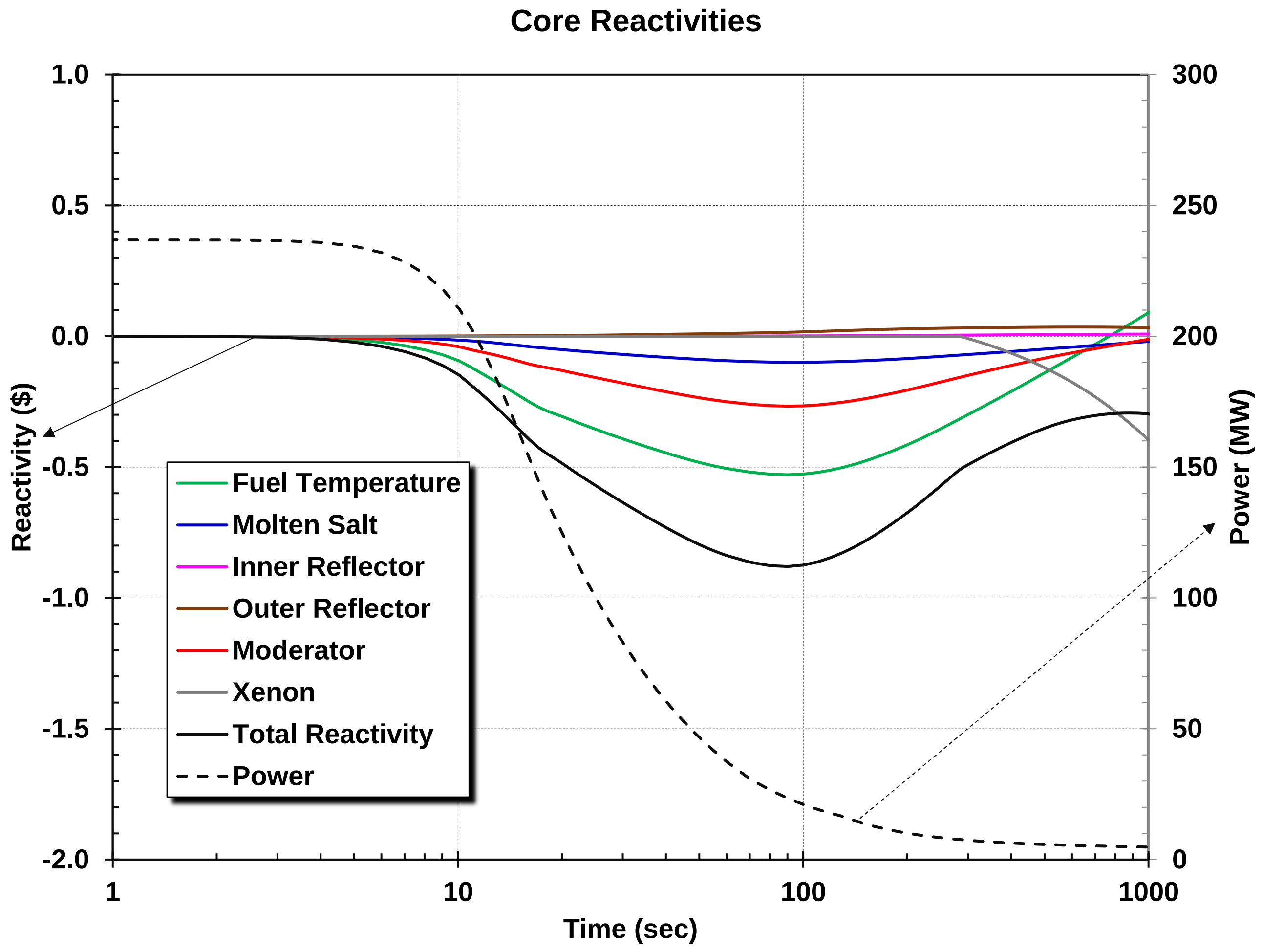

Molten Salt Chemistry and Radionuclide Release

Model Scope

Evaluation of thermochemical state

- Gibbs Energy Minimization with Thermochimica
- Provides solubilities and vapor pressures

Thermodynamic database

- Generalized approach to utilize any thermodynamic database
- An example is the Molten Salt Thermal Database
  - FLiBe-based systems
  - Chloride-based systems

Radionuclides grouped into forms found in the Molten Salt Reactor Experiment

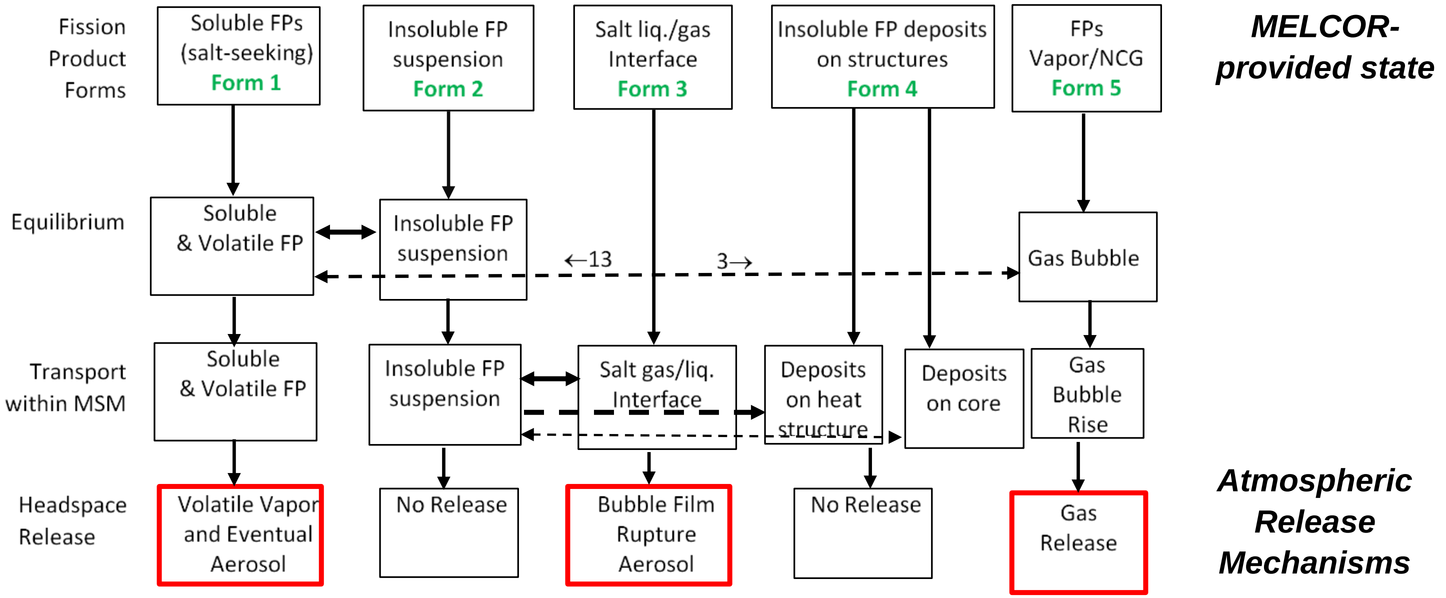

Initial Model Form

Solubility determined from empirical evidence (P. Britt ORNL 2017)

Solubilities mapped to 17 MELCOR fission product classes

Insoluble MELCOR classes are assigned to be colloidal

Core and reactor vessel

Core nodalization – light blue lines

- Assumes azimuthal symmetry
- Subdivided into 11 axial levels and 8 radial rings
- Core cells model molten salt fluid volume, reflector structures, the pebble-bed core, and the pebbles in the defueling chute

Fluid flow nodalization – black boxes

- Molten salt enters through the downcomer and flows into the center reflector and into the bottom of the pebble bed
- Molten salt leaves through the periphery of the core and upwards through the refueling chute
- Unfueled graphite pebbles in box labeled “180”

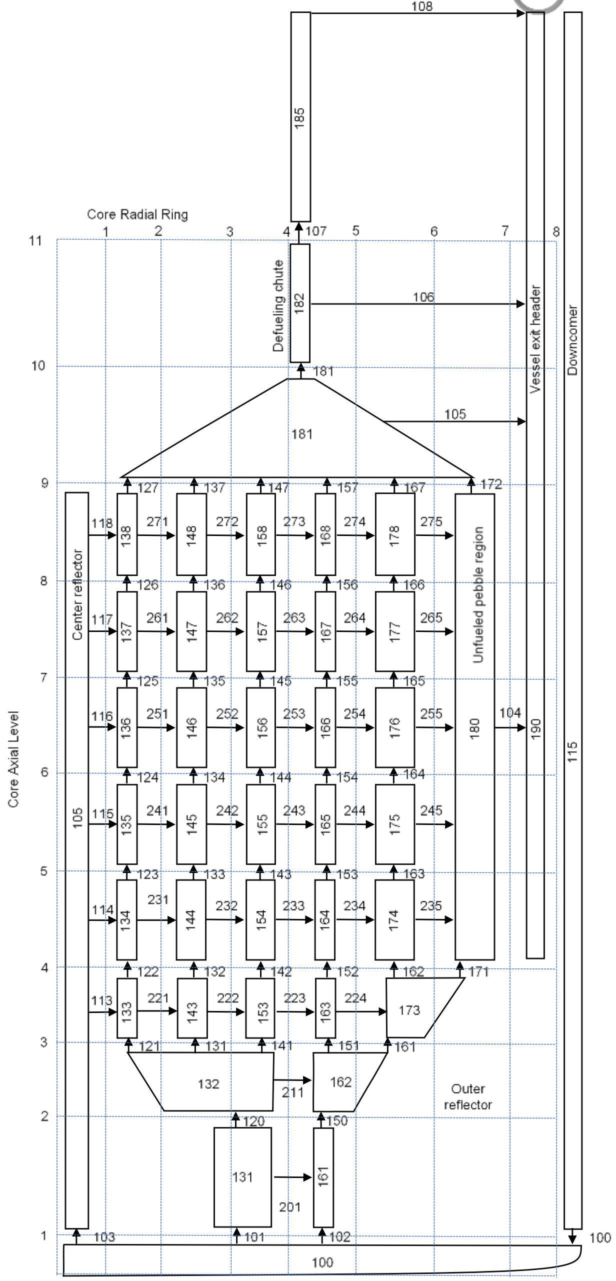

Recirculation loops

Each loop has a pump, a heat exchanger, and a standpipe

Molten salt has free surface in the hotwell and the standpipes

Argon gas above the free surfaces with connection to the cover-gas system

- Over-pressurization relief passes through the cover gas system
- Cover gas enclosure leaks into the containment when over-pressurized

Secondary-side air cools primary-side molten salt

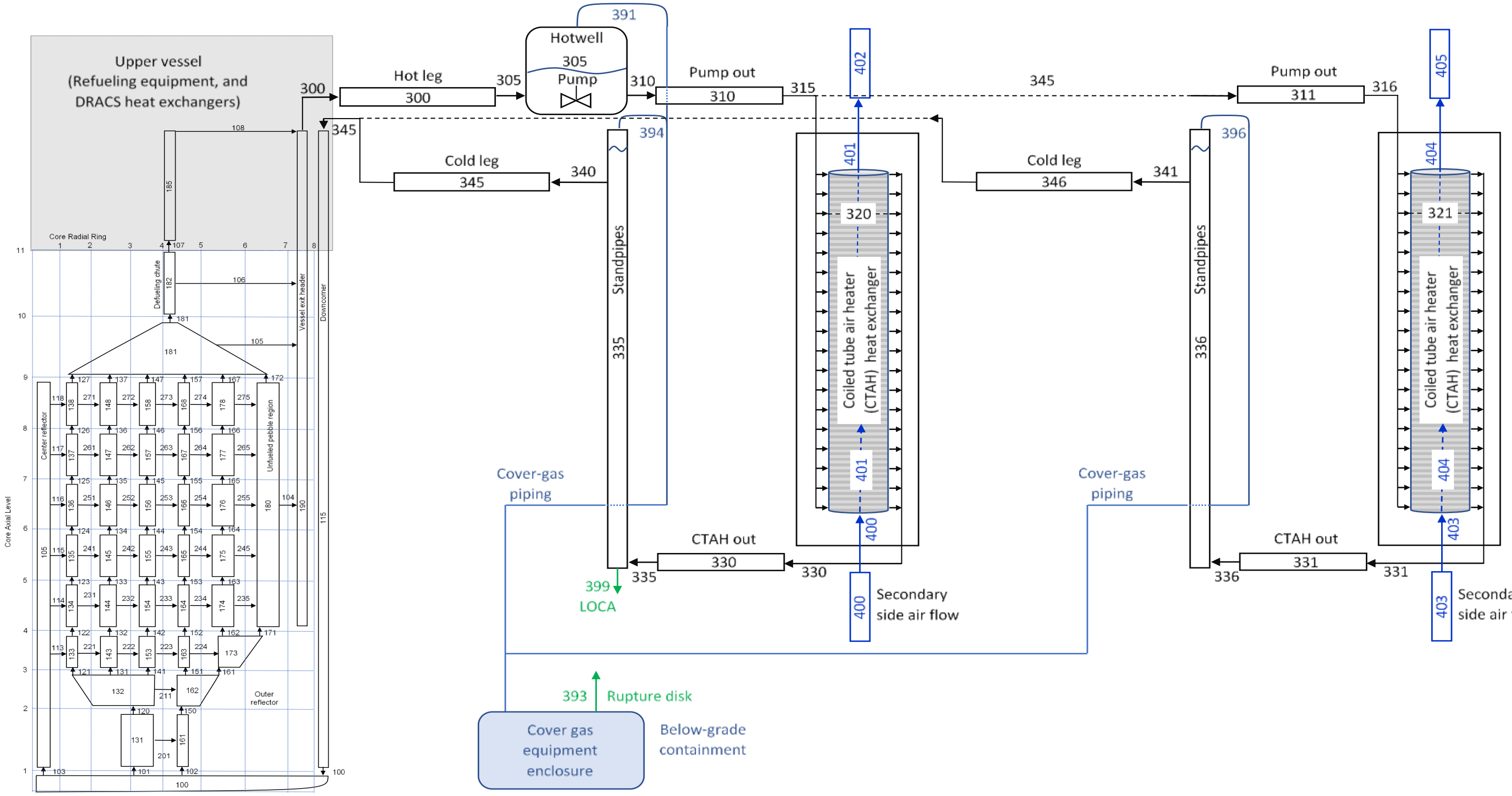

Direct Reactor Auxiliary Cooling System (DRACS)

3 trains – 2.36 MW/train

- 236 MWt reactor

Each train has 4 loops in series

- Primary coolant circulates to DRACS heat exchanger
- Molten-salt loop circulates to the thermosyphon-cooled heat exchangers (TCHX)
- Water circulates adjacent to the secondary salt tube loop in the TCHX
- Natural circulation air circuit cools and condenses steam

Start-up: RCS-pump trip causes ball in valve to drop

Additional system information

- DHXs are in the reactor vessel
- TCHXs are in the shield building

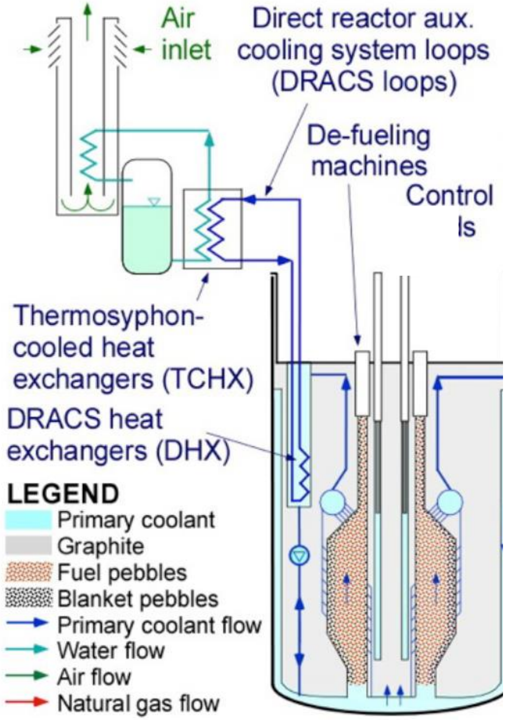

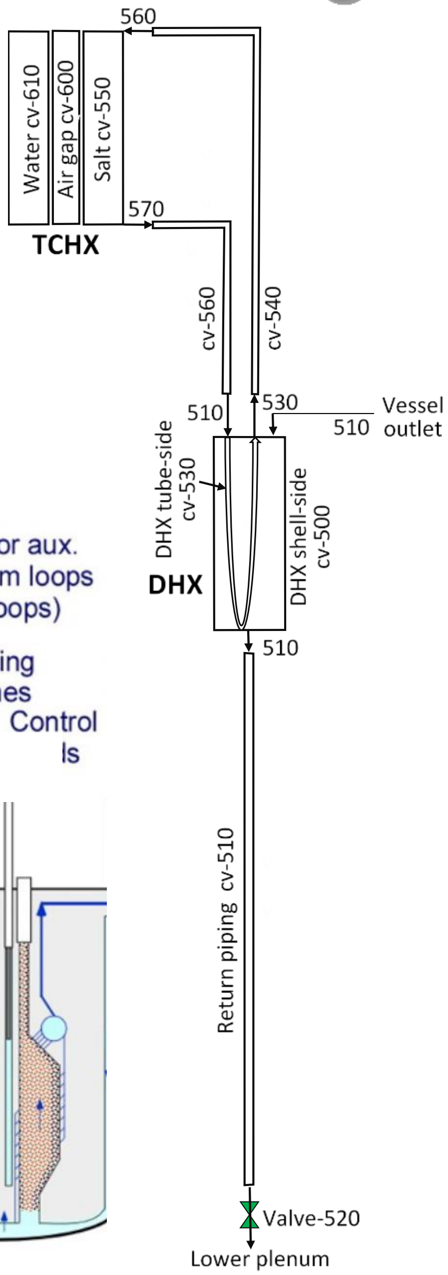

Containment

Shield dome

- Protection against aircraft and natural gas detonations (co-fired turbine concept)
- Contains water for DRACS and RCCS
- DRACS air natural circulation chimneys connected to the shield dome

Reactor cavity

- Fire-brick insulation
- Low free volume
- Low-leakage bellows between reactor cavity and adjacent cavities

Separate compartments for the other RCS components

- Below-grade compartment includes the cover-gas enclosure for reactor cavity over-pressurization

Reactor cavity cooling subsystem in reactor cavity wall

- Water circulation
- Cooling tubes affixed to reactor cavity steel liner
- Cools concrete during normal operation

Leak rate assumed consistent with BWR Mark 1 reactor building

- 100% vol/day at 0.25 psig

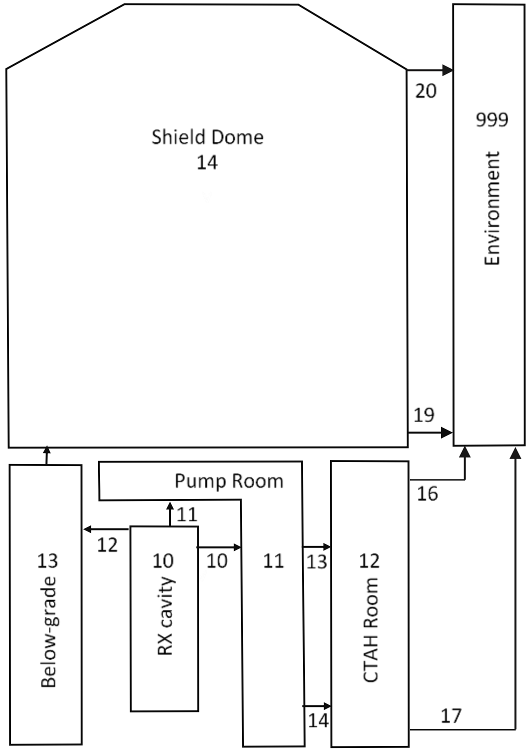

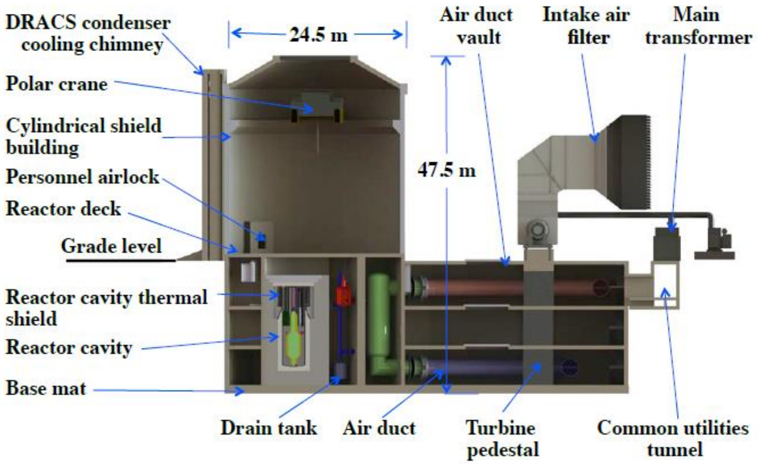

MELCOR model inputs (2/2)

Fission product diffusivities through the TRISO and the pebble matrix from IAEA-TECDOC-978, Appendix A

- Primarily based on values from German experiments with UO_2 TRISO pebbles
  - UO_2 data can be easily updated to UCO data*
- Limited data based on nuclides of Xe, Cs, Sr, and Ag
- Iodine assumed to behave like Kr

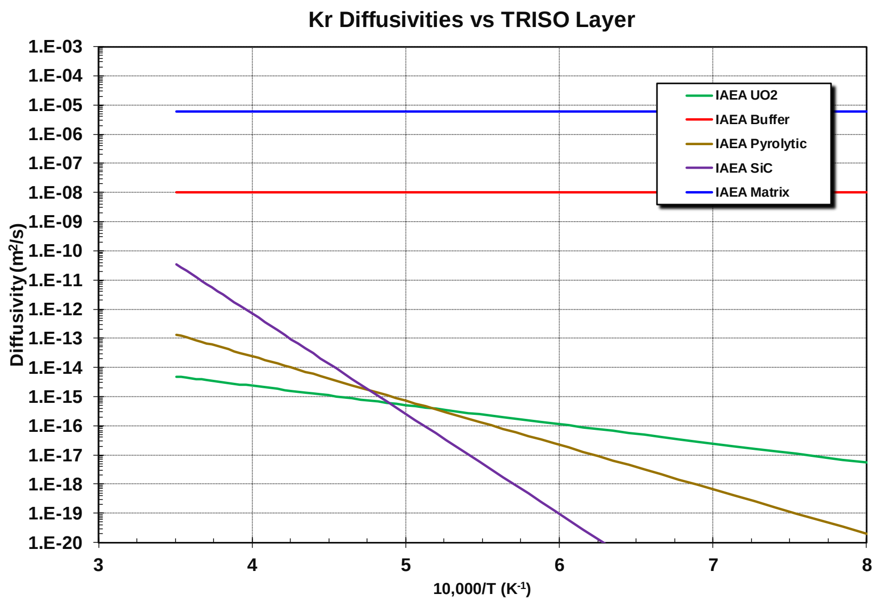

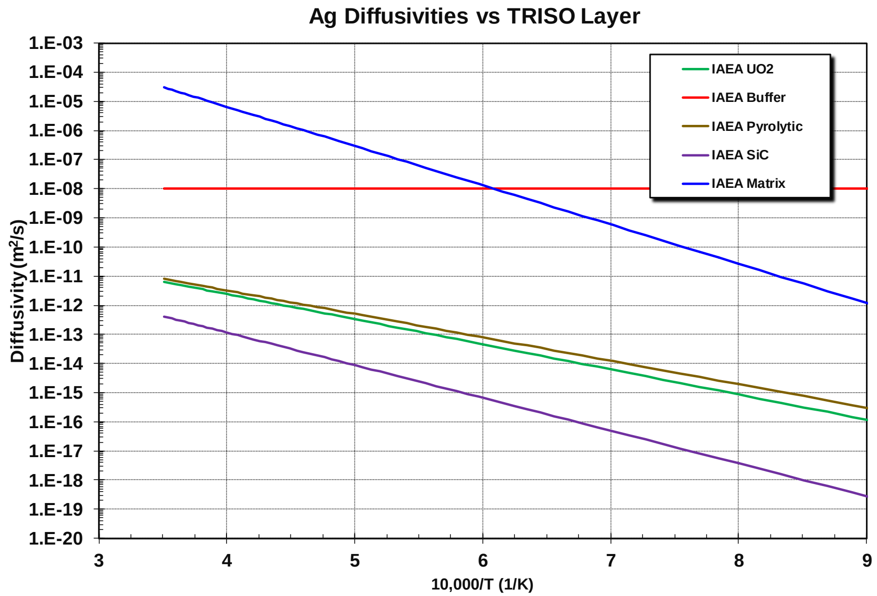

* UCO TRISO thermal failure characteristics were not available, so UO_2 TRISO diffusivity and UO_2 failure data were used. Both are changeable through user input with design-specific data.

ATWS

Loss-of-onsite power with failure to SCRAM

- Salt pumps shut off
- Reactor fails to SCRAM
- Secondary heat removal ends
- 0 to 3 trains of DRACS operating

Includes preliminary analysis with xenon transient

- Guided by ORNL calculations
- Xenon reactivity feedback model being implemented into MELCOR

ATWS with 3xDRACS

Initial fuel heatup has strong negative fuel and moderator feedback that offsets positive reflector feedbacks

Strong negative xenon transient feedback *

3xDRACS exceeds core power after 330 s

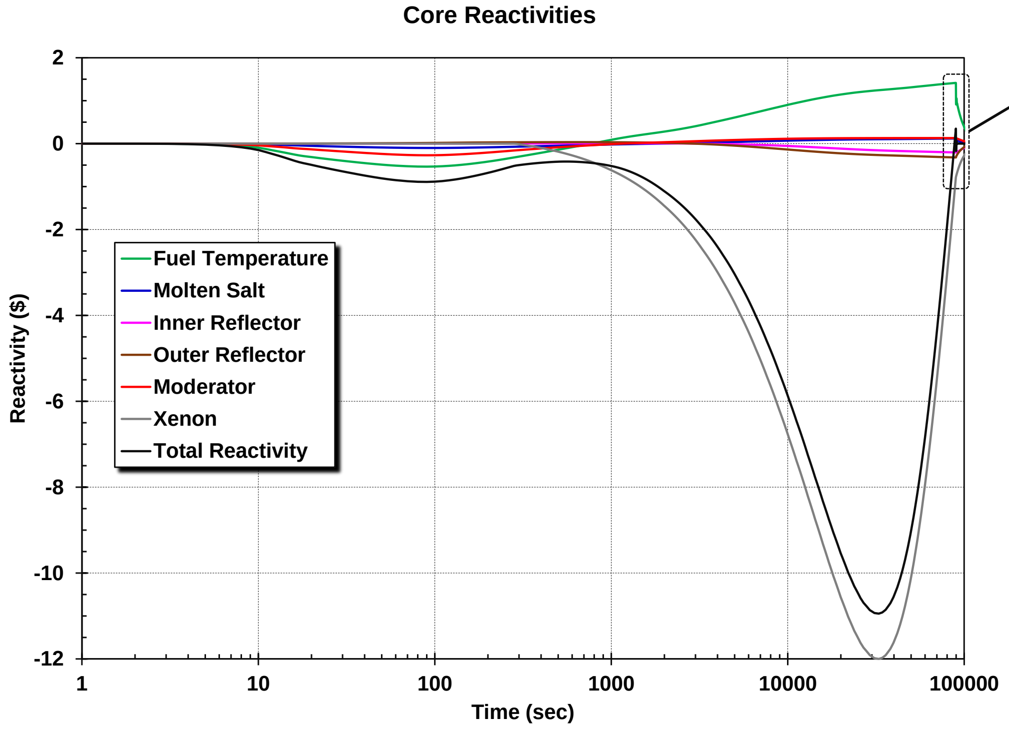

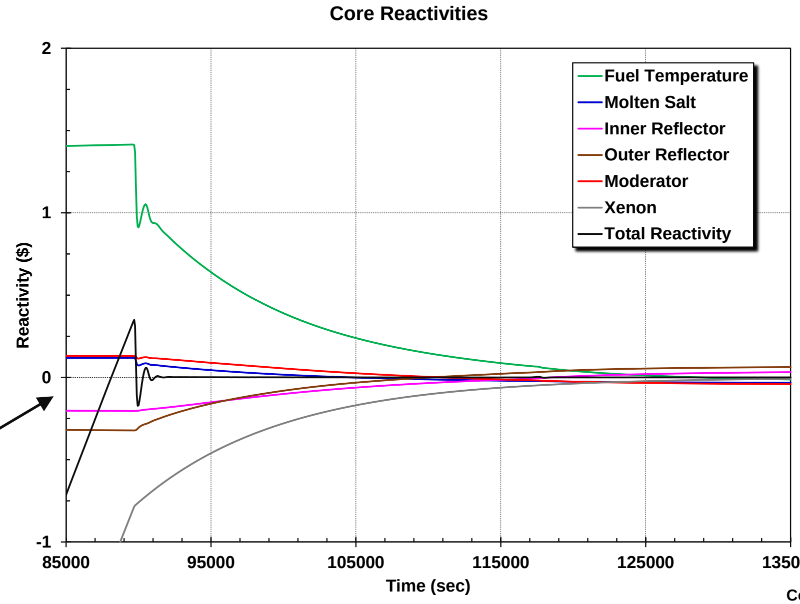

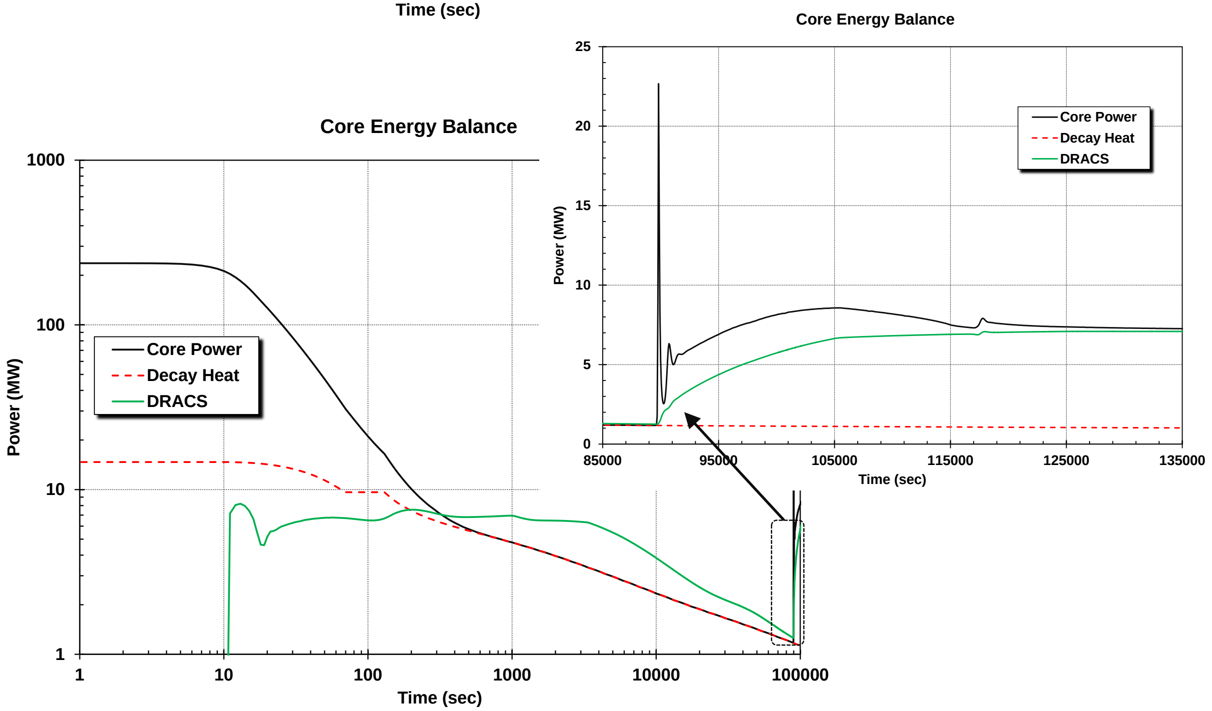

* Xenon transient approximated.

ATWS with variable DRACS (semi-log)

Early power decrease to decay heat level is similar for all cases

- 1xDRACS and 2xDRACS cases exceed decay heat later

Fuel temperatures cool down according to DRACS heat removal rate

- 0xDRACS peak fuel temperature = 990 °C at 10^5 s (T_{sat}~ 1350 °C)

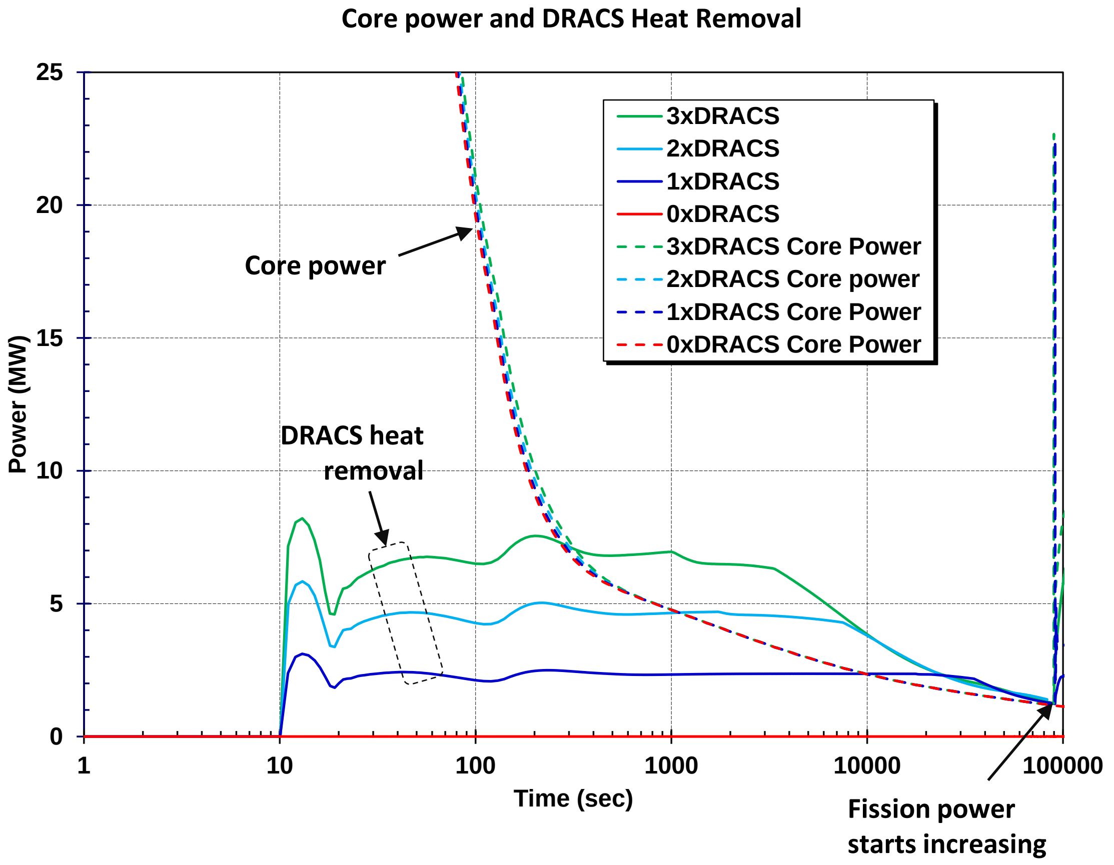

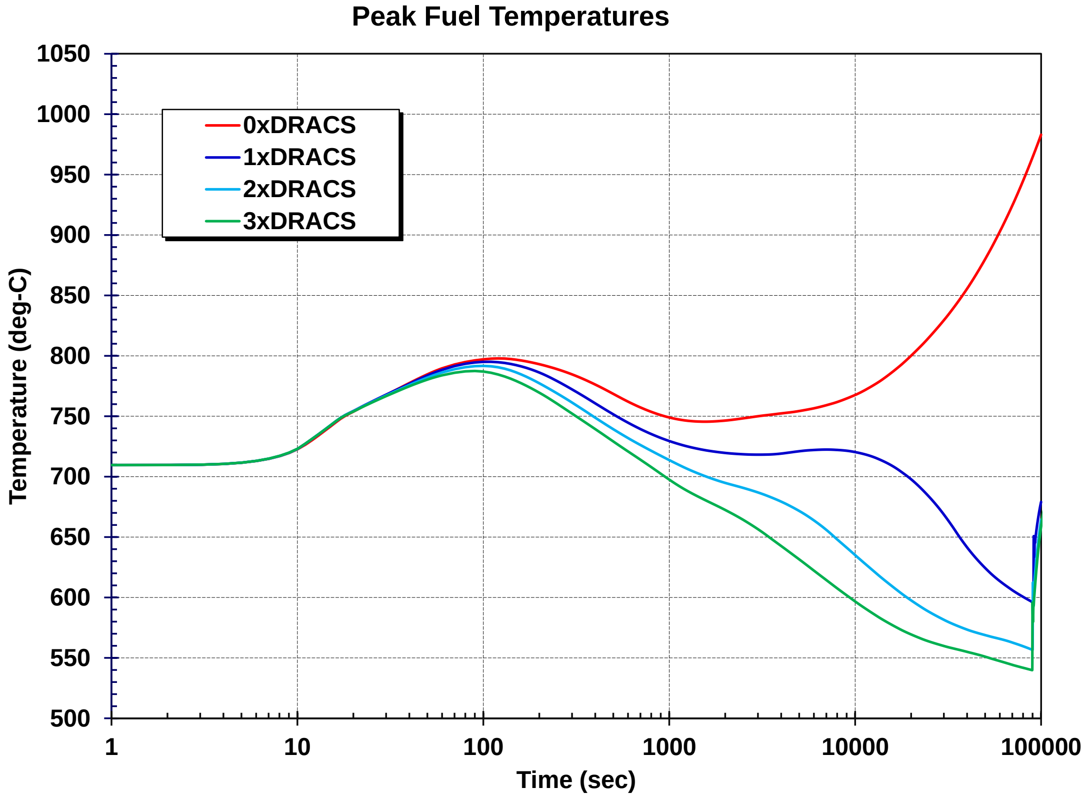

* Xenon transient approximated.

ATWS with variable DRACS – (Linear scale)

When the total reactivity exceeds zero, the core power increases

- Increased power heats the fuel and reduces the positive fuel reactivity
- Core power eventually converges on the DRACS heat removal rate

The long-term fuel temperatures increase to offset changes in the xenon feedback

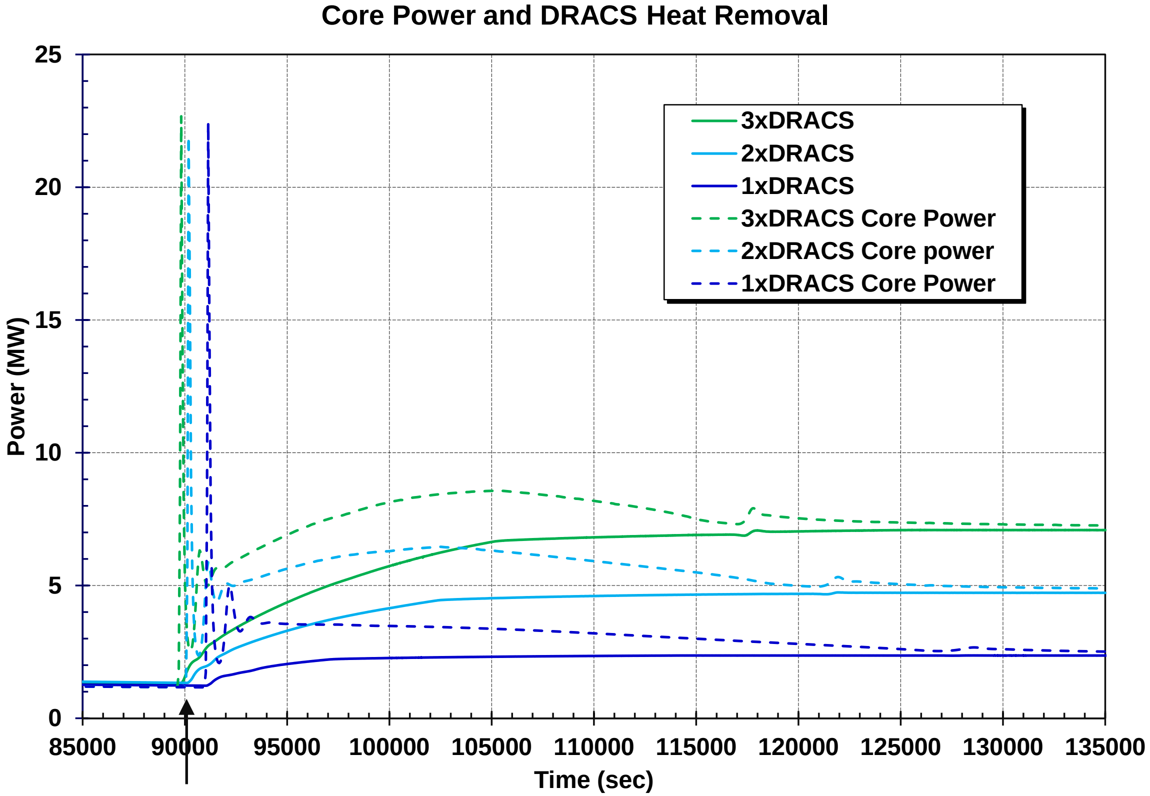

Fission power starts increasing

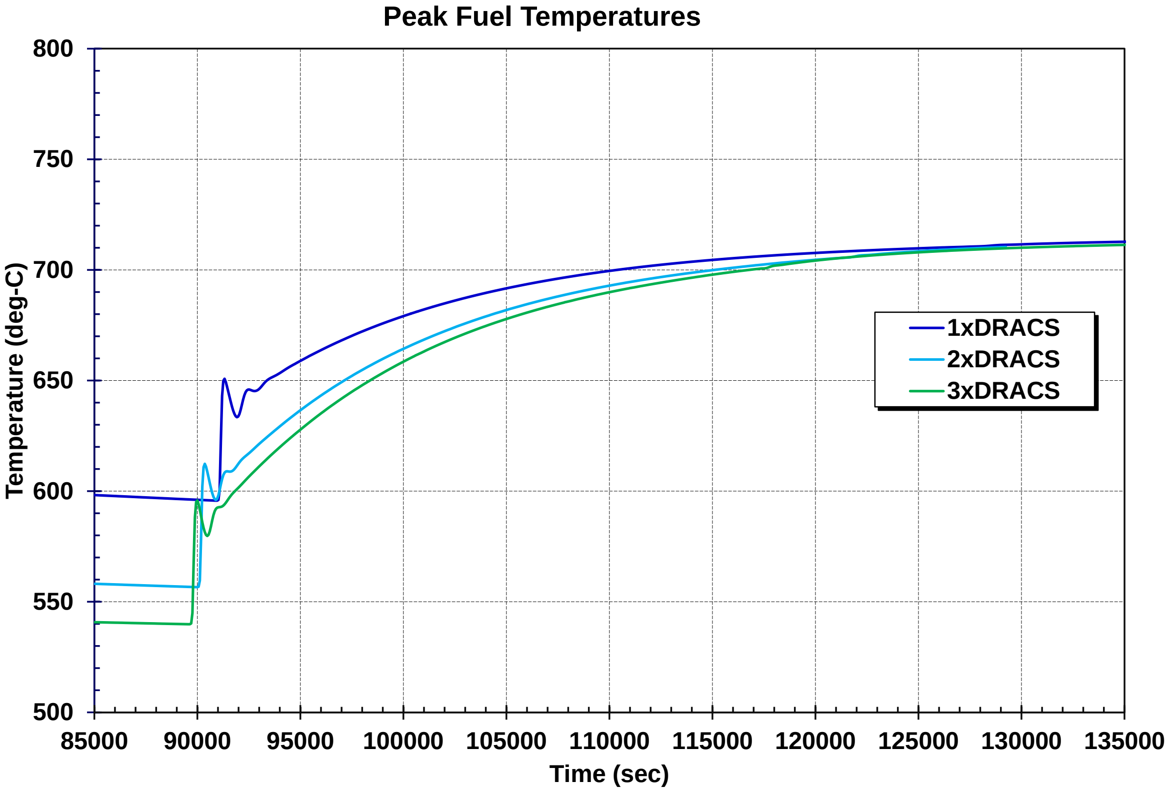

* Xenon transient approximated.

SAND2022-12146 PE

SCALE/MELCOR Non-LWR Source Term Demonstration Project – Molten Salt Reactor (MSR)

September 13, 2022

Fluid Core and Power Distribution

Fluid fuel core defined within the graphite stringers

- The fluid volume within the graphite stringers comprise the active “Core”
- “Loop” volumes comprise a portion of the primary fuel flow loop OUTSIDE the active core
- Allows specification of the axial and radial power distribution from SCALE
  - Feedbacks and power governed by flowing fluid fuel point reactor kinetics model

Fission power generation in “core” and “loop” control volumes

- Fission power and feedbacks are calculated for the “core” volumes
- No fission power energy generation in “loop” volumes
- Decay heat (due to radionuclide class mass carried in pool) for both volume types
- Graphite heating due to neutron absorption
- Provisions for shutdown in a spill accident

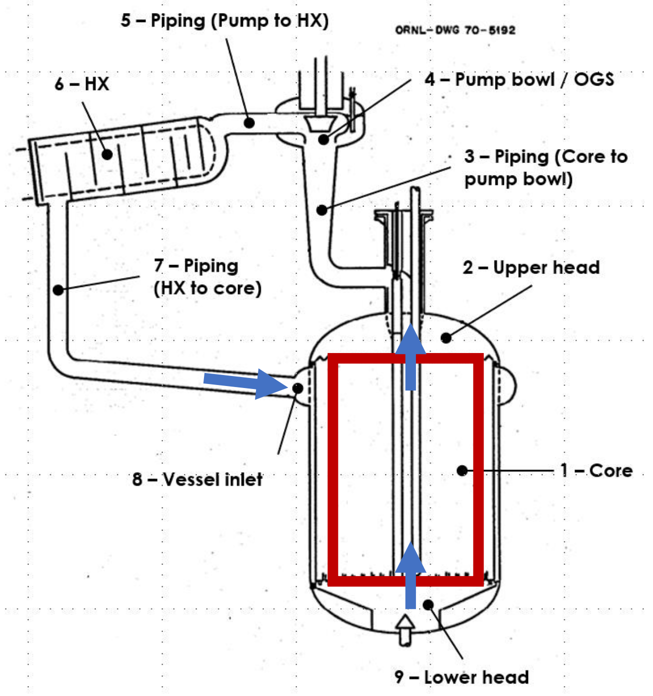

Fluid Fuel Neutronic Transients – Modified Point Kinetics

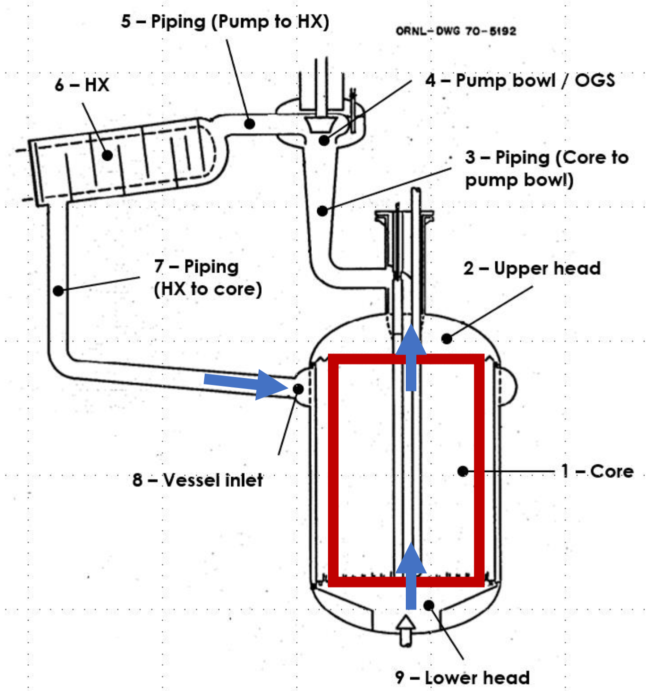

Fission inside **core**

- Neutrons generated and moderated
- **DNPs** generated

DNPs that do not decay in core-region flow into loop

- Decay in loop or advect back into core-region

$$\frac{dP(t)}{dt} = \left(\frac{\rho(t) - \bar{\beta}}{\Lambda}\right)P(t) + \sum_{i=1}^{6} \lambda_i C_i^C + S_0$$

$$\frac{dC_i^C(t)}{dt} = \overset{A}{\left(\frac{\beta_i}{\Lambda}\right)P(t)} - \overset{B}{\left(\lambda_i + {}^{1}/_{\tau_C}\right)C_i^C(t)} + \overset{C}{\left(\frac{V_L}{\tau_L V_C}\right)C_i^L(t-\tau_L)}, \qquad for\ i = 1 \ldots 6$$

$$\frac{dC_i^L(t)}{dt} = \overset{D}{\left(\frac{V_C}{\tau_C V_L}\right)C_i^C(t)} - \overset{E}{\left(\lambda_i + {}^{1}/_{\tau_L}\right)C_i^L(t)}, \qquad for\ i = 1 \ldots 6$$

$$\bar{\beta} = \beta - \left(\frac{\Lambda}{P(t)}\right)\sum_{i=1}^{6} \lambda_i C_i^L(t)$$

A – In-Vessel DNP gain by fission
B – In-Vessel DNP loss by decay and flow
C – In-Vessel DNP gain by Ex-Vessel DNP flow
D – Ex-Vessel DNP gain by In-Vessel DNP flow
E – Ex-Vessel DNP loss by decay, flow

** **DNP** = Delayed Neutron Precursor

MELCOR nodalization - core and reactor vessel

Vessel nodalization

- Assumes azimuthal symmetry
- The graphite core structure is subdivided into 10 axial levels and 5 radial rings
  - Next slide shows mapping from SCALE
- Molten fuel salt enters through an annular distributor (cv-100) that directs the flow into the annular downcomer (cv-105) and the core inlet plenum (cv-110)
- The core is formed by graphite stringers that include flow channels
- The molten fuel salt flows through the stringers (CV-210 through CV-259), where the fuel fissions

Core region

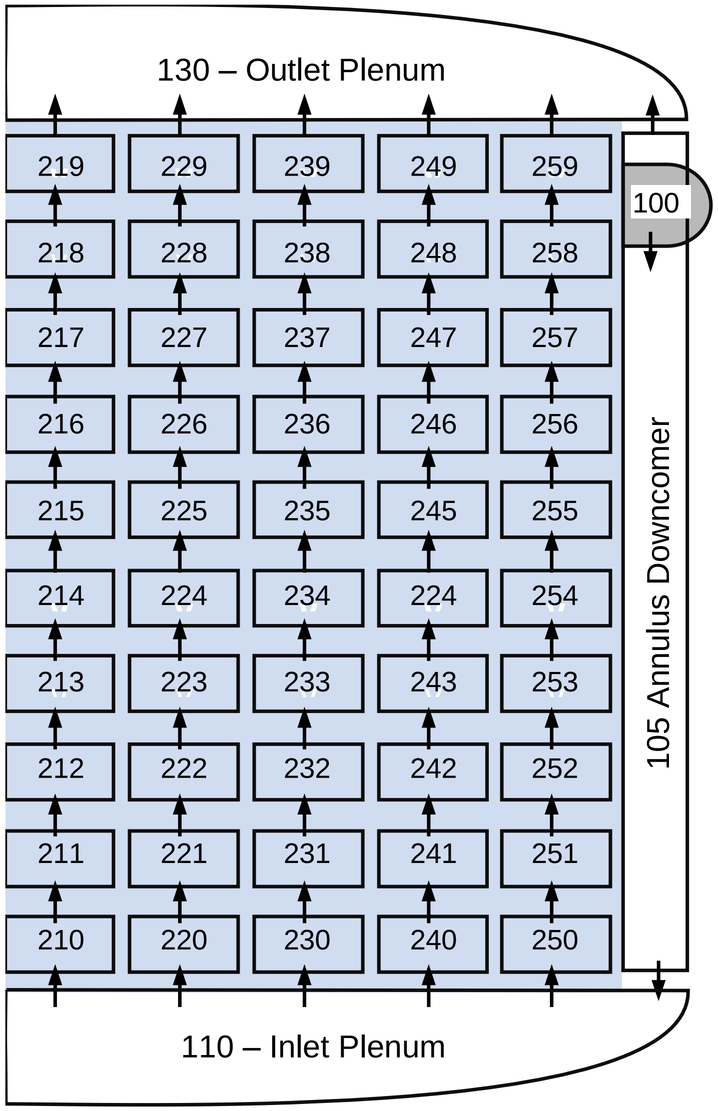

MELCOR nodalization - primary recirculation loop

Recirculation flows

- Pump bowl spray = 50 gpm
- Pump shaft = 15 gpm

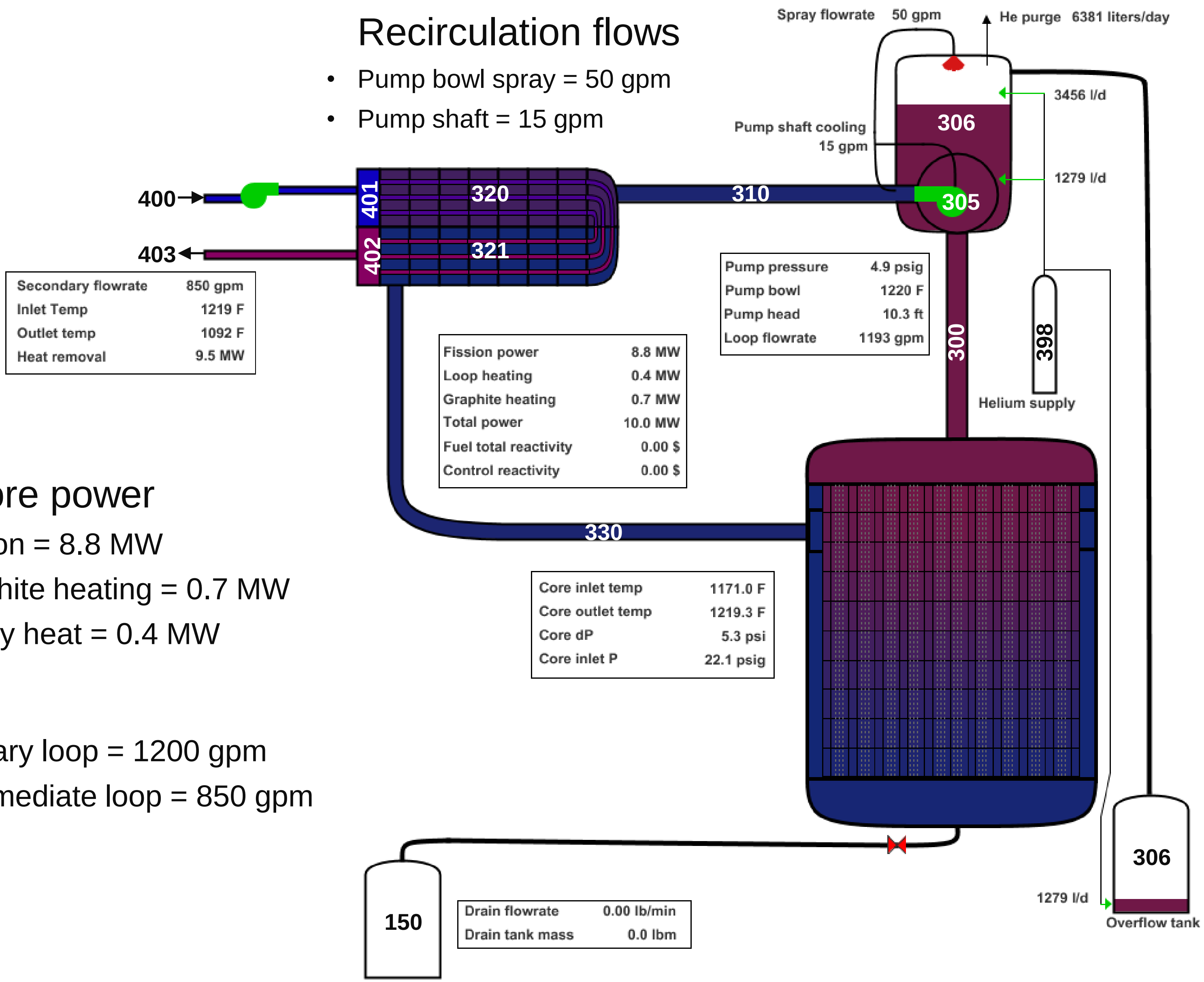

Helium off-gas flows

- Pump shaft = 1279 l/d
- Pump bowl = 3456 l/d
- Overflow tank = 1279 l/d

Total core power

- Fission = 8.8 MW
- Graphite heating = 0.7 MW
- Decay heat = 0.4 MW

Flows

- Primary loop = 1200 gpm
- Intermediate loop = 850 gpm

MELCOR nodalization – reactor cell, condensing tank, and reactor building

Leakages

- Reactor cell = 0.42 scfh at 12.7 psia
- Reactor bldg = 10% per day at 0.25 psig

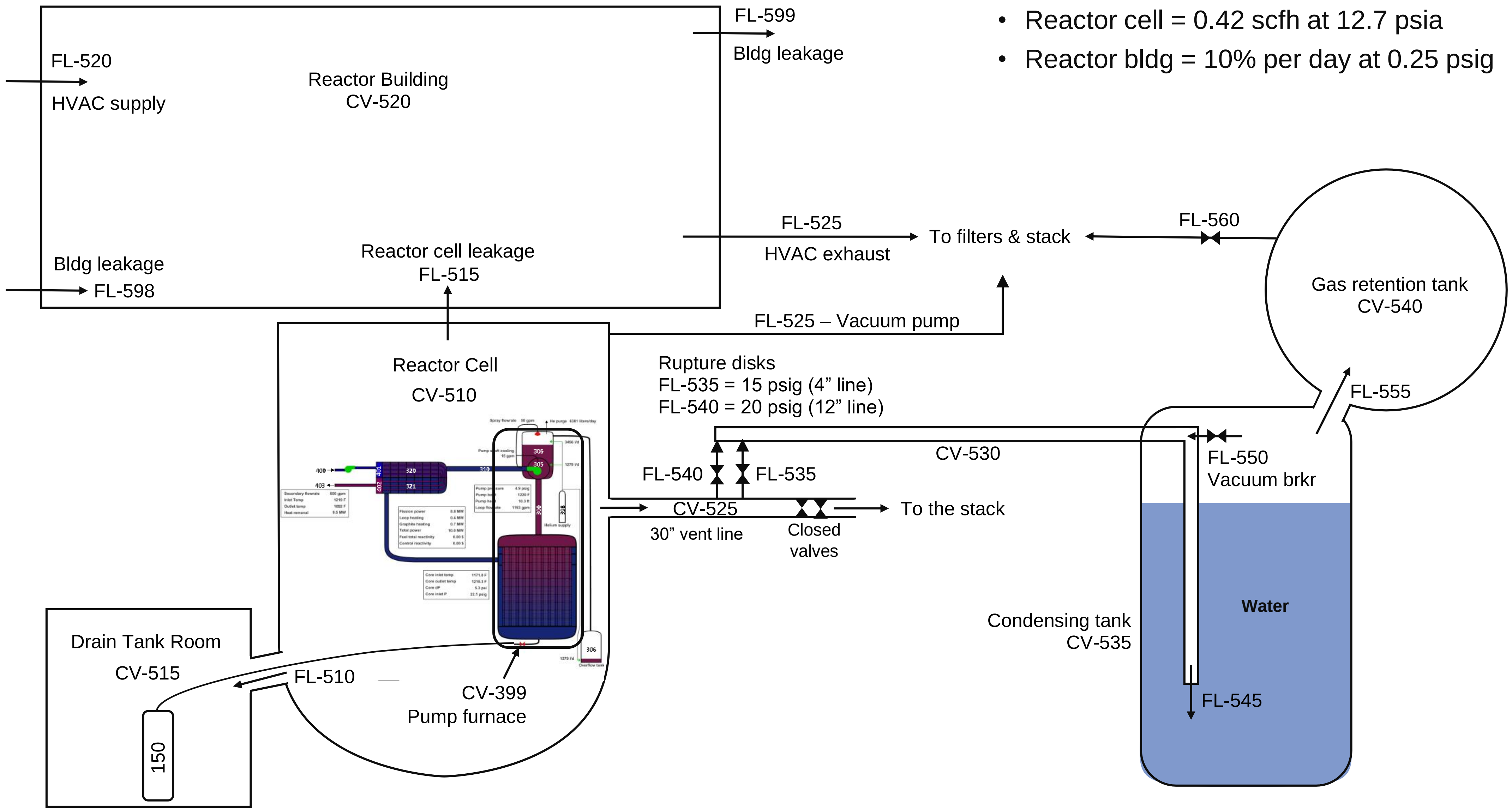

MELCOR nodalization - offgas system

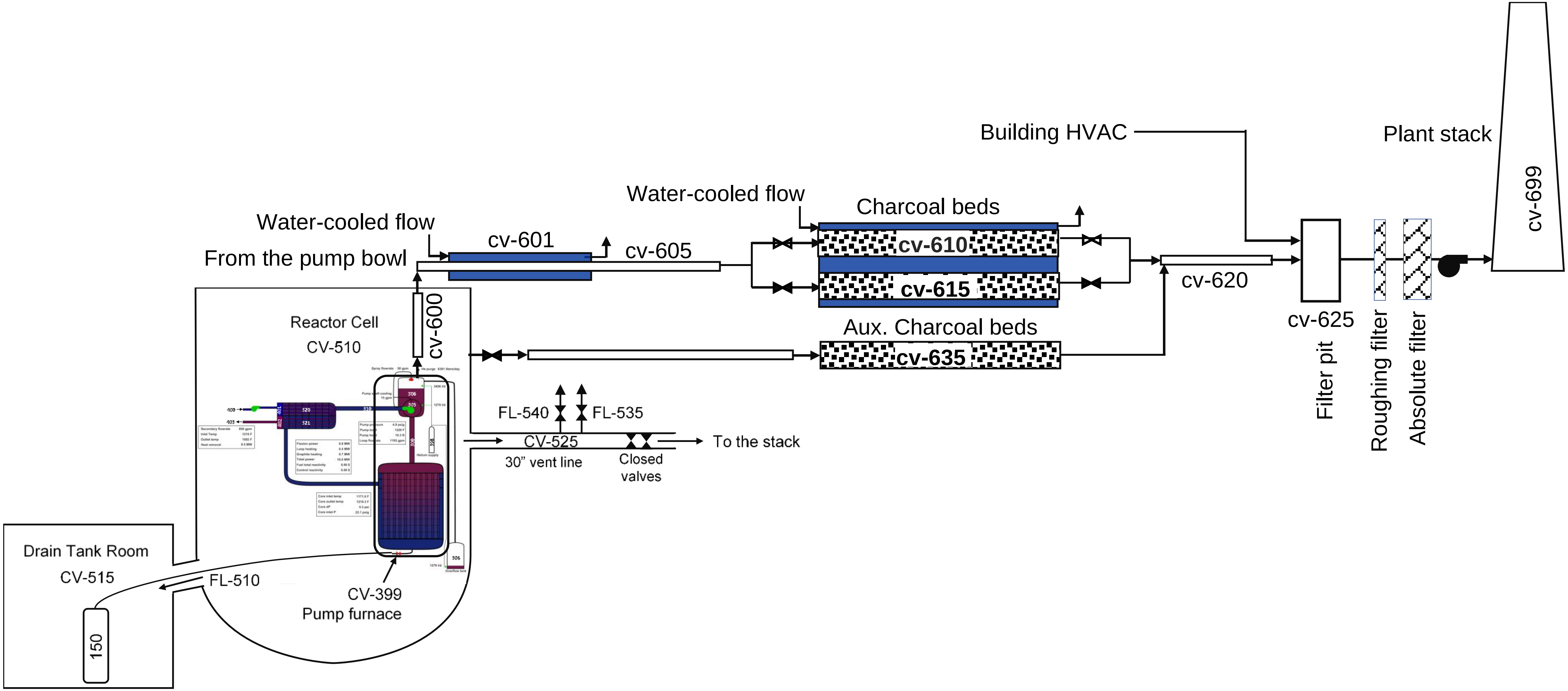

MCA1 salt spill base case – Primary System Response

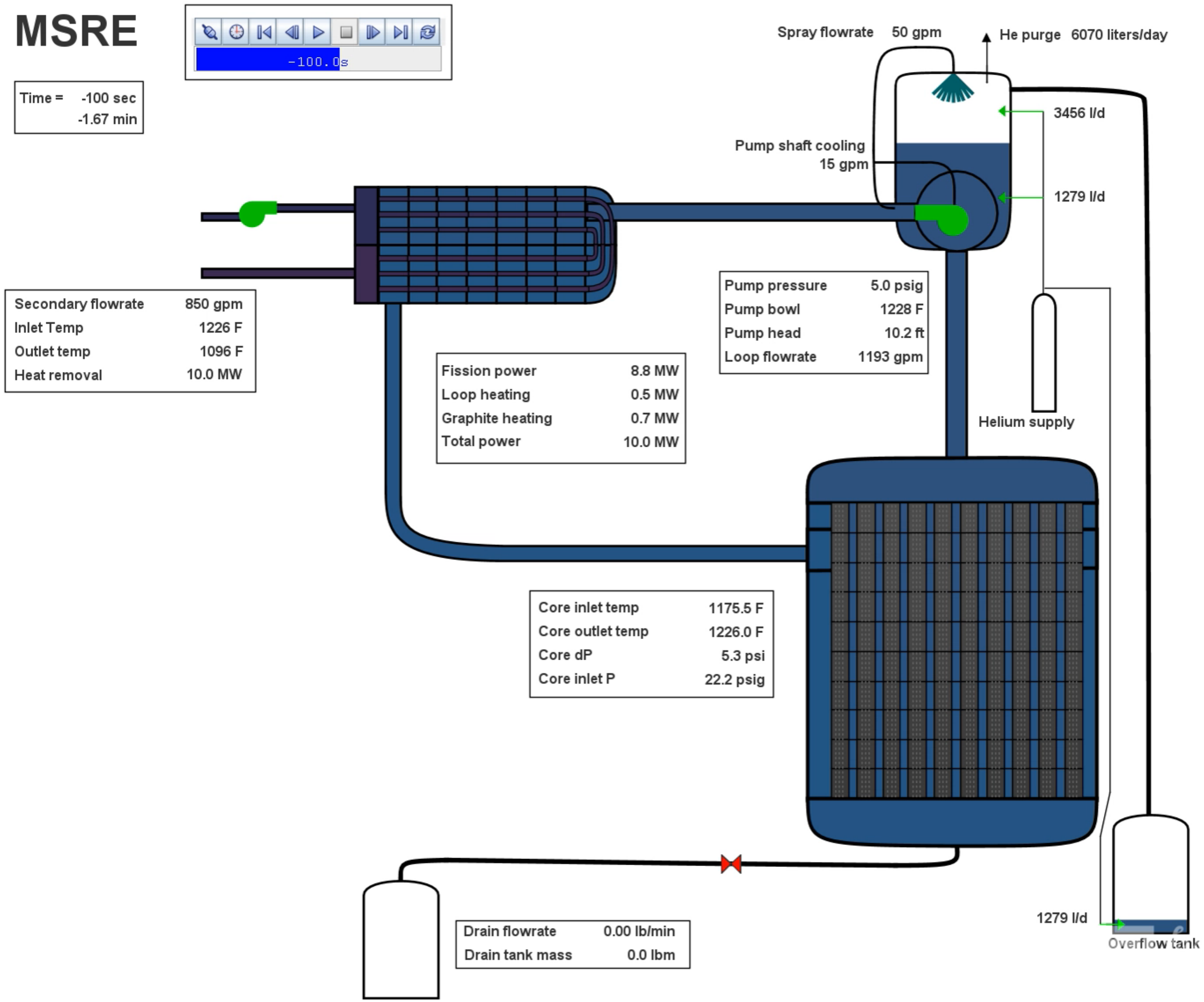

MCA1 salt spill base case – Reactor Cell Response

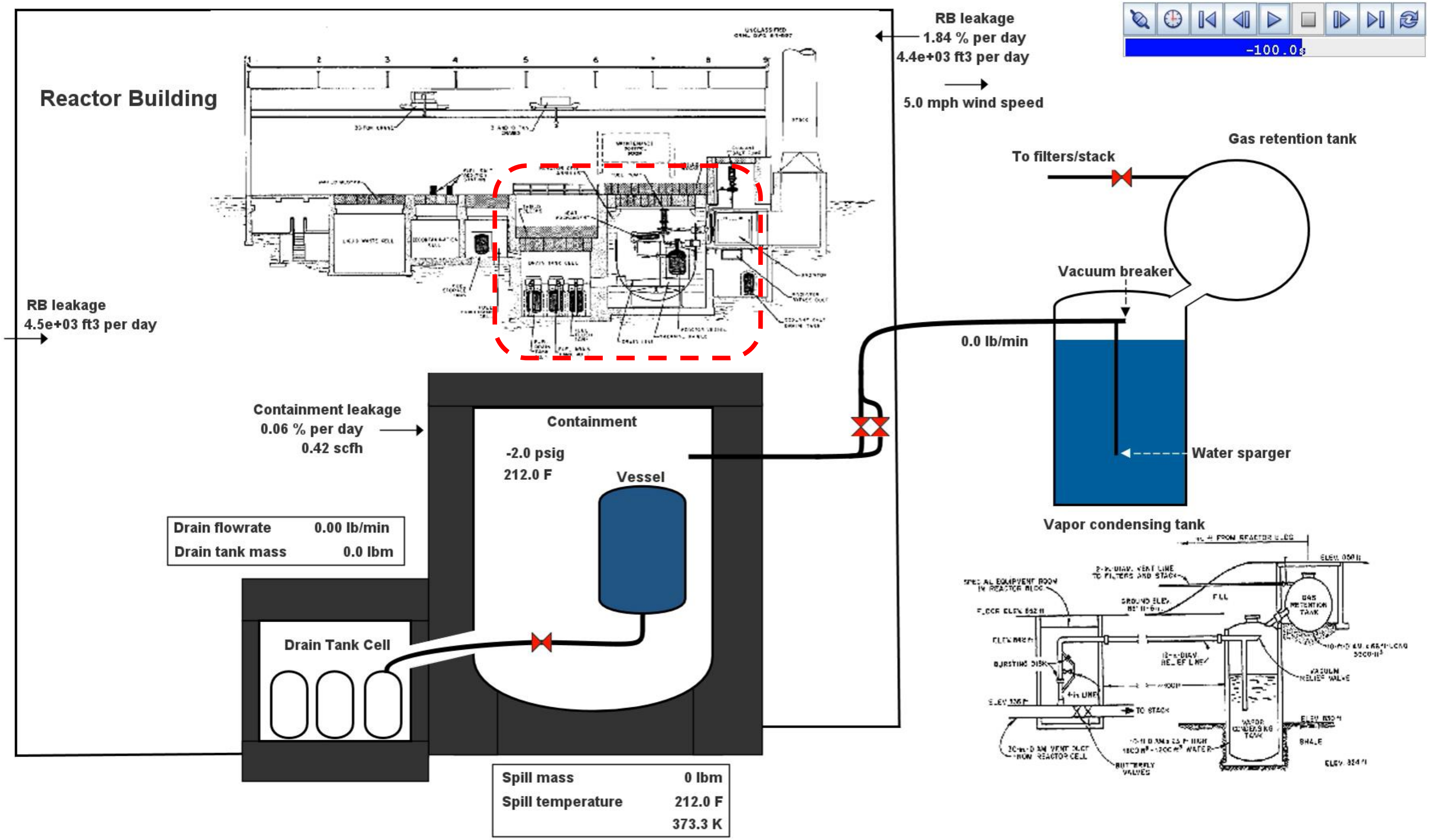

SAND2022-12412 PE

SCALE/MELCOR Non-LWR Source Term Demonstration Project – Sodium Fast Reactor (SFR)

September 20, 2022

Sandia National Laboratories is a multimission laboratory managed and operated by National Technology and Engineering Solutions of Sandia LLC, a wholly owned subsidiary of Honeywell International Inc. for the U.S. Department of Energy's National Nuclear Security Administration under contract DE-NA0003525. SAND20XX-XXXX P

ABTR – Reactor Design

- Selected for the SCALE/MELCOR SFR demonstration
- ABTR Design Specifics
  - 250 MW_{th}
  - Pool-type SFR, near atmospheric pressures
  - 355°C core inlet / 510°C core outlet
  - 1260 kg/s core flowrate
  - 2 mechanical or EM pumps
  - 2 internal intermediate heat exchangers
- Design features
  - Guard vessel
  - Short-term fuel storage in the reactor
  - Primary connects to an intermediate loop inside the vessel
  - Power conversion system: Super-critical CO_2 Brayton cycle

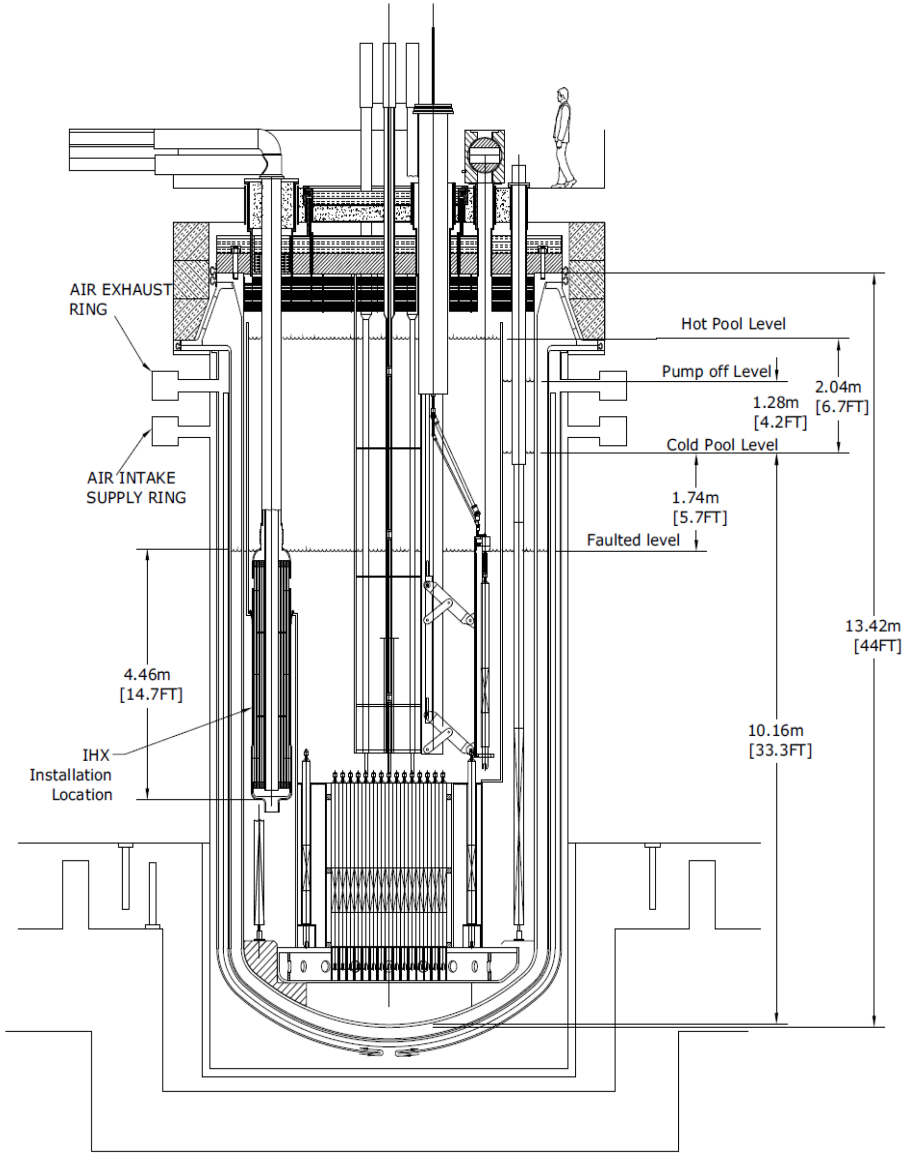

ABTR Vessel
[ANL-AFCI-173]

SCALE SFR Inventory, Decay Heat, Power, and Reactivity Methods and Results

U.S.NRC

Oak Ridge National Laboratory

Sandia National Laboratories

Reactivity Coefficients

- Litany of model perturbations were performed to calculate reactivity coefficients
- Axial Fuel Expansion:
  - A 1% expansion was considered, representing a 575K increase in fuel temperature
  - Density was correspondingly adjusted
- Radial Grid Plate Expansion:
  - Uniform, radial thermal expansion of the SS-316 grid plate (increasing assembly pitch)
  - Cold (293K) to operating (628K)
  - Pitch increase of 0.087 cm (0.6%)

Feedback Effect	SCALE
Axial Fuel Expansion Coefficient (cents/K)	-0.135 ± 0.003
Radial Grid Plate Expansion Coefficient (cents/K)	-0.338 ± 0.007

Reactivity Coefficients, cont.

- Fuel Density:
  - A 1% density reduction while conserving dimensions (decreasing mass)
  - Enhanced response relative to axial fuel expansion due to lost mass
- Structure Density:
  - All HT-9 components (cladding, ducts, reflector, structure, followers, barrel)
  - A 1% density reduction results from a 720K increase (decreasing mass)
- Sodium Void Worth:
  - Flowing sodium was voided within fuel assembly ducts, active fuel region and above
  - Varied from literature values, but known issues exist in calculating void worth with homogenized methods common for SFRs, as well as an XS library dependence [4,5]

Feedback Effect	SCALE
Fuel Density Coefficient (cents/K)	−0.244 ± 0.004
Structure Density Coefficient (cents/K)	−0.013 ± 0.002
Sodium Void Worth ($)	−0.462 ± 0.016

[4] W. S. Yang, et al. (2007).Preliminary Validation Studies of Existing Neutronics Analysis Tools for Advanced Burner Reactor Design Applications Technical Report ANL-AFCI-186, Argonne National Laboratory.
[5] NEA (2016).Benchmark for Neutronic Analysis of Sodium-cooled Fast Reactor Cores with Various Fuel Types and Core Sizes Technical Report NEA/NSC/R(2015)9, Nuclear Energy Agency.

Reactivity Coefficients, cont.

- Doppler:
  - Nine fuel temperatures were utilized to determine the Doppler coefficient
  - Logarithmic response expected from fast spectrum HPR experience, so coefficient is calculated as derivative at nominal fuel temperature (with respect to reactivity, not k_{eff})

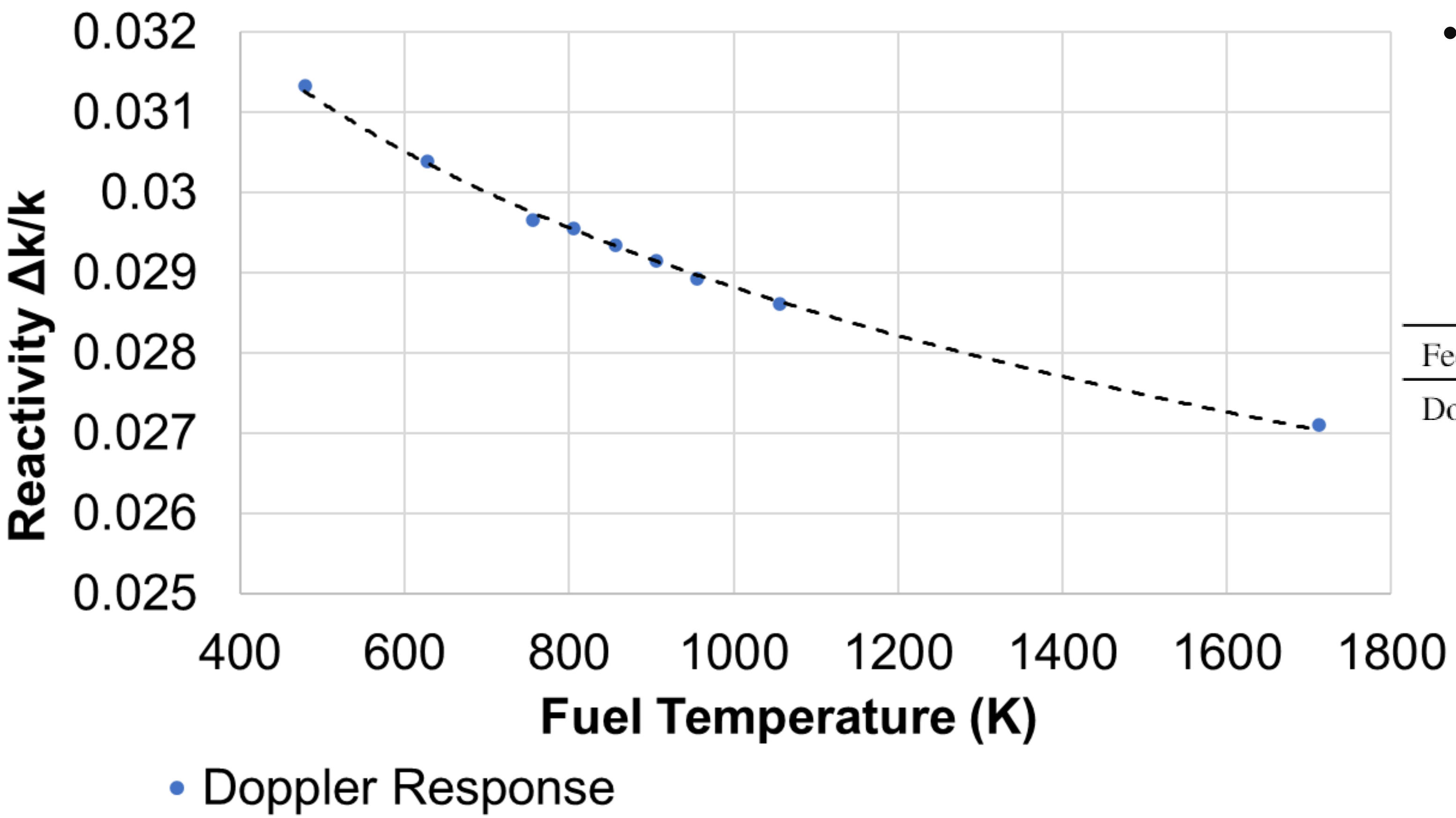

- Linear approach can cause underestimation of Doppler coefficient
  - -0.079 cents/K linear with 2 points
  - -0.098 cents/K linear with 9 points

Feedback Effect	SCALE
Doppler Coefficient (cents/K)	–0.117 ± 0.003

MELCOR SFR Plant Model and Source Term Analysis

Core

Core nodalization – light blue lines

- Subdivided into 15 axial levels and 8 radial rings
- Core divided according to assembly power and function (similar to SFP modeling)
  - Ring 1 through 6 = 60 fueled assemblies combined according to power
  - Ring 7 = 10 control and 3 material test assemblies
  - Ring 8 = 78 reflector and 58 shield assemblies
  - The 8 rings share a common inlet plenum and the lower cold pool

Fluid flow nodalization – black boxes

- Sodium enters through the inlet plenum and flows into the assemblies

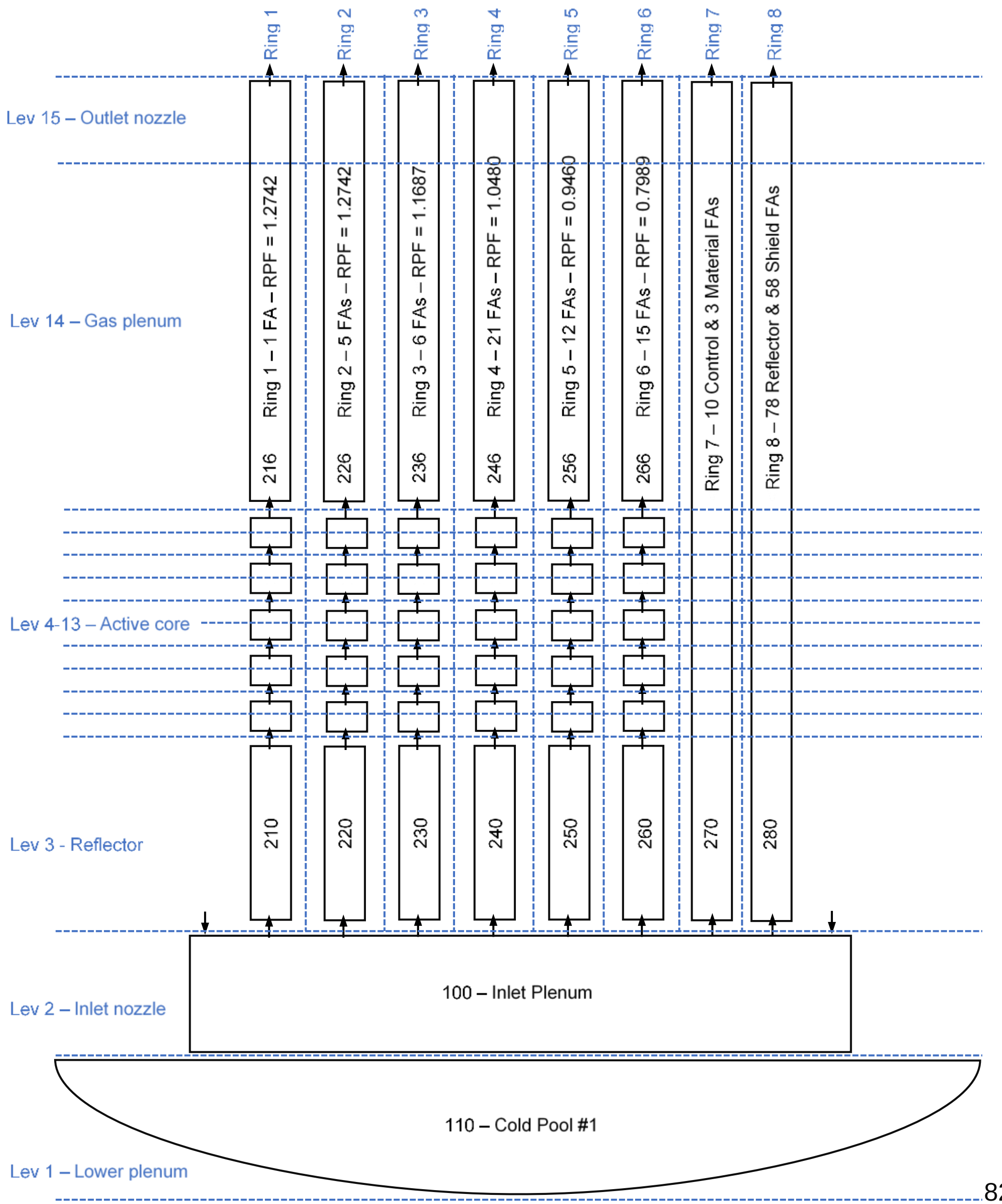

Vessel

All primary system sodium is contained within the vessel

Sodium exits into a hot pool and circulates through the shell side of 2 intermediate heat exchangers (iHX)

A redan (wall) separates the hot pool from the cold pool

2 EM or mechanical pumps circulate sodium into the vessel inlet

Free surfaces at the top of the hot and cold pools

Argon gas above the free surfaces with connection to the cover-gas system

- Assumed leak path for fission products

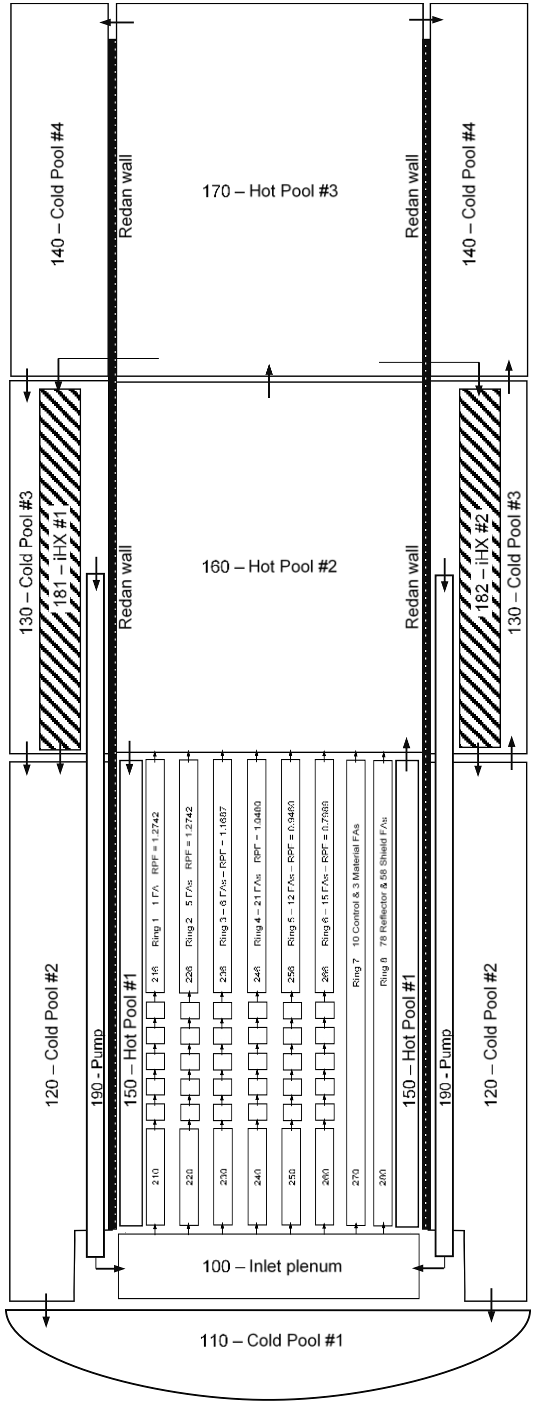

Direct Reactor Auxiliary Cooling System (DRACS)

4 trains – 625 kW/train

- 0.25% of rated power per train (passive mode)
- Passive or forced circulation operation (only passive mode modeled)

Each train has 3 loops in series

- Cold pool primary coolant circulates through DRACS heat exchanger
- A Na-K secondary side loop transfers heat from the DRACS HX to the natural draft heat exchanger (NDHX)
  - Pump-driven or passive (only passive flow modeled)
- Air flows through the NDHX to the plant stack
  - Fan-driven or passive (only passive flow modeled)

Start-up: Damper on air flow springs open

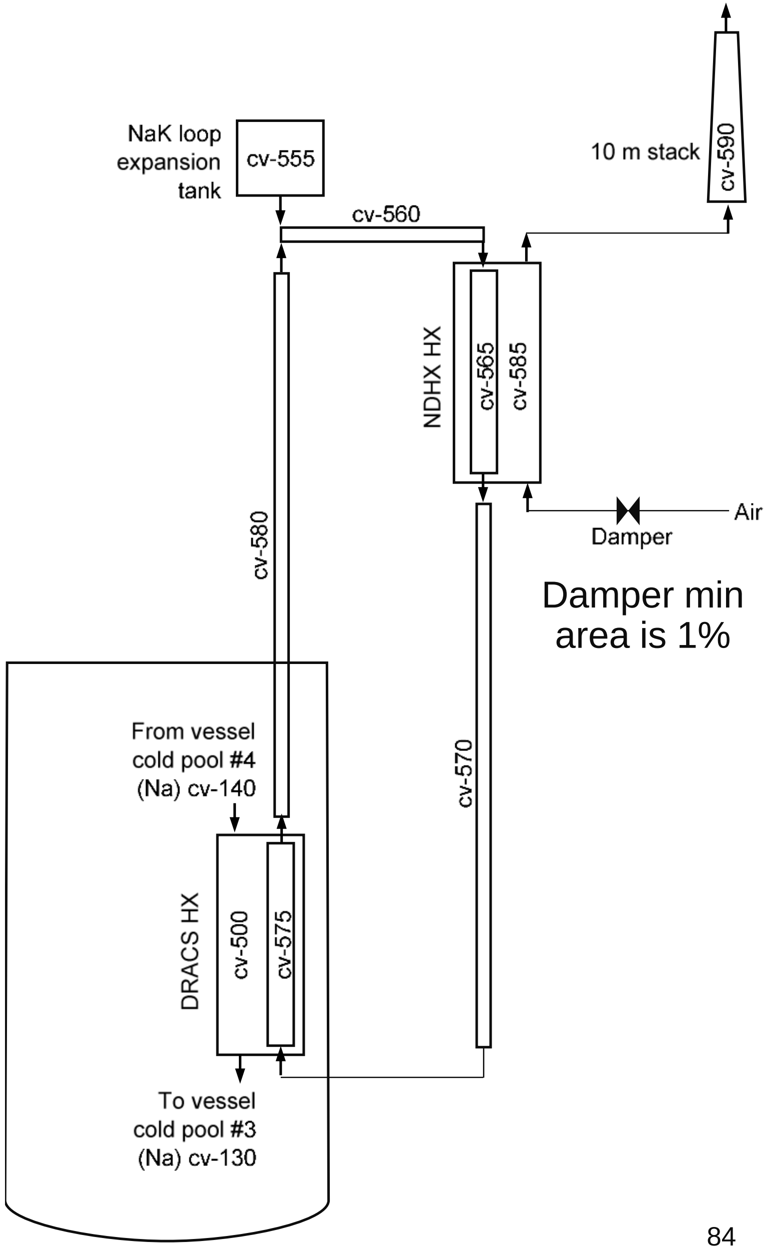

Damper min area is 1%

Unprotected loss-of-flow (ULOF)

Initial and boundary conditions

- Primary and intermediate pumps trip resulting in no secondary heat removal
- Reactor safety control rods fail to insert
- 4 DRACS trains are available in passive mode

Sensitivity analysis on DRACS availability

- 0, 1, 2, and 3 DRACS trains available

ULOF

The initial fuel heatup has strong negative expansion, fuel density, and fuel Doppler fuel feedbacks that greatly offsets the positive sodium density feedback that shuts down fission

The net reactivity oscillates near zero after 1000 sec

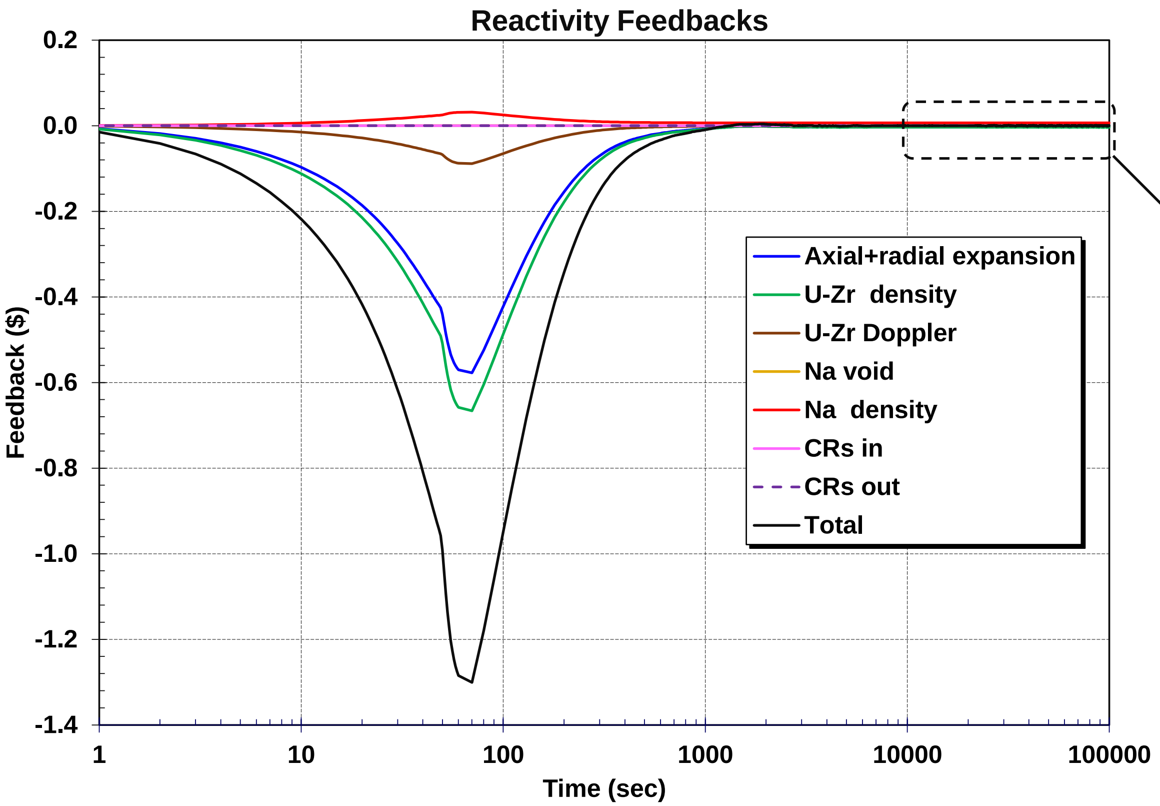

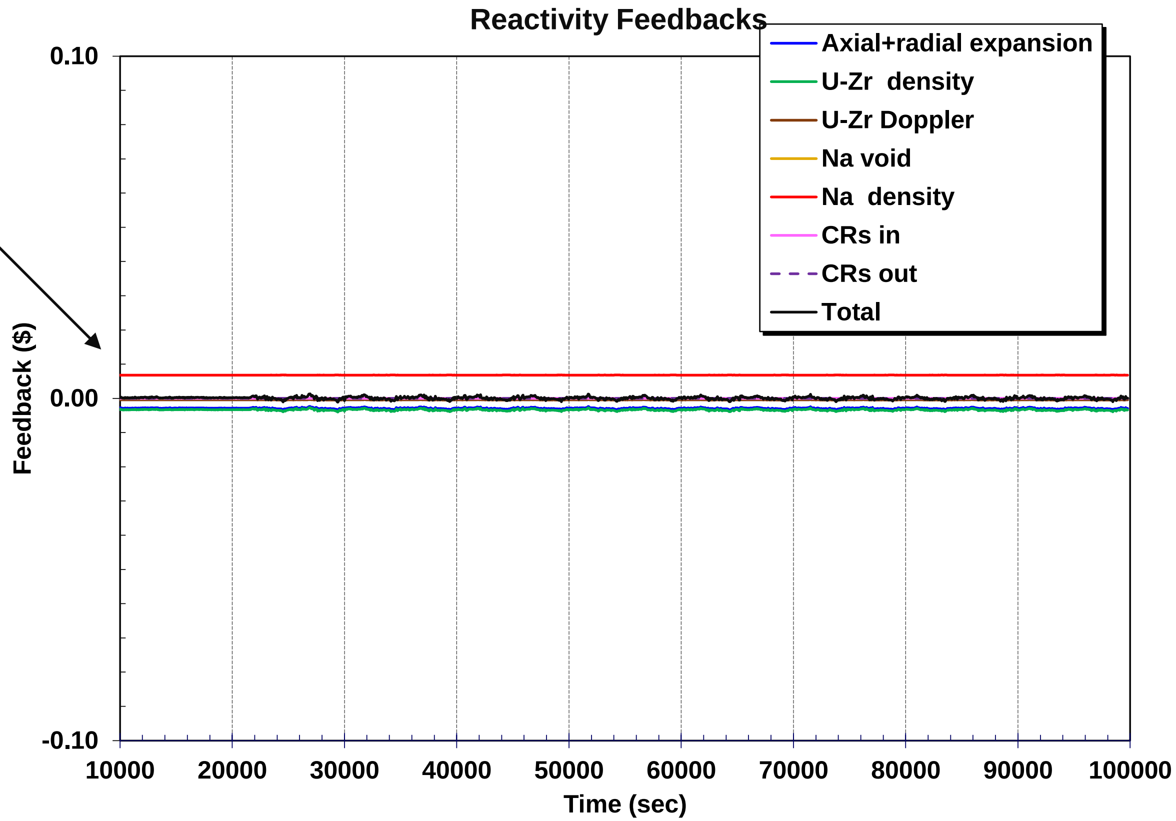

ULOF

The long-term core power matches the DRACS heat removal rate after 20,000 sec (5.6 hr)

The fission power is 1000 kW at 10,000 sec and gradually increases to offset the decrease in decay heat

The fuel and vessel liquid sodium temperatures quickly stabilize

The natural circulation flow moves heat from the core, through the iHXs to the cold pool, and through the DRACS

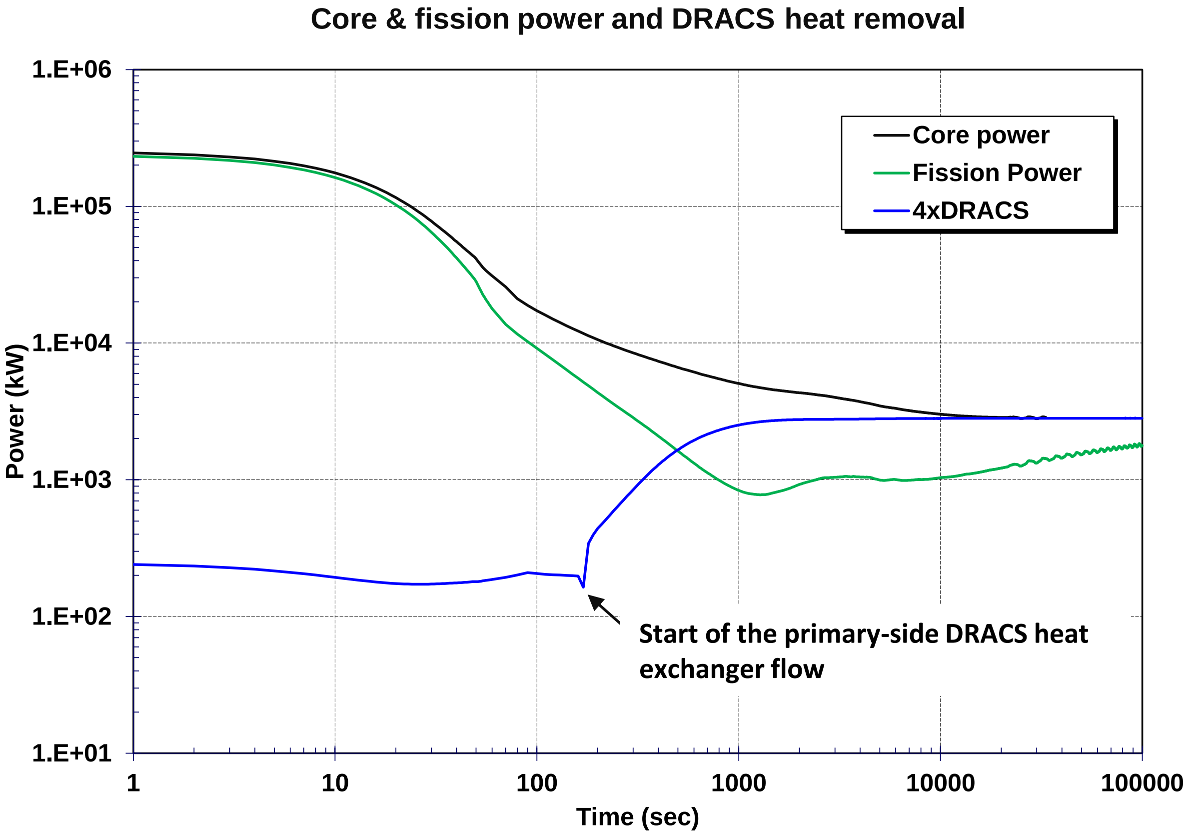

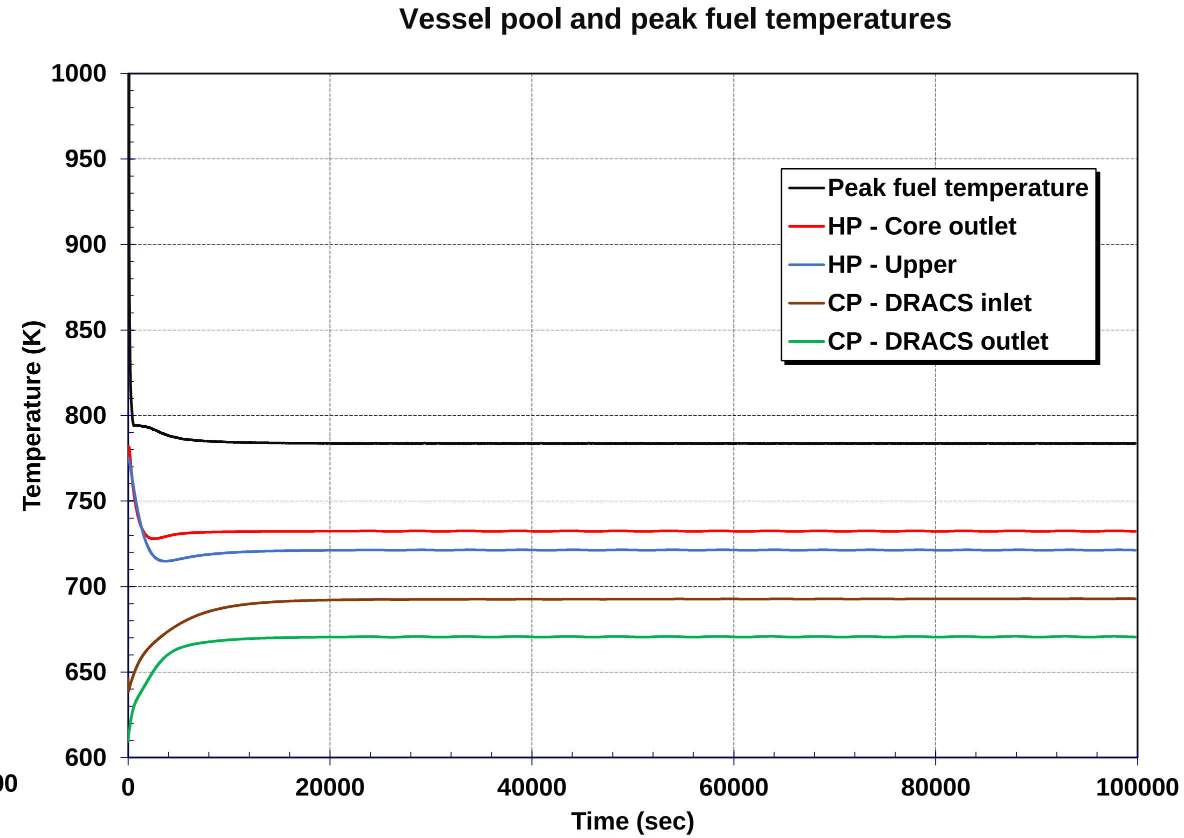

ULOF – with variable DRACS sensitivity

- Core power eventually converges on the DRACS heat removal rate
- Dampers are normally 1% open

1xDRACS case shows a small heatup but other DRACS cases have similar responses

- Thermal inertia of the DRACS and vessel mitigate heatups

Expansion of sodium leads to hot to cold pool spill-over and eventually a filled vessel in 1% damper case

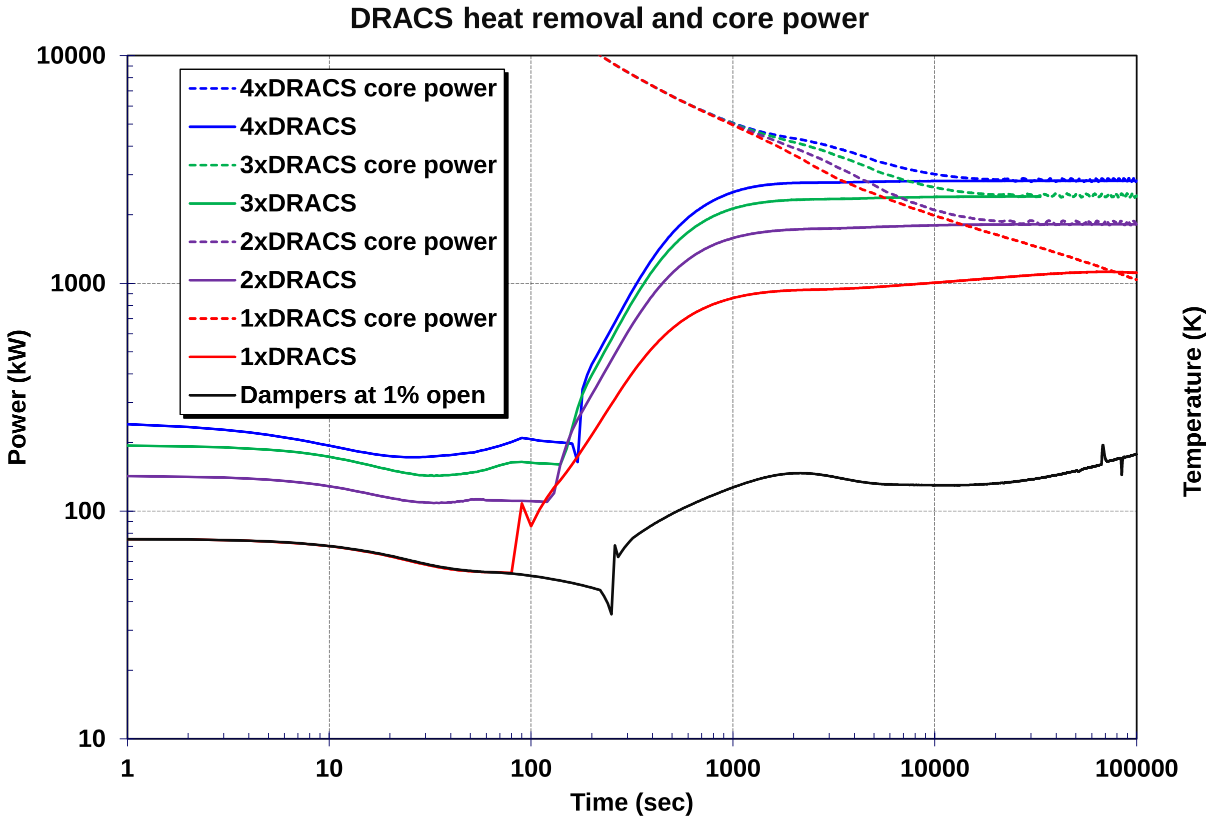

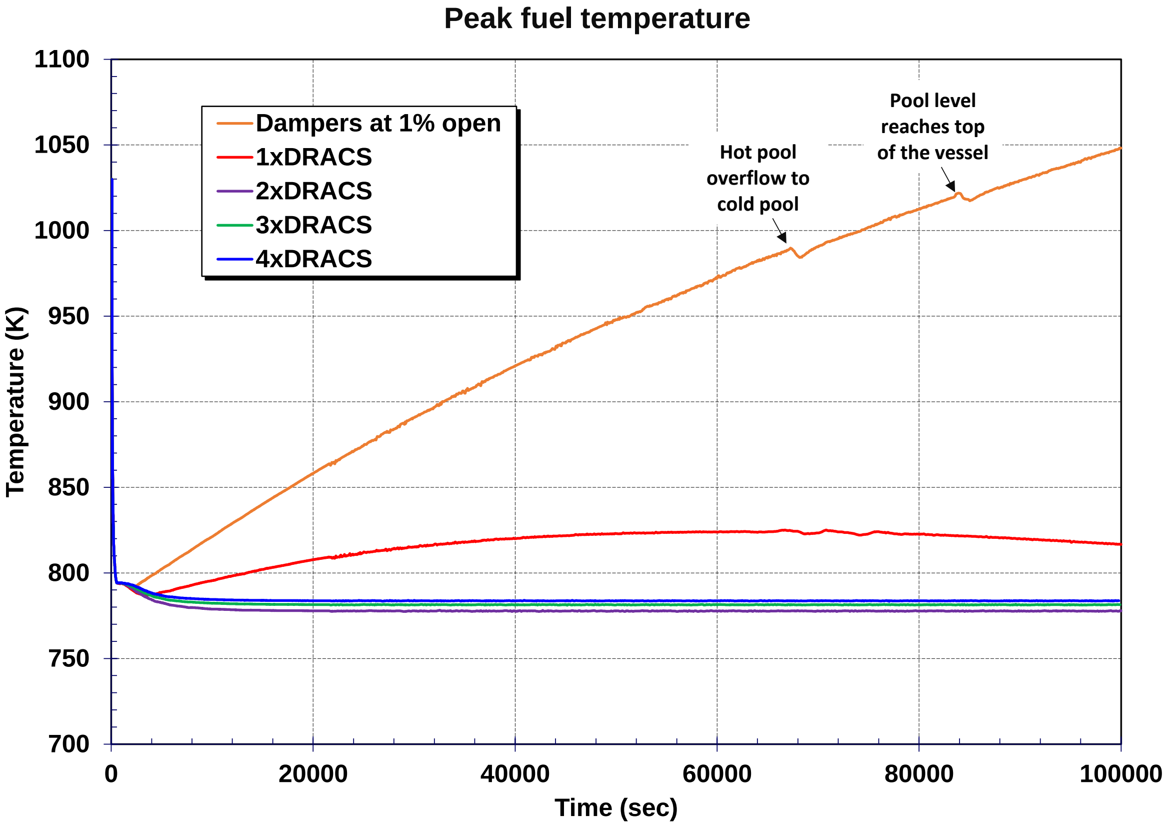

Single blocked fuel assembly

Initial and boundary conditions

- Inlet to a fuel assembly is blocked
- Primary and intermediate pumps remain running
- Control rods are assumed to insert after an off-gas high-radiation signal
- The cover gas system leaks in the containment
  - Assumed radionuclide release pathway

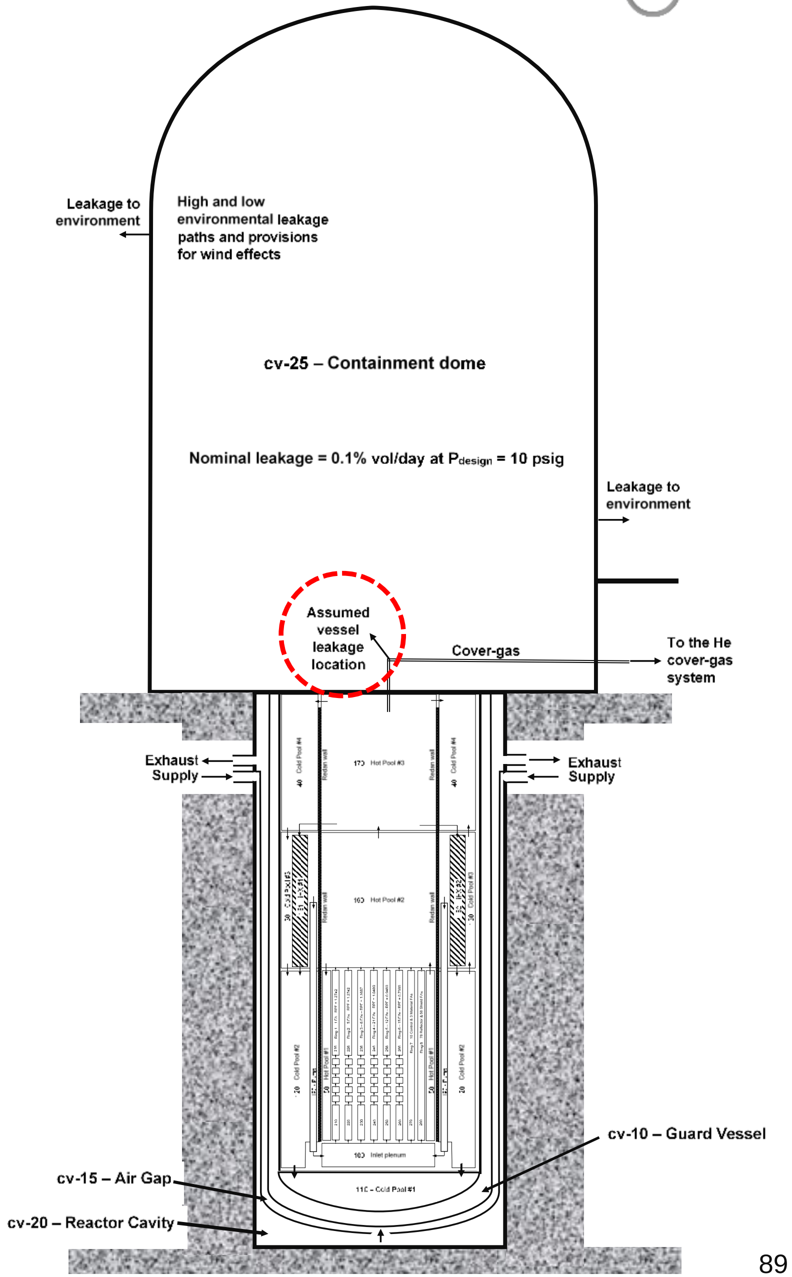

Single blocked fuel assembly

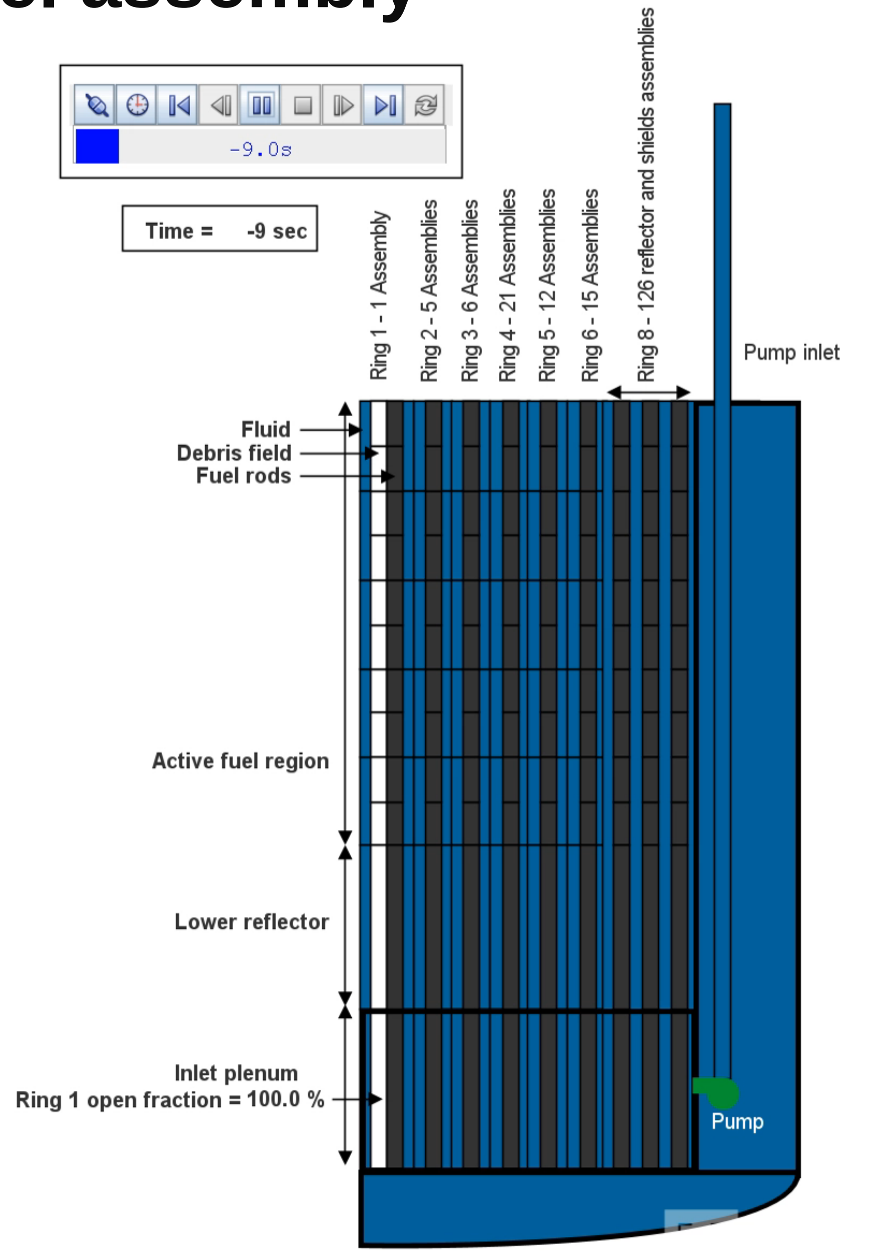

Single blocked fuel assembly

- The fluid in the duct starts voiding within 3 seconds
- The assembly sodium is boiled and expelled within ~10 sec
- The fuel cladding temperature responses (below) also indicate the fuel temperature response
- The cladding temperature rise pauses while the fuel melts and then increases to the cladding melting temperature
- The cladding melts and collapses when the minimum thickness reaches a structural integrity limit

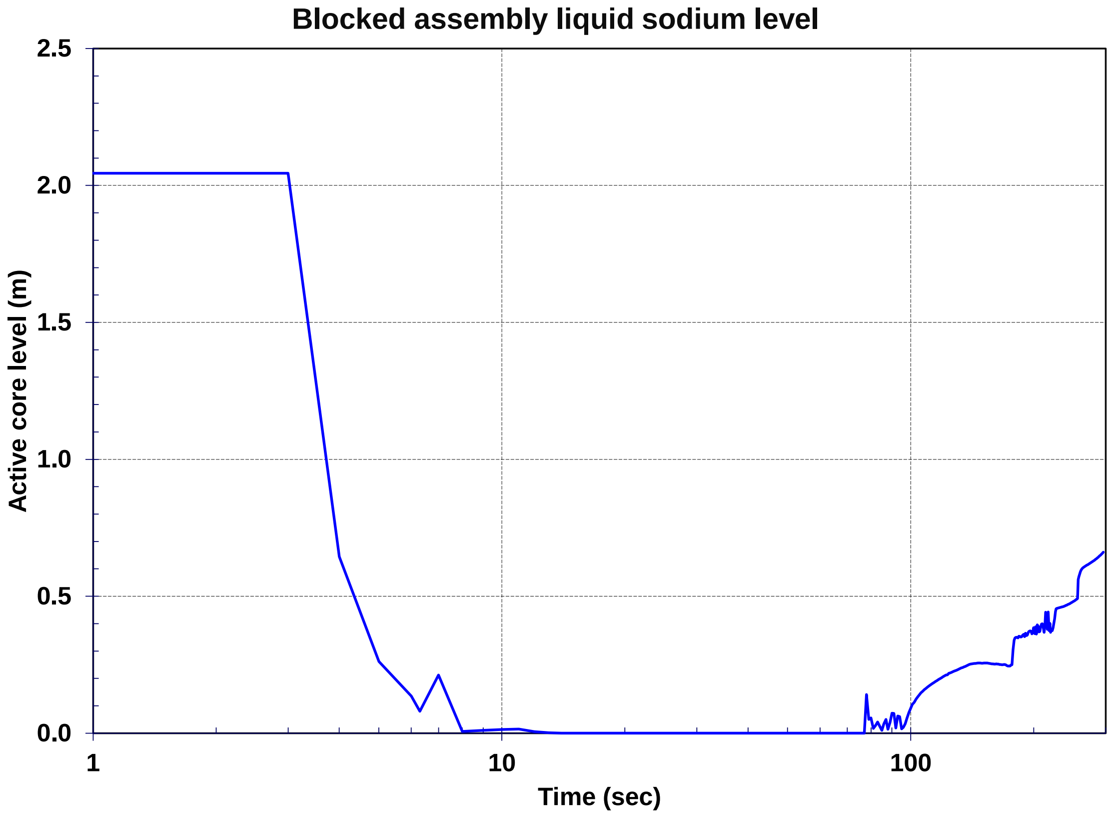

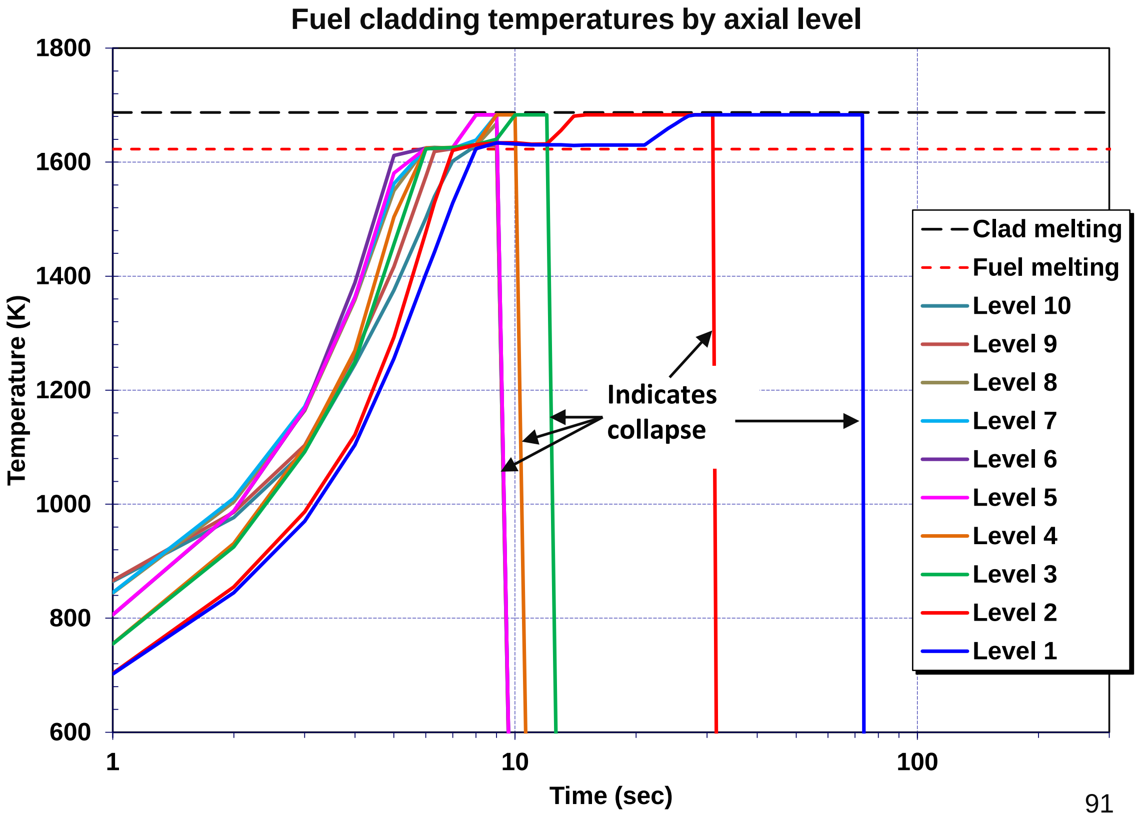

Single blocked fuel assembly

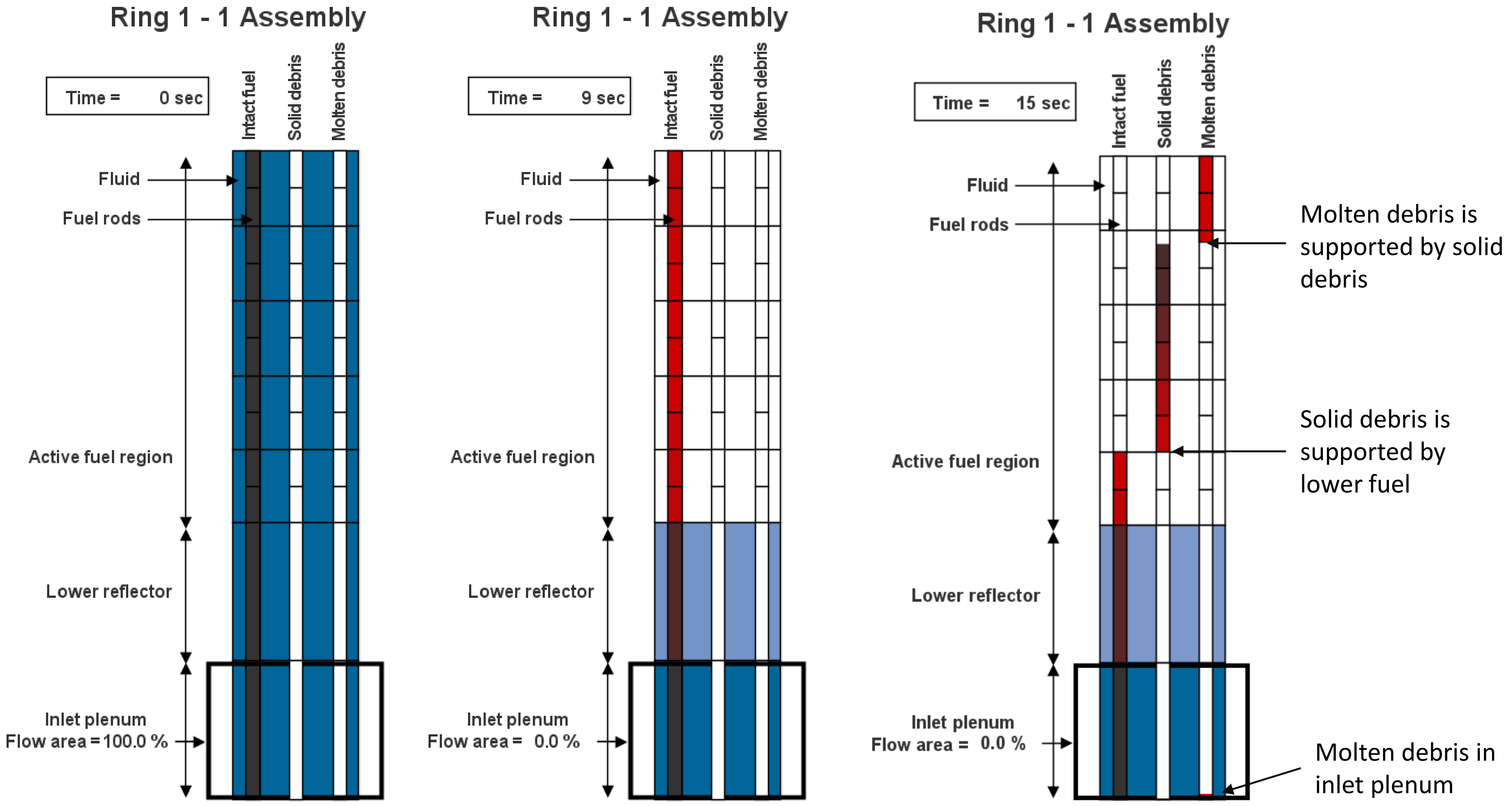

Single blocked fuel assembly

- After the cladding failure, there is a prompt release of the plenum gas inventory followed by thermal releases from the hot debris
- The analysis assumed blockage of a high-powered center assembly with approximately 2.2% of the core radionuclides
  - 97% of the noble gases
  - ~6% of iodine and cesium

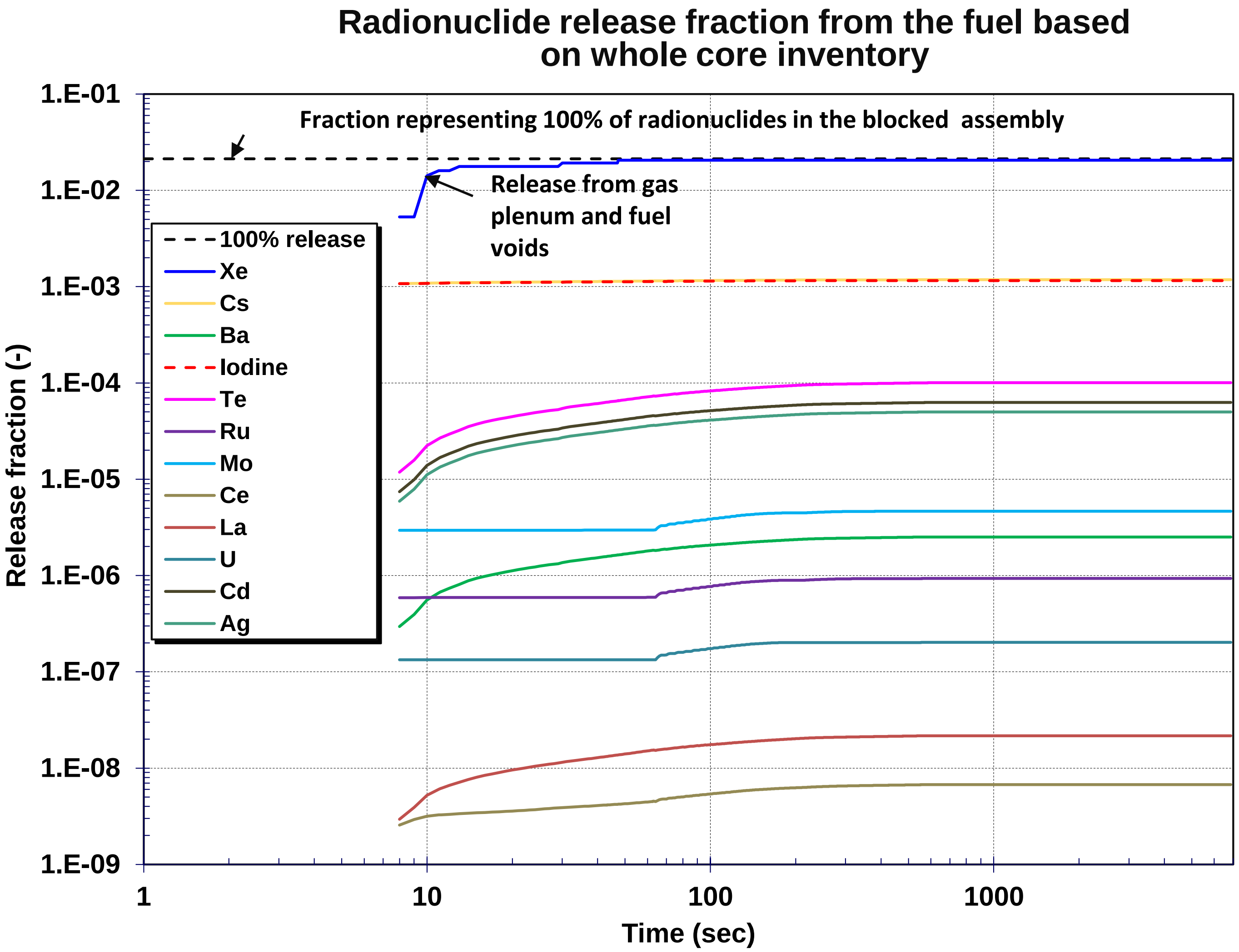

Single blocked fuel assembly

- Xe bubbles through the hot sodium pool above the core to the gas space.
- Leakage rate through the failed off-gas line to the containment
  - Assumed a sweep flow of 1 reactor gas space change per hour persisted during the transient
  - Xe environmental release is very small due to the large containment volume and the low leak rate
- The cesium and other radionuclides retained in the sodium

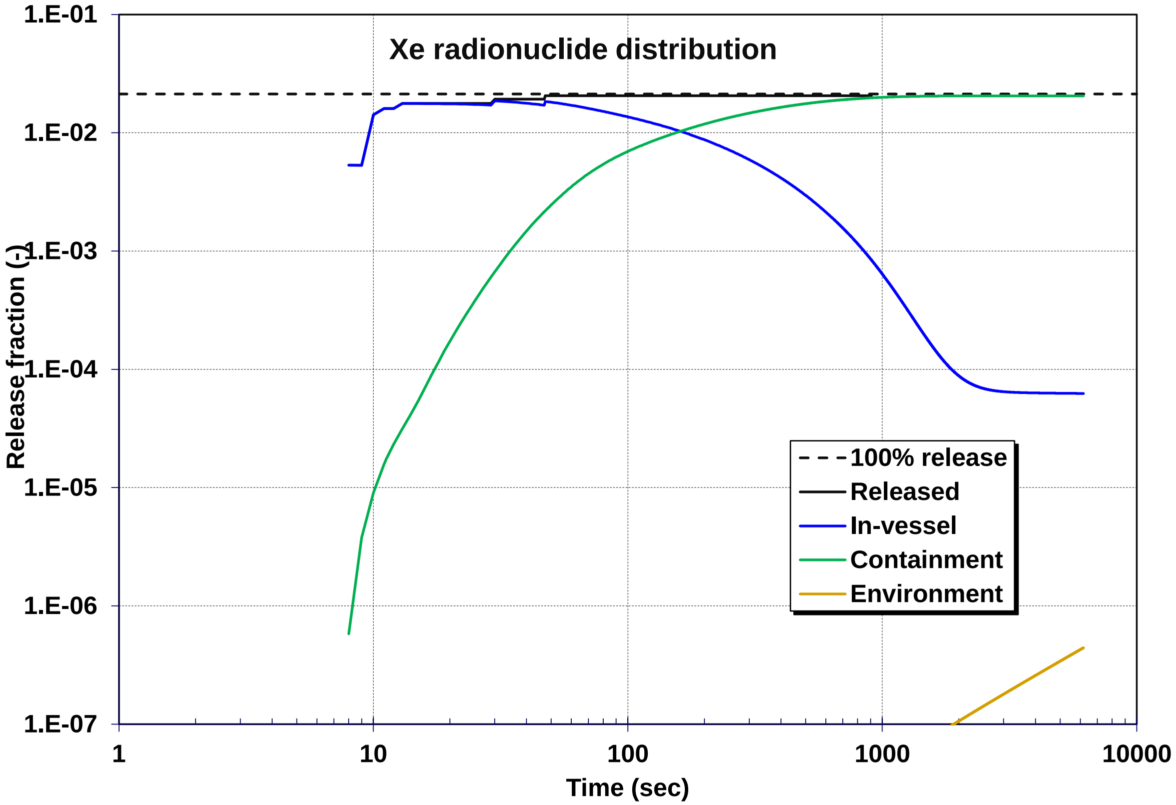

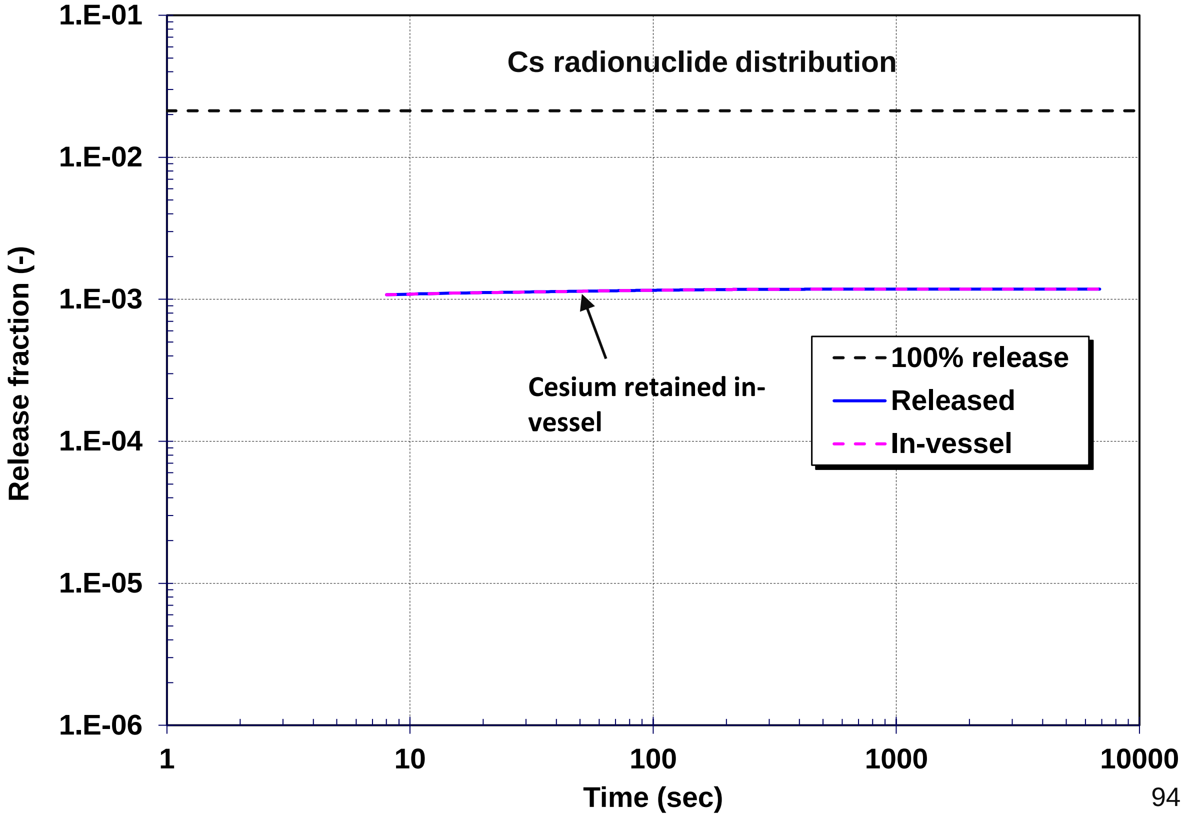

MELCOR Point Kinetics Feedback Example

MELCOR Point Kinetics

Required inputs (cor_pkm0x)

- All relevant feedbacks in dollars [$] – example uses vector control functions
- Control rod worth for SCRAM [$]
- Any neutron sources [neutron/s]

cor_tavg & cor_pkm03 input is optional

- Not used in non-LWR models

Disable built-in feedbacks (sensitivity coefficient 1404)

- Default feedbacks originally formulated for high-temperature gas reactor (HTGR)

```
cor_sc      6
            1    1404    0.0     1
            2    1404    0.0     2
            3    1404    0.0     3
            4    1404    0.0     4
            5    1404    0.0     5
            6    1404    0.0     6
            7    1404    0.0     7
```

MELCOR Point Kinetics

6 delayed-neutron group decay constants in sensitivity coefficient 1405

- Default developed for a high-temperature gas reactor (HTGR) (thermal neutron reactor)

Other reactor-specific point kinetics data in sensitivity coefficient 1406

- For example, sc-1406(2) is the total effective delayed neutron fraction, **β**

SFR feedback example

Feedback Effect	SCALE Value
Axial fuel expansion coefficient (cents/K)	-0.1347 ± 0.0033
Radial grid plate expansion coefficient (cents/K)	-0.3376 ± 0.0067
Fuel density coefficient (cents/K)	-0.2444 ± 0.0044
Structure density coefficient (cents/K)	-0.0125 ± 0.0021
Sodium void worth ($)	-0.4623 ± 0.0165
Sodium density coefficient (cents/K)	-0.1252 ± 0.0389
Doppler coefficient ($ with T in K)	-1.004 ln(T) + 15.67
Sodium voided Doppler coefficient ($ with T in K)	-0.776 ln(T) + 13.68
Primary control assemblies ($)	-22.07
Secondary control assemblies ($)	-15.77

SFR fuel Doppler feedback example

First, define fuel temperatures vector range

```
cf_range    RANGEFU cells 1
construct   1   ! Axial Radial
            1     4-13   1-6
```

Second, get fuel temperatures

```
cf_id        'Tfu'   4001   formula
cf_sai       1.0     0.0    0.0000E+00
cf_vcf       #RANGEFU
cf_formula   1  T
             1  T  cor-celltemp(#RANGEFU,fu)
```

Third, calculate feedback

```
cf_id       'fb-Dopp0'   4014   formula
cf_sai      1.0          0.0    0.0000E+00
cf_vcf      #RANGEFU
cf_formula  3    a*ln(T)+b
            1    a   -1.004
            2    b   15.67
            3    T   cf-valu('Tfu')
```

SFR fuel Doppler feedback example

Fourth, apply weighting factors (e.g., volume, power, power^2)

```
cf_id        'fb-Dopp1'   4015     add
cf_sai       1.0          0.0      0.0000E+00
cf_arg       60
             1      cf-valu('fb-Dopp0')[1]     1.7647E-03
             2      cf-valu('fb-Dopp0')[2]     8.8236E-03
             3      cf-valu('fb-Dopp0')[3]     9.7116E-03
             4      cf-valu('fb-Dopp0')[4]     3.0481E-02
             5      cf-valu('fb-Dopp0')[5]     1.5723E-02
…
             58     cf-valu('fb-Dopp0')[58]    2.4429E-02
             59     cf-valu('fb-Dopp0')[59]    1.2601E-02
             60     cf-valu('fb-Dopp0')[60]    1.3301E-02
!                                              1.0000E+00
```

Fifth, freeze steady state values

```
cf_id        'fb_Dopp-ss'    4016       formula
cf_sai       1.0    0.0      0.0000E+00
cf_formula   4      l-a-ifte(t>t0,self,fb)
             1      t        exec-time
             2      t0       -10.0
             3      self     cf-valu('fb_Dopp-ss')
             4      fb       cf-valu('fb-Dopp1')
```

SFR fuel Doppler feedback example

Sixth, calculate the Doppler change from full-power steady state conditions

```
cf_id        'del_Dopp'    4017    formula
cf_sai       1.0           0.0     0.0000E+00
cf_formula   2   fb-fbss
             1   fb          cf-valu('fb-Dopp1')
             2   fbss        cf-valu('fb_Dopp-ss')
```

Seventh, sum feedbacks

```
cf_id        'React'       4029    formula
cf_sai       1.0           0.0     0.0000E+00
cf_formula   8     Axial+Radial+FuRho+Doppler+NaVoid+NaRho+CRout+CRin
             1     Axial      cf-valu('fb-FuExp')
             2     Radial     cf-valu('fb-RadExp')
             3     FuRho      cf-valu('fb-FuRho')
             4     Doppler    cf-valu('del_Dopp')
             5     NaVoid     cf-valu('del_void')
             6     NaRho      cf-valu('del_NaRho')
             7     CRout      cf-valu('CR-out')
             8     CRin       cf-valu('CRs-in')
```

SFR fuel Doppler feedback example